# Synthesis of 1,2-Glycosidic Polymers via Ring-Opening Condensation Polymerization of Cyclic Sulfite

環状サルファイトの開環縮合重合による

1,2-グリコシド型ポリマーの合成

**Sangeetha Shetty Srinivasa**

サンゲータ　シェティー　スウェニバサ

**Hokkaido University**

北海道大学

**2016**

# Contents

# Chapter 1

# General Introduction

## 1.1 Polysaccharides

A carbohydrate is a biological molecule consisting of carbon (C), hydrogen (H), and oxygen (O) atoms, usually with a hydrogen–oxygen atom ratio of 2:1. The term "polysaccharide" means polymeric carbohydrate joined together by glycosidic linkages. Polysaccharides are also called as glycans. They are structurally divided into linear and branched polymers. Polysaccharide exit as storage and structural materials in a living body. Figure 1.1 shows a matrix for the categorization of polysaccharides.

| | **Linear** | **Branched** |
|---|---|---|
| **Storage material** | Amylose<br>Curdlan | Amylopectin, Dextran<br>Glycogen |
| **Structural material** | Cellulose<br>Chitin, Chitosan | Hemicellulose<br>Arabinoxylan |

**Figure 1.1** categories of polysaccharides.

Plants make starch as their storage units, which is found in many plants such as potatoes, rice, wheat, and cereal grains, while animals make glycogen as an energy storage in the liver, muscle tissue, and brain. Glycogen acts as a fuel reserve. When blood sugars become low, the pancreas releases the

hormone *glucagon*, which travels to the liver and triggers the conversion of glycogen to glucose. This process can also be activated by adrenaline as a stress response.

Starch and glycogen consist of glucose as a repeating unit. Starch includes two polymers, amylose and amylopectin. Amylose is an unbranched chain of hundreds of glucose units, while amylopectin is a chain of thousands of units that is branched. The structure of amylopectin is very similar to that of glycogen, although glycogen includes protein at the polymer terminus. Amylose and amylopectin have α-glycosidic linkages without any β-linkage. The anomeric acetal bonds with α-stereochemistry can be easily cleaved, which makes glucose released.

In addition to the storage polysaccharides, structural polysaccharides with other structures are also found in a living body. The polymers give rigidity to cells. They are also comprised of saccharide units with β-anomeric linkages, whose cleavage is more difficult compared with that of α-linkage. Cellulose is a member of the structural polysaccharides, which helps to give plant walls their strength.

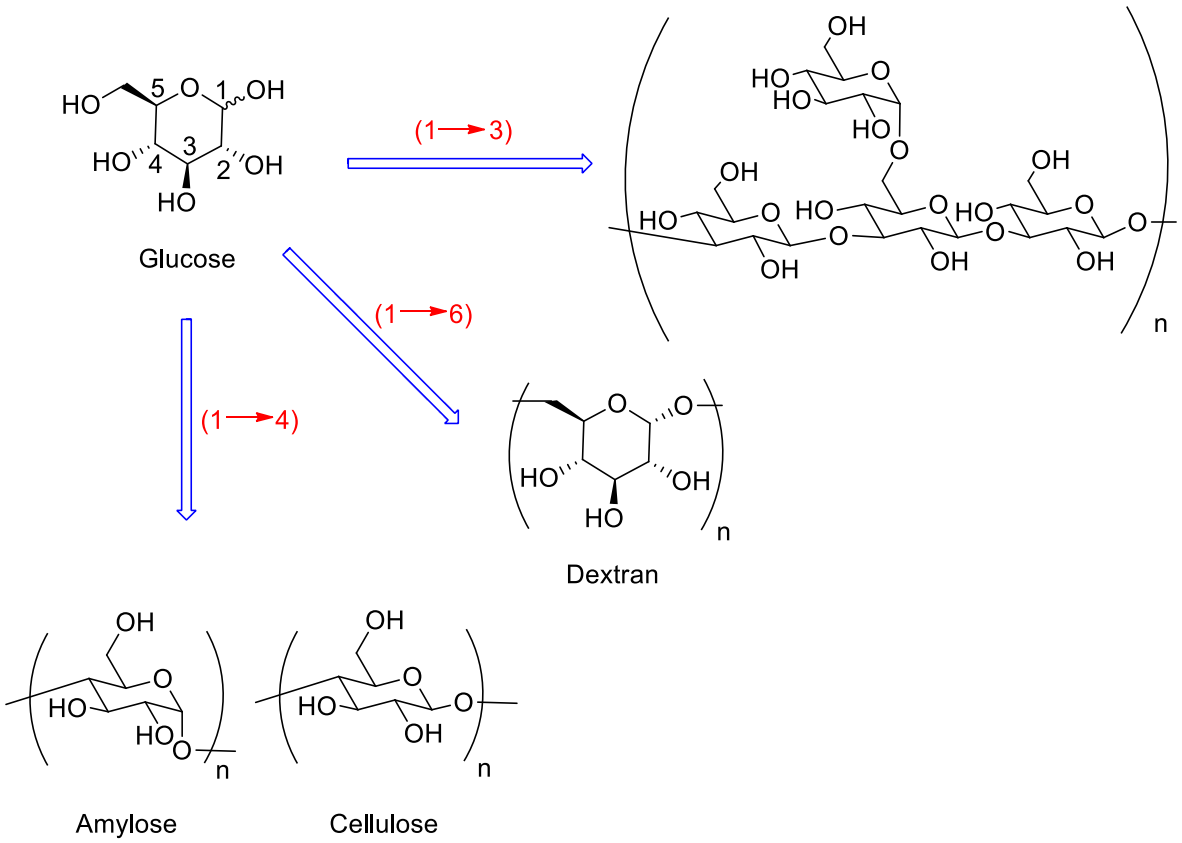


**Figure 1.2** Polysaccharides with (1→3), (1→4), and (1→6)-glycosidic linkages

Figure 1.2 shows the structures of polysaccharides consisting of glucose as a repeating unit. It is very interesting that the different position of glycosidic linkage for example (1→6) (dextran), (1→4) (amylose, cellulose, chitin, and chitosan), (1→3) (schizophyllan and lentinan) linkages provides different higher-order-structure and unique properties.

Together with the unique structures and activity of polysaccharides, the properties such as atoxicity, hydrophilicity, biocompatibility, multichirality, and multifunctionality confer the additional

importance to polysaccharides as valuable and renewable resources.[1] The chemical modification of polysaccharides is still underestimated regarding the properties of materials.

Wide variety of polymeric carbohydrates are produced by the living organisms.[2] For long years, the attention has been centered mainly on polysaccharides composed of sugar residues. Noncarbohydrate materials were found in polysaccharide preparations were in fact considered as an impurity. With the improvements in methods for isolation, purification, and characterization of high-molecular-weight natural compounds, it became evident that hybridization between carbohydrates and other constituents occurs widely in nature.

Recently, the research activities have increased in simple and abundant homopolysaccharides like cellulose, chitin, and amylose and less readily obtainable mucopolysaccharides, and polysaccharide moieties of glycoproteins,[3] glycopeptides, and lipopolysaccharides. In addition, the interests in polysaccharide biosynthesis[4] and analytical techniques have markedly increased.

Many natural polysaccharides and oligosaccharides participate in a variety of biochemical reactions *in vivo*. However, it is quite difficult to elucidate the mechanism of the biological activity of the polysaccharide itself, because of the complicated chemical structure of the natural saccharide chain and the existence of impurities.

## 1.2 Polysaccharides consisting of (1→4)-glycosidic bonds

### 1.2.1 Amylose

Amylose is a storage polysaccharide composed of an unbranched chain of D-glucose units, bound to each other through α-(1→4)-glycosidic bonds having one reducing end (Figure 1.3). Amylose is one of the two components of starch, making up approximately 20-30% of the structure. The other component is amylopectin, which makes up 70–80% of the structure, branched at every 20-35 glucose units via α-(1→6) linkage.

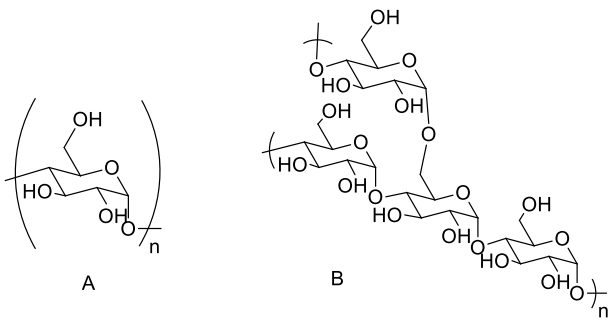


**Figure 1.3** Structures of amylose (A) and amylopectin (B)


Corn starch,
copied from free picture

The structural characteristics of amylose and amylopectin lead them to very different uses. For instance, amylopectin is easily digested in the body and is therefore a major source of dietary glucose. It also has several industrial uses because its highly branched nature makes it an excellent thickner and texturant. By contrast, amylose cannot be digested well in human body because its glucose chains tend to repack together even after cooking. Because of its tightly packed structure, amylose is an

important form of resistant starch. Amylose is isolated from plant components like corn starch,[5] cotton leaves,[6] potato starch, etc. Starch is made from both plant (potato phosphorylase) and animal (muscle phosphorylase) sources, by glycogen phosphorylase.

Amylose forms a left- handed helical structure with a chiral inner cavity.[7] The helical structure has been reported to be stabilized by a combination of inter-turn hydrogen bonding interactions at the 6-positions and a hydrophobic interaction of its main chain,[8] the introduction of hydrogen-bond functionalities at the 6-positions with respect to the amylose backbone is an important issue in the structural design for advanced functions such as chiral separation,[9] asymmetric catalysis,[10] and optical anisotropy.[11] Several amylose derivatives are known to behave as a host polymer for various compounds such as iodine[12] and linear organic molecules,[13] accompanied by intermolecular chirality transfer from amylose to achiral guest molecules.[14] Hydrophobic linear polymers also form inclusion complexes with amylose derivatives in water.[15]

A lot of functional materials exploiting amylose backbone have been reported to date. The most impressive work is a creation of chiral column reported by Prof. Okamoto and Prof. Yashima.[16] They reported that, the fully protected polymers by carbamates or esters are useful as chiral separation resins to recognize a pair of enantiomers, enabling the optical resolution of racemic compounds

.

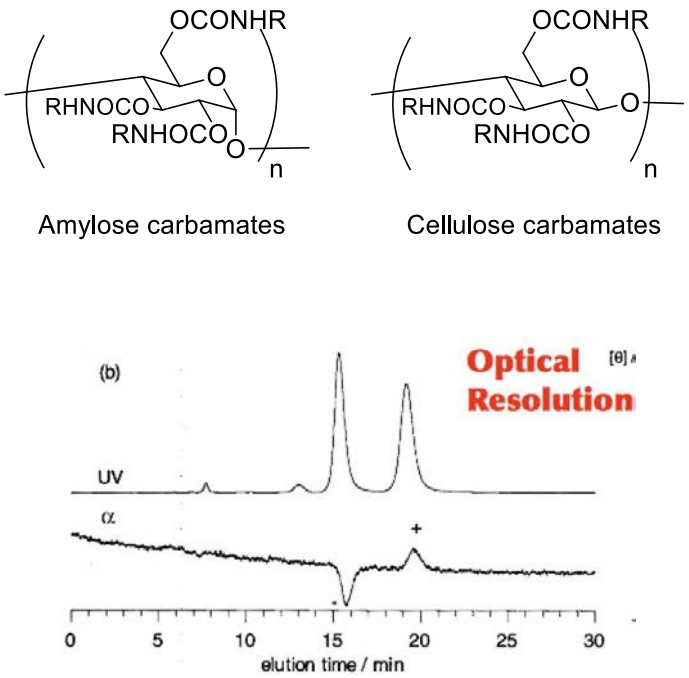


**Figure 1.4** Representative structures of chiral stationary phase in chiral column.

### 1.2.2 Cellulose

Cellulose is a structural polysaccharide consisting of repeated glucose units bonded together by β-(1→4) linkages (Figure 1.5). Wood is largely cellulose and lignin, while paper and cotton are nearly pure cellulose. It is the most abundant carbohydrate in nature. Humans and many animals lack an enzyme to break the β-linkages, so they do not digest cellulose. Certain animals such as termites can digest cellulose, because the bacteria possessing the enzyme are present in their gut. Cellulose is insoluble in water. It does not change color when mixed with iodine.

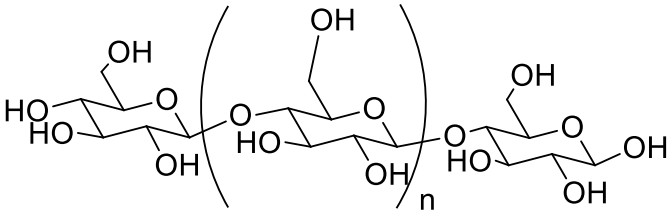

**Figure 1.5** Structure of cellulose

Cotton, one of cellulose source, copied from free picture

As for the synthesis of cellulose, Prof. Shoda has reported enzymatic synthesis of cellulose utilizing glycosyl fluoride via cellulase-catalyzed polymerization (Scheme 1.1).[17] The polymerization features perfect control of regioselectivity of glycosidation points and stereoselectivity on the anomeric centers.

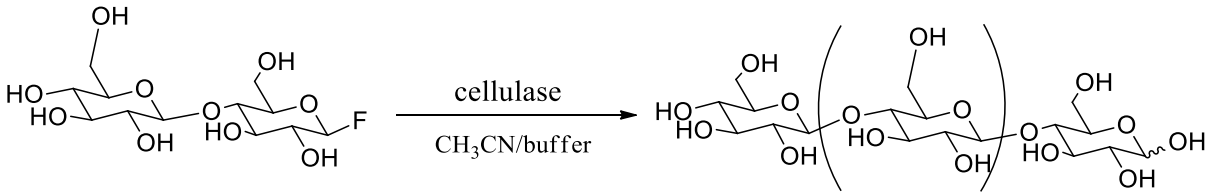


**Scheme 1.1** Enzymatic synthesis of cellulose.

Even though cellulose is the most abundant resource, its application become limited because of its insolubility. However the conversion or depolymerization of cellulose plays a very important role to make it usefull material for biomass conversion processes and equipment to produce fuels, power, heat, and value-added chemicals. Prof. Fukuoka and Prof. Kobayashi reported the catalytic degradation

method of cellulose to glucose and the catalytic transformation method of cellulose to its useful chemicals (Scheme 1.2). [18]

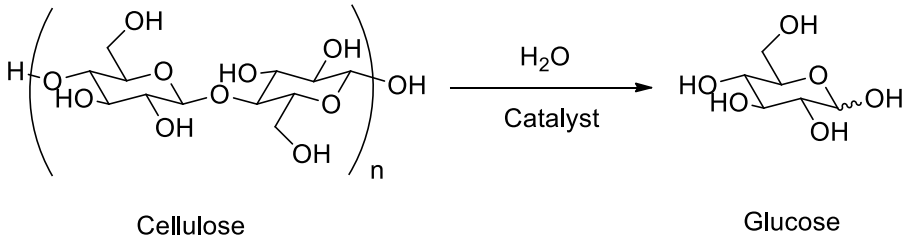


**Scheme 1.2** Hydrolysis of cellulose.[18c]

### 1.2.3 Chitin

Chitin is one of the naturally occurring polymers (Figure 1.6). It is a linear-chain polymer of *N*-acetyl glucosamine and the structural material of cellwall, for instance, fungal cell walls, insect and crustacean exoskeletons (e.g., crabs, lobsters, and shrimps), arthropods, mollusk radulas, and on the scales and other soft tissues of fish and lissamphibians.

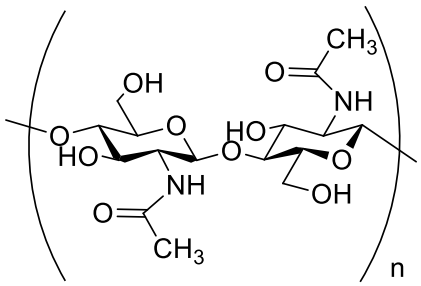


**Figure 1.6** Structure of chitin.

Shrimp, one of chitin and chitosan source, copied from free picture

It is bio-degradable in the natural environment. Chemically, chitin is closely related to chitosan (a more water-soluble derivative of chitin). Chitosan is the most important derivative of chitin, produced commercially by deacetylation of chitin. These are also closely related to cellulose. Both chitin and chitosan have unbranched chains consisting of glucosamine derivatives.

Natural marine chitin and chitin residues are the exclusive nutrient source for many marine bacteria, which use them efficiently as metabolic fuels. Microbial chitin utilization involves enzymatic breakdown of the biopolymer into short-chain chito-oligomers by secreted chitinases[18] and subsequent efficient internalization of the resultant chitosugars through specialized bacterial outer membrane proteins ("chitoporins").[19] Man-made chitin waste from seafood processing. On the other hand, it is a common starting material for production of commercial purified chitin by processes involving harsh chemical treatment. Both chitin and chitosan has been used in the application of electrochemical biosensors.[20] Many reserchers developed the synthetic route for the production of chitin derivatives. Kobayashi *et al.* reported the synthesis of artificial chitin. The method allows the production of the perfectly *N*-acetylated chitins without any damage to *N*-acetyl group (Scheme 1.3).[21]

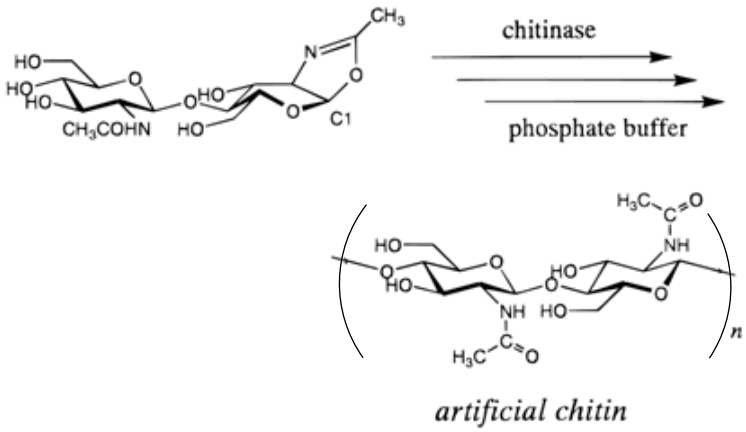


**Scheme 1.3** Synthesis of artificial chitin.

### 1.2.4 Chitosan

Chitosan is a linear polysaccharide composed of randomly distributed β-(1→4)-D-glucosamine (deacetylated unit) and *N*-acetyl-D-glucosamine (acetylated unit) (Figure 1.7). It is made by treating shrimp and other crustacean shells with sodium hydroxide and is more water-soluble. The solubility can be controlled by varying the chain length of the precursor material or the degree of chemical depolymerisation and the extent of deacetylation, which provides useful polymers for a broad range of chemical and physical applications.

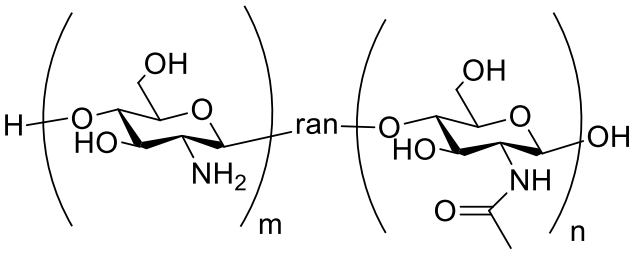


**Figure 1.7** Structure of chitosan.

One of chitin, chitosan Source, copied from free picture

Chitosan derivatives have practical applications in the form of films, gels, suspensions, microscopic threads, fibers, and also in the fields of biotechnology,[22] human[23] and veterinary medicine,[24] pharmacy, agriculture,[25] food engineering,[26] environmental technology,[27] and textile and paper industries.[28]

## 1.3 Polysaccharides consisting of (1→3)-glycosidic bonds

### 1.3.1 Schizophyllan

Schizophyllan is an extracellular polysaccharide composed of glucose units derived from the cell wall of the Schizophyllum commune mushroom (Figure 1.8). Schizophyllum species are known collectively as the "split gill" (schizo-) mushrooms. Schizophyllan is a proven biological defense modifier that nutritionally potentiates the immune response. The structure of beta-glucans with the 1,3-glycosidic bonds provides a better molecular "fit", translating into enhanced activation of the immune cascade and a more effective physiological response.

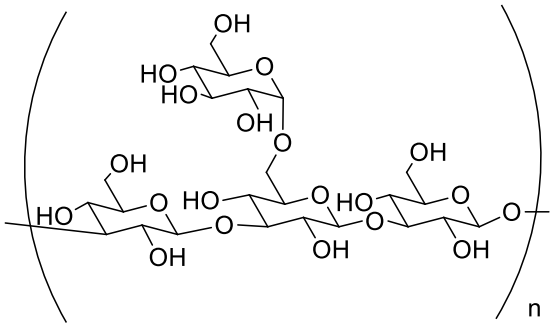


**Figure 1.8** Structure of schizophyllans.

The synthesis of 1,3-glycosidic polymer is achievable by cationic ring-opening polymerization of the corresponding anhydro sugar derivatives (Scheme 1.4). The stereoselectivity of ring-opening polymerization of oxetane is controllable by changing of catalyst. The low temperature reaction with $Tf_2O$ takes place through $S_N2$-type mechanism to give stereoregular glycopyranan at the inversion manner, while the high-temperature reaction affords the other polymer with retention of stereochemistry.

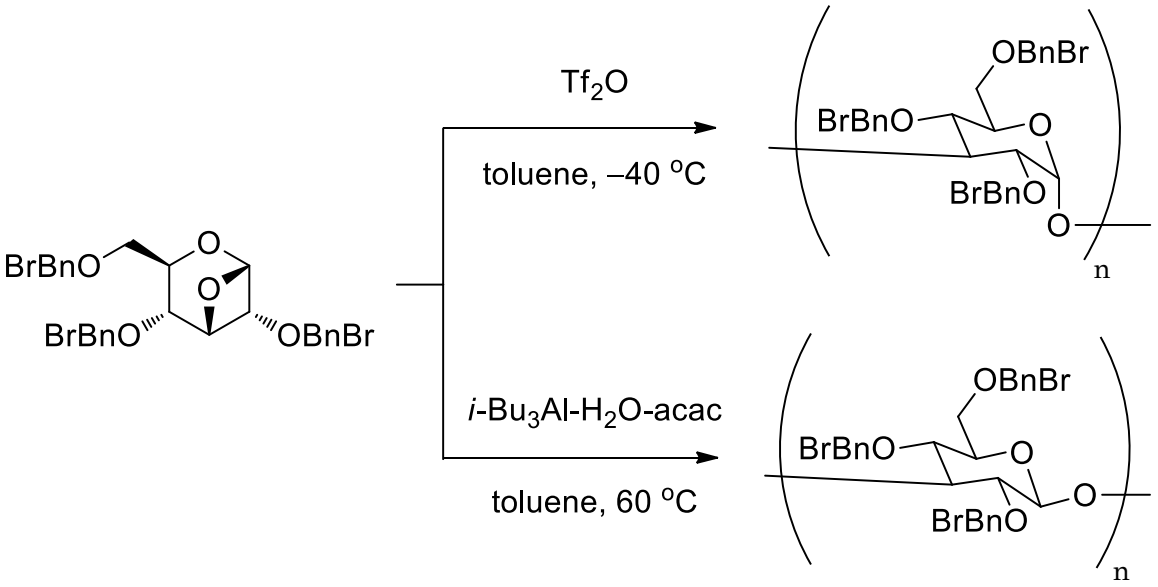


**Scheme 1.4** Synthesis of (1→3)-glucopyranans via ring-opening polymerization.

Since schizophyllan is bound by beta-1,3-glycosidic linkages in the main chain, it forms triple helix with chiral inner cavity, which works as a chiral host polymer for achiral guest molecules.[29] For example, it has been reported that oligothiophene guest adopts twisted conformation in the chiral inner cavity (Figure 1.9).

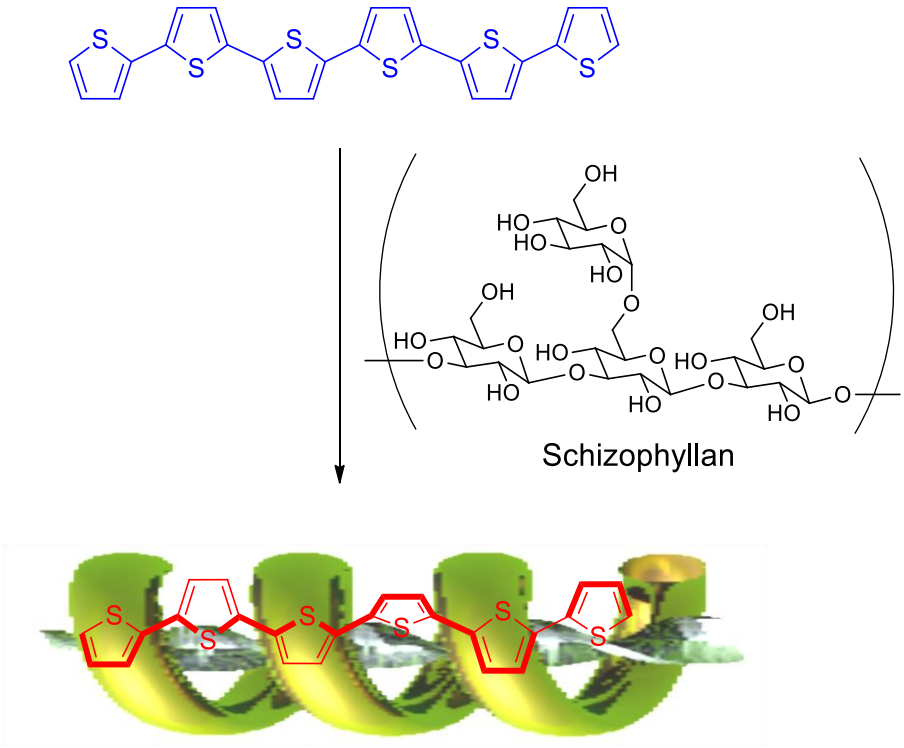


**Figure 1.9** Chirality-induced host for achiral guest

### 1.3.2 Lentinan

Lentinan is also a 1,3-glycosidic polymer (Figure 1.10), which is an intravenous anti-tumor polysaccharide isolated from the fruit body of shiitake mushroom. Lentinan has been approved as an adjuvant for stomach cancer in Japan since 1985. Lentinan is one of the host-mediated anti-cancer drugs which has been shown to affect host defense immune systems.

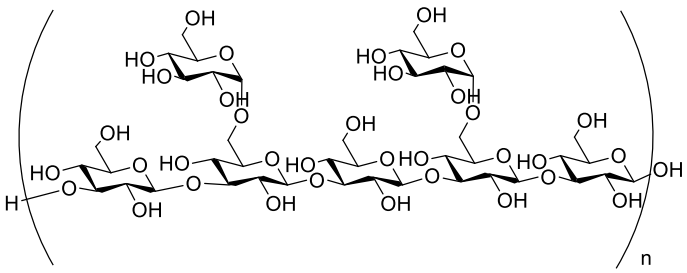

**Figure 1.10** Structure of lentinan

shiitake mushroom,
copied from free picture

## 1.4 Polysaccharides consisting of (1→6)-glycosidic bonds

### 1.4.1 Dextran

Dextran is a complex branched glucan composed of chains of varying lengths (from 3 to 2000 kilodaltons) (Figure 1.11). The straight chain consists of α-(1→6)-glycosidic linkages between glucose molecules, while branches begin from α-(1→3) linkages. Dextran is synthesized from sucrose by certain lactic acid bacteria, the best-known being *Leuconostoc mesenteroides* and *Streptococcus mutans*. It is used medicinally as an antithrombotic to reduce blood viscosity, and as a volume expander in hypovolaemia. Dextran was first discovered by Louis Pasteur as a microbial product in wine.

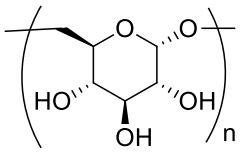

**Figure 1.11** Structure of dextran.

The syntheses of 1,6-glycosidic polymer is also achievable by cationic ring-opening polymerization of the corresponding anhydro sugar derivatives (Scheme 1.5). Dextran with α-(1→6)-glycosidic linkages is also preparable by the low-temperature ring-opening polymerization.

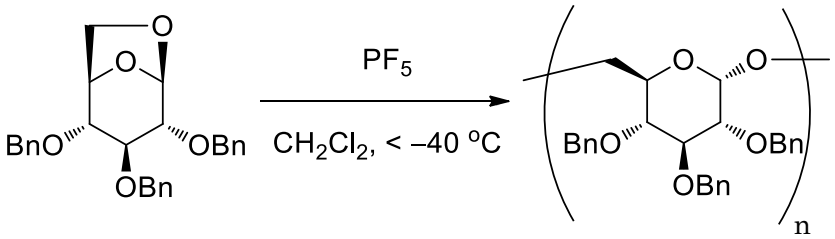


**Scheme 1.5** Synthesis of (1→6)-glucopyranans via ring-opening polymerization.

## 1.5 Polysaccharides consisting of (1→2)-glycosidic bond

### 1.5.1 (1→2)-β-D-Glucopyranan (nD-β-Glcp-(1-2))

Recently, the author is focussed on the studies of the remaining 1,2-glycosidic polymers. (1→2)-β-Glucopyranan is a natural polysaccharide (Figure 1.12), isolated from *Agrobacterium tumefaciens*. This polymer has glucose units linked together by (1→2)-glycosidic bonds, and has a rigid helical structure having side-chain hydroxyl groups with regulated orientations that may be useful in molecular integration.

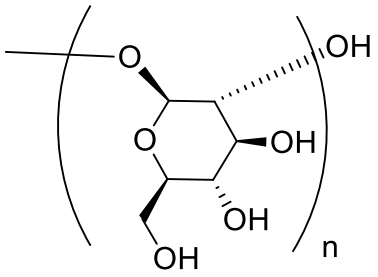


**Figure 1.12** Structure of (1→2)-β-D-glucopyranan

The soil bacteria can convert nitrogen gas to ammonia after becoming established inside root nodules of legumes. Therefore, legumes such as clover, beans, and soy can sufficiently grow without fertilizer. Although it is strongly expected that this polymer may play a significant role in the interaction between the bacteria and their host plant cell, the interaction mechanism is not clear at the present stage due to a lack of supplied amount of the polymer. The production is affected by external osmolarity, implying the capability to recognize ions.[30-32]

In spite of such interests, only one pioneering work has been reported as long as I know. The reaction is based on the cationic ring-opening polymerization of highly unstable glycal epoxide, which provides 1,2-glycosidic polymer in middle yield as an anomeric mixture (Scheme 1.6).[33,34] Therefore, I conceived that there still remains synthetic challenges of 1,2-glucopyranan as follows. First one is the development of practical monomer with improved stability and second is the control of polymerization degree. Third is the introduction of glycosylation reaction-active site to the one polymer terminus, which might be useful for a creation of hybridized materials. Final challenge is the

perfect control of stereochemistry on the anomeric centers.

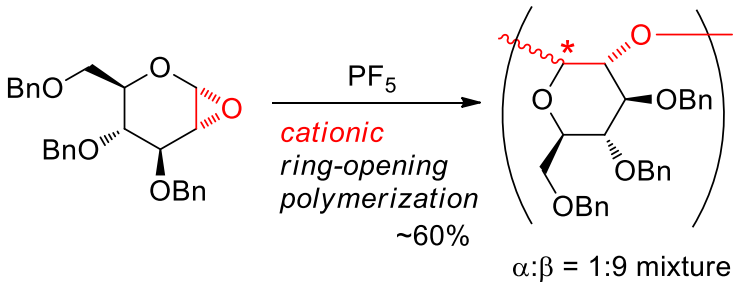


**Scheme 1.6** Synthesis of 1,2-glycosidic polymer from glycal epoxide by cationic ring-opening polymerization.

## 1.6 Glycosides

Glycosides are compounds containing a sugar unit and a non-sugar residue in the same molecule joined together by glocosidic bond at the anomeric carbon atom. The nonsugar component is called as an aglycone. The sugar component is called as a glycone. Glycosides can be linked by an *O*- (an *O-glycoside*), *N*-(a *glycosylamine*), *S*-(a *thioglycoside*), or *C*-(a *C-glycoside*) glycosidic bond. Enzymes can form and break the glycosidic bonds. The representative enzymes are glycoside hydrolases for cleavage and glycosyltransferases for the connection.

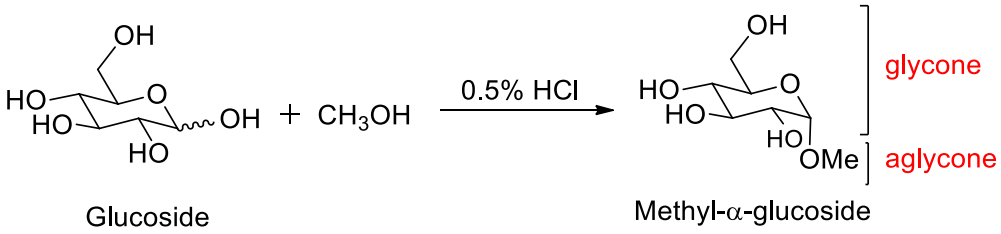


**Scheme 1.7** Methyl-α-glucoside

Most of glycosides are bioactive compounds. They comprise several important classes of compounds such as hormones, alkaloids, flavonoids, and antibiotics. Several natural glycosides have been used for long time as a folk medicine. It is generally accepted that glycosides are more water soluble than the respective aglycons. Attachment of sugar moiety into the aglycone molecule increases its hydrophilicity and reduces the toxicity. Attachment of polyglycoside to aglycone dramatically increases the solubility in water. The glycone moiety can govern the pharmacokinetic characteristics of glycosides, *e.g.*, circulation, elimination, and the concentrations in the body fluids. Modified hydrophilicity, however, influences mainly the membrane transport. Some compounds enter the cells just because of their "solubility" in the membrane components. Therefore, the solubility of glycoside is very important for the use as a drug when it enters the human body.

Glycosides play important roles in our lives. Many plants store medicinally important chemicals in the form of inactive glycosides. The aglycone contains the biochemically active properties of medical interest. For example, digitalis is a glycoside. The indigestion of the digitalis causes the heart to contract (pump) more forcefully. The glycone and aglycone portions can be chemically separated

by hydrolysis in the presence of acid because the acetal bond is labile under acidic condition. There are also numerous enzymes that can form and break the glycosidic bonds.

### 1.6.1 Monosaccharide- containing glycosides

An example for monosaccharide- containing glycoside is salicin, which is found in the genus *salix* (Figure 1.13). Salicin is converted in the body into salicylic acid, which is closely related to aspirin and has analgesic, antipyretic, and anti-inflammatory effects.

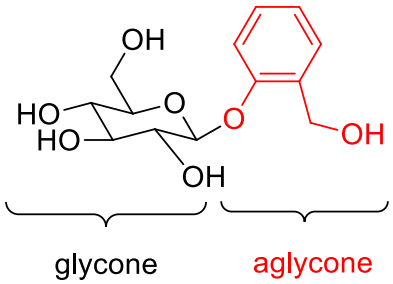


**Figure 1.13** Salicin, a glycoside related to aspirin**.**

Salicin is obtained from different species of *Salix* and *Populus*, but the principal commercial source is *Salix fragilis* (White Willow). Salicin has been used for many years as a remedy in the treatment of fever and rheumatism. It is now used as an analgesic-antipyretic and in case of periodic fever. It is better tolerated in the stomach than sodium salicylate, aspirin, and other antipyretics and anti-

inflammatory agents, which have largely displaced it in medical practice.

Salicin is hydrolyzed by the enzyme emulsin into saligenin (salicyl alcohol) and glucose. Acid hydrolysis of salicin gives glucose and a phenolic ether, saliretin. Oxidation of saligenin gives salicylic acid, and this accounts for the medicinal value of salicin.

### 1.6.2 Oligosaccharide containing glycosides

An example for oligosaccharide containing glycoside is glycyrrhizin (or glycyrrhizic acid or glycyrrhizinic acid), which has a disaccharide unit and the aglycone (Figure 1.14). The compound is chief sweet-tasting constituent of *Glycyrrhiza glabra* (liquorice) root, which is known that it is 50 times sweeter than sugar. It is a saponin and has been used as an emulsifier and gel-forming agent in foodstuff and cosmetics. Its aglycone is enoxolone and it has therefore been used as a prodrug for that compound, to prevent liver carcinogenesis in patients with chronic hepatitis C. The other examples for natural oligosaccharide-containing glycosides like cyanidine-3-*O*-sophoroside[35] and quercetin-3-*O*-sophoroside[36] are reported. These three compounds have (1→2)-glycosidic linkages in the glycone moieties. The effective synthetic method for the introduction of such oligosaccharide to the aglycone has been strongly urged from the view point of the creation of drug.

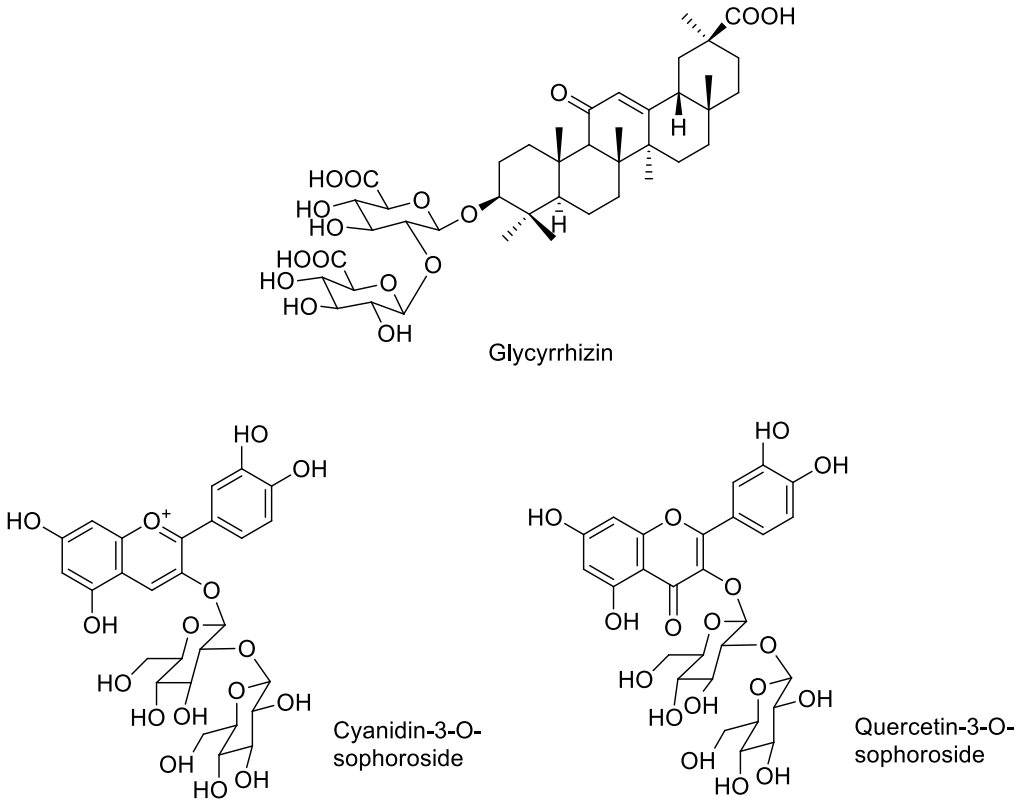


**Figure 1.14** oligosaccharide- containing glycosides**.**

## 1.7 Outline of this thesis

This thesis focuses on the development of new synthetic method for 1,2-glycosidic polymers via ring-opening condensation polymerization of a sugar-based cyclic sulfite. In this work, the author discovered the usefulness of the cyclic sulfite a new monomer, for the synthesis of (1→2)-linked polysaccharide. Cationic polymerization of the cyclic sulfite afforded (1→2)-D-glycopyranan along with the elimination of $SO_2$. The method was also applied to both grafting-onto and grafting-from polymerizations to give the corresponding glycosides. Scheme 1.8 shows the outline of this thesis.

In chapter 2, the author discusses the chemical stability and reactivity of cyclic sulfite as a monomer,

mainly by the comparison with those of glycal epoxide as a conventional monomer. Kinetic studies for the degradations evaluated the higher stability of the cyclic sulfite than the epoxide.

In chapter 3, the author describes the cationic polymerization of cyclic sulfite, where I achieved the synthesis of 1,2-glycosidic polymer bearing pentenoyl group at the polymer terminus.

In chapter 4, the author describes the new grafting reaction using cyclic sulfite from glycyrrhetic acid to give glycyrrhetic polyglycosides in one-pot. The reaction enables the rapid preparation of glycyrrhizin derivatives consisting of oligosaccharides with arbitrary polymerization degree.

In chapter 5, this thesis is summarized and concluded, and the future prospect of this work is described.

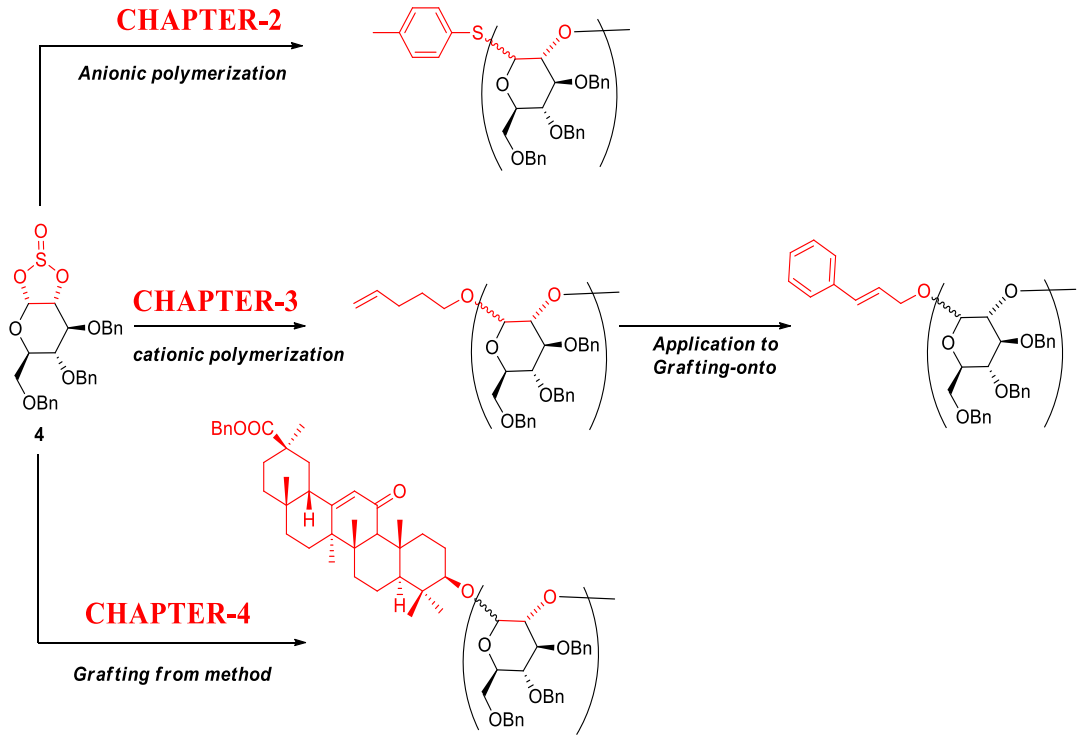


**Scheme 1.8** Outline of this thesis.

## References


1) Habibi, Y.; Lucia, L. A. Polysaccharide building blocks- A sustainable Approach to the Development of Renewable Biomaterials, First edition, **2012**.

2) Sharon, N. *Annu. Rev. Biochem.* **1966**, *35*, 485-520.

3) (a) Lloyd, A. G. *Postgrad. Med. J*. **1965**, *41*, 382-391.

4) (a) Ashwell, G. *Ann. Rev. Biochem*. **1964**, *33*, 101-138. (b) Neufeld, E. F.; Ginsburg, V. *Ann. Rev. Biochem.* **1965**, *34*, 297-312.

5) Taylor, T.C.; Lifschitz, D. *Journal of ACS*, **1932**, *54*, 1054-1063.

6) Chang, C.W. *Plant physiology*, **1979**, *64*, 833-836.

7) (a) Buleon, A.; Colonna, P.; Planchot, V.; Ball, S. *Int. J. Biologic. Macromol*. **1998**, *23*, 85-112. (b) Ohdan, K.; Fujii, K.; Yanase, M.; Takaha, T.; Kuriki, T. *Biocat. Biotrans*. **2006**, *24*, 77-81. (c) Buleon, A.; Veronese, G.; Putaux, J. –L. *Aust. J. Chem*. **2007**, *60*, 706-718. (d) Putseys, J. A.; Lamberts, L.; Delcour, J. A. *J. Cer. Sci*. **2010**, *51*, 238-247. (e) Perez, S.; Bertoft, E. *Starch/Starke* **2010**, *62*, 389-420.

8) Hui, Y.; Gai, Y. *Makromol. Chem*. **1988**, *189*, 1287-1294.

9) For a selected review, see: Yashima, E.; Yamamoto, C.; Okamoto, Y. *Synlett*. **1998**, 344-355.

10) For a selected report, see: Ikai, T.; Muro, M.; Maeda, K.; Kanoh, S. *React. Funct. Polym*. **2011**, *71*, 1055-1058.

11) For a selected review, see: Gray, D. G. *Carbohydr. Polym*. **1994**, *25*, 277-284.

12) (a) Rundle, R. E.; Baldwin, R. R. *J. Am. Chem. Soc*. **1943**, *65*, 554-558. (b) Rundle, R. E.; French, D. *J. Am. Chem. Soc*. **1943**, *65*, 558-561. (c) Rundle, R. E.; French, D. *J. Am. Chem. Soc*. **1943**, *65*, 1707-1710. (d) Rundle, R. E.; Edwards, F. C. *J. Am. Chem. Soc*. **1943**, *65*, 2200-2203. (e) Rundle, R. E. *J. Am. Chem. Soc*. **1947**, *69*, 1769-1772. (f) Wulff, G.; Steinert, A.; Holler, O. *Carbohydr. Res*. **1998**, *307*, 19-31. (g) Immel, S.; Lichtenthaler, F. W. *Starch/Starke* **2000**, *52*, 1-8.

13) (a) Hinrichs, W.; Buttner, G.; Steifa, M.; Betzel, C. –H.; Zabel, V.; Pfannemuller, B.; Saenger, W. *Science*, **1987**, *238*, 205-208. (b) Nimz, O.; Gessler, K.; Uson, I.; Sheldrick, G. M.; Saenger, W. *Carbohydr. Res*. **2004**, *339*, 1427-1437. (c) Sanji, T.; Kato, N.; Tanaka, M. *Org. Lett*. **2006**, *8*, 235-238. (d) Sanji, T.; Kato, N.; Tanaka, M. *Angew. Chem. Int. Ed*. **2009**, *48*, 1130-1132.

14) For a review indicating the concept and importance of organic-inorganic hybrid polymers (element-block polymers), see: Chujo, Y.; Tanaka, K. *Bull. Chem. Soc. Jpn*. **2015**, *88*, 633-643.

15) (a)Kadokawa, J.; Kaneko, Y.; Tagaya, H.; Chiba, K. *Chem. Commun.* **2001**, 449-450. (b) Kida, T.; Minabe, T.; Okabe, S.; Akashi, M. *Chem. Commun*. **2007**, 1559-1561. (c) Kaneko, Y.; Saito, Y.; Nakaya, A.; Kadokawa, J.; Tagaya, H. *Macromolecules* **2008**, *41*, 5665-5670. (d) Rachmawati, R.; Woortman, A. J. J.; Loos, K. *Boimacromolecules* **2013**, *14*, 575-583. (e) Kumar, K.; Woortman, A. J. J.; Loos, K. *Biomacromolecules* **2013**, *14*, 1955-1960. (f) Kadokawa, J.; Nomura, S.; Hatanaka, D.; Yamamoto, K. *Carbohydr. Polym*. **2013**, *98*, 611-617. (g) Star, A.; Steuerman, D. W.; Heath, J. R.; Stoddart, J. R. *Angew. Chem., Int. Ed.* **2002**,

*41*, 2508-2512. (h) Kim, O. –K., Je, J.; Baldwin, J. W.; Kooi, S.; Pehrsson, P. E.; Buckley, L. J. *J. Am. Chem. Soc.* **2003**, *125*, 4426-4427.

16) Yashima, E.; Yamamoto, C.; Okamoto, Y. *Synlett*, **1998**, *4*, 344-360.

17) Kobayashi, S.; Kashiwa, K.; Kawasaki, T.; Shoda, S. *J. Am. Chem. Soc.* **1991**, *113*, 3079-3084.

18) (a) Komanoya, T.; Kobayashi, H.; Hara, K.; Chun, W. –J.; Fukuoka, A. *Chem. Cat. Chem.* **2014**, *6*, 230-236. (b) Yabushita, M.; Kobayashi, H.; Fukuoka, A. *Applied Catalysis B: Environmental* **2014**, *145*, 1-9. (c) Kobayashi, H.; Kaiki, H.; Shrotri, A.; Techikawara, K.; Fukuoka, A. *Chem. Sci.* **2016**, *7*, 692-696.

19) (a) Suginta, W.; Chumjan, W.; Mahendran, K. R.; Janning, P.; Schulte, A.; Winterhalter, M. *PLoS One,* **2013**, *8*, e55126. (b) Meibom, K. L.; Li, X. B.; Nielsen, A. T.; Wu, C. Y.; Roseman, S.; Schoolnik, G. K. *Proc. Natl. Acad. Sci. U.S.A.*, **2004**, *101*, 2524-2529.

20) Suginta, W.; Khunkaewla, P.; Schulte, A. *Chem. Rev.*, **2013**, *113*, 5458−5479.

21) Kobayashi, S.; Kiyosada, T.; Shoda, S.-I. *J. Am. Chem. Soc*., **1996**, *118*, 13113-13114.

22) Guibal, E. *Prog. Polym. Sci*. **2005**, *30*, 71-109.

23) Alves, N. M; Mano, J. F. *Int. J. Biol. Macromol*. **2008**, *43*, 401-414.

24) Senel, S.; McClure, S. J. *Adv. Drug Delivery Rev*. **2004**, *56*, 1467-1480.

25) (a) Zhang, H. Y.; Li, R. P.; Liu, W. M. *Int. J. Mol. Sci*. **2011**, *12*, 917-934. (b) Badawy, M. E. I.; Rabea, E. I. *Int. J. Carbohydr. Chem*. **2011**, *2011*, 1-29.

26) Shahidi, F.; Vidana Arachchi, J. K.; Jeon, Y.-J. *Food Sci. Technol*. **1999**, *10*, 37-50.

27) Dutta, P. K.; Tripathi, S.; Mehrotra, G. K.; Dutta, J. *Food Chem*. **2009**, *114*, 1173-1182.

28) Balakrishnan, B.; Banerjee, R. *Chem. Rev*. **2011**, *111*, 4453-4474.

29) (a*)* Kong, F.; Schuerch, C. *Macromolecules*, **1984**, *17*, 983-989; (b) Ruckel, E. R.; Schuerch, C. *J. Org.Chem.*, **1966**, *31*, 2233-2239.

30) Sanji, T.; Kato, N.; Tanaka, M. *Org. Lett.*, **2006**, *8*, 235-238.

31) York, W. S.; McNeil, M.; Darvill, A. G.; Albersheim, P. *J. Bacteriol.* **1980**, *142*, 243-248.

32) Choma, A.; Komaniecka, I. *Acta Biochimica Polonica*, **2003**, *50*, 1273-1281.

33) Song, R. J.; Zhou, J. *J. Chromatogr. B*, **2015**, *995-996*, 8–14.

34) Sharkey, P. F.; Eby, R.; Schuerch, C. *Carbohydr. Res.* **1981**, *96*, 223-229.

35) Chaturvedula, V. S. P.; Yu, O.; Mao, G. *Journal of pharmacy*, **2014**, *4*, 44-48.

36) Wu, X.; Gu, L.; Prior, R. L.; McKay, S. *J. Agric. Food Chem*. **2004**, *52*, 7846–7856

# Chapter 2

# Synthesis, Kinetic Study and Anionic Ring-Opening Condensation Polymerization of Cyclic Sulfite

## 2.1 Introduction

Polysaccharide is a representative class of biopolymers, which consists of sugars with regularly-aligned stereogenic centers as a monomeric unit.[1] The polysaccharide scaffolds are expected to be an indispensable motif for advanced materials such as chiral separation materials,[2] asymmetric catalysts,[3] and optical materials.[4] To date, the synthetic studies of polysaccharides have been extensively investigated to disclose several fruitful methods for a part of polysaccharides such as cationic ring-opening polymerization of anhydro-sugars[5] and enzymatic polymerizations using non-protected sugars.[6] Branched and cyclic (1→2)-β-D-glucopyranan (nD-β-Glcp-(1-2)) derivatives are natural polysaccharides isolated from *Agrobacterium* and *Sinorhizobium* genera to cause crown gall disease of dicotyledonous plants.[7,8] The bacterium exhibits nitrogen gas-fixing ability to provide ammonia to the plants. Although it is invoked that nD-β-Glcp-(1-2) derivatives would play an important role to interact between the bacterium and the plant hosts, the interaction mechanism has not been systematically unveiled, urging the chemical synthesis of the structural analogues with a variety of molecular weights and different stereocenters. Meanwhile, the polymer skeleton of nD-β-Glcp-(1-2) can be regarded as a helical polyoxyethylene (PEO) possessing hydroxyl groups as the side chain functionalities. Because PEO skeleton recognizes metal cations to change the higher-order structure,[9] nD-β-Glcp-(1-2) might be a unique asymmetric scaffold available for molecular integration to produce stimuli-responsive optically active materials.

In spite of such interests of nD-β-Glcp-(1-2), the synthetic method has not been sufficiently

developed yet; only the synthesis leading to broad polydispersity indices via cationic polymerization of highly unstable glycal epoxide has been reported, where the anomeric carbons of the polymer have ~95% β-configurations.[10] The stereo-selectivity at the anomeric centers depends on three reasons: (i) The polymerization would proceed via an intermediary formation of oxocarbenium cation and (ii) the acetal linkages in the kinetically obtained polymer would undergo further epimerization to give the thermally stable polymer during the acidic condition, which make the stereo-control difficult. In addition, (iii) the $S_N2$ reaction-based anionic polymerization of the glycal epoxide was infeasible, which seems to provide the stereo-regulated polymer, because the epoxide was highly unstable at the temperature required on the anionic polymerization. Therefore, I planned the development of a new synthetic method of nD-β-Glcp-(1-2) including the following improvements; (i) the use of practical monomer with improved stability, (ii) the controls of polymerization degree and anomeric stereochemistry, and (iii) the introduction of glycosydation-active site to the polymer terminus that might be useful for a creation of the cyclic polymers. Thus I focus on the use of shelf-stable 1,2-*O*-sulfinyl glucopyranose (Scheme 2.1) as a substitute of the unstable epoxy monomer, considering the reports concerning stereospecific introductions of azide,[11] diethyloxoglutarate,[12] and cyanide[13] to the anomeric center of the cyclic sulfite[14].

Schematic illustration for the synthesis of nD-β-Glcp-(1-2) is shown in Scheme 2.1. The thiolate initiator with high nucleophilicity would attack to the anomeric center to give monomeric alkoxide **I** accompanying with a removal of $SO_2$. Subsequent nucleophilic addition of **I** to the other monomer

would give the corresponding dimer **II** at the stereo-selective manner attributed to an $S_N2$ reaction. The successive propagation would afford structure-defined nD-β-Glcp-(1-2) skeleton with thioglycoside terminus, which could be easily converted to the corresponding hemi-acetal to give the natural polymer.[15] The thioglycoside could be useful for glycosidation reaction[16] to connect nD-β-Glcp-(1-2) skeleton to aglycons and to graft nD-β-Glcp-(1-2) onto the other polymers (discussed in chapter 4). Moreover, the cyclization reaction under highly diluted condition might also enable the access to cyclic nD-β-Glcp-(1-2) derivative as a natural product.[8] In this chapter, I describe the synthesis, kinetic study and anionic ring-opening polymerization of the cyclic sulfite.

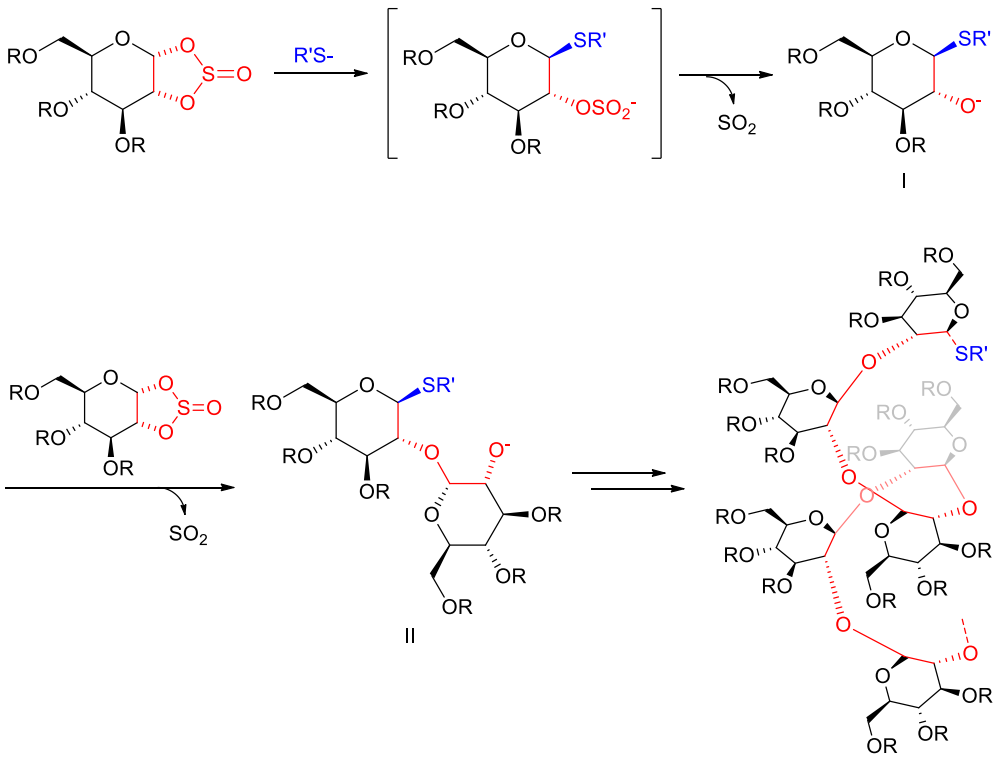


**Scheme 2.1** Schematic illustration for a thiolate-initiated anionic ring-opening polymerization of cyclic sulfite to prepare nD-β-Glcp-(1→2) framework.

## 2.2 Results and Discussion

Cyclic sulfite **4** was prepared from tribenzyl-D-glycal **1** according to the literature with a slight modification (Scheme 2.2).[10-12] Glycal **1** was treated with Oxone® to give an epoxide **2** with small amount of impurities[18]. The purification of **2** was quite difficult due to the unstability of **2**. Epoxide **2** was exposed to silica gel in ethyl acetate (EtOAc) to give a diol **3** as an anomeric mixture. A formation of cyclic sulfite **4** was performed by a reaction of **3** with freshly prepared thionyl diimidazole in tetrahydrofuran (THF) at room temperature for 30 minutes to give a mixture of two products. From the $^1$H NMR spectrum and the literature, it turned out that the products are an *endo/exo*-mixture on the sulfur atom and both compounds are α-anomers.

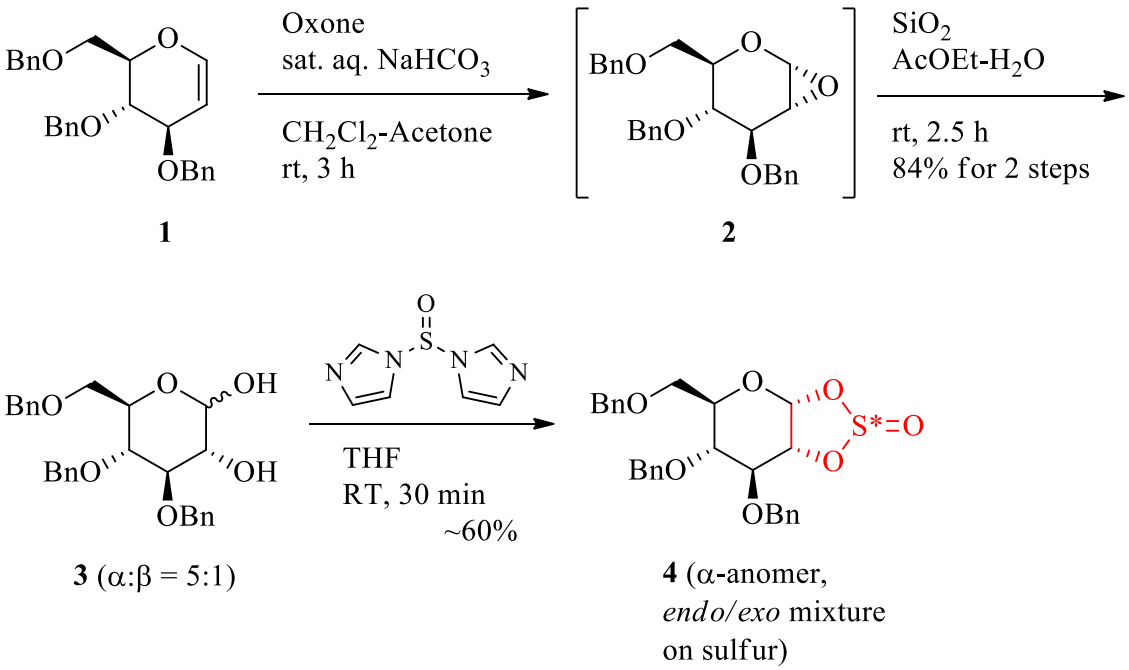


**Scheme 2.2** Synthesis of epoxide **2** and cyclic sulfite **4**.

At first I investigated the usefullness of cyclic sulfite over glycal epoxide by a kinetic studies.[19] Through the measurements of $^1$H NMR spectra I calculated the thermodynamic parameters for both glycal epoxide and cyclic sulfite discussed below.

**Determination of kinetic parameters for the degradation of cyclic sulfite and glycal epoxide.**

**Degradation of glucal cyclic sulfite 4 and epoxide 2 in $CDCl_3$.**

Cyclic sulfite **4** or epoxide **2** (0.01-0.02 mg) was dissolved in $CDCl_3$ (0.60 mL) in an NMR tube and the solution was heated at defined temperatures (293.15 K, 313.15 K, and 333.15 K). The $^1$H NMR spectra were measured after the defined time (Figure 2.4 & 2.5, see page 53). For the cyclic sulfite **4**, the signals corresponding to the anomeric protons at 6.3 and 5.9 ppm progressively decreased and the other peaks changed the shapes along with the degradation of **4**. In the case of epoxide **2**, the anomeric signal at 5.3 ppm decreased faster than that of **4**. These phenomena suggest the chemical stability of **4** is higher than that of **2**. From the integral ratio between the anomeric proton signals and the other aliphatic proton signals**,** the conversion [**4**]/[**4**]$_0$ was determined.

**Table 1.** Kinetic analysis for degradation of **4**.[a]

| 293.15 K | | 313.15 K | | 333.15 K | |
|---|---|---|---|---|---|
| Time /h | [**4**]/[**4**]$_0$ | Time /h | [**4**]/[**4**]$_0$ | Time /h | [**4**]/[**4**]$_0$ |
| 3 | 0.984 | 3 | 0.987 | 1 | 0.796 |
| 7 | 0.968 | 7 | 0.976 | 4 | 0.756 |
| 21 | 0.967 | 21 | 0.955 | 6 | 0.755 |
| 25 | 0.962 | 25 | 0.871 | 7 | 0.559 |

[a][**4**]$_0$ = 0.992.

**Table 2.** Kinetic analysis for degradation of **2**.[a]

| 293.15 K | | 313.15 K | | 333.15 K | |
|---|---|---|---|---|---|
| Time /h | [**2**]/[**2**]$_0$ | Time /h | [**2**]/[**2**]$_0$ | Time /h | [**2**]/[**2**]$_0$ |
| 1 | 0.860 | 1 | 0.818 | 1 | 0.823 |
| 2 | 0.828 | 2 | 0.806 | 2 | 0.789 |
| 3 | 0.810 | 3 | 0.800 | 3 | 0.749 |
| 4 | 0.814 | 4 | 0.755 | 4 | 0.734 |
| 5 | 0.803 | 5 | 0.743 | 5 | 0.712 |
| 6 | 0.800 | 6 | 0.748 | 6 | 0.687 |
| 7 | 0.804 | 7 | 0.738 | 7 | 0.659 |
| 25 | 0.789 | 25 | 0.660 | 25 | 0.341 |
| 27 | 0.788 | 27 | 0.639 | 27 | 0.301 |
| 29 | 0.773 | 29 | 0.629 | 29 | 0.242 |
| 71 | 0.747 | 71 | 0.457 | 71 | –[b] |
| 101 | 0.746 | 101 | 0.424 | 101 | –[b] |

[a][**2**]$_0$ = 0.864. [b]Not determined.

Assuming that the degradation reaction obeyed the first-order kinetics, the reaction rate is described with the following equation:

$$-d[\mathbf{4}]/dt = -k_4[\mathbf{4}] \quad (1)$$

It was converted to equation (2);

$$ln\,[\mathbf{4}]/[\mathbf{4}]_0 = -k_4 t \quad (2)$$

In a similar way, the conversion $[\mathbf{2}]/[\mathbf{2}]_0$ was also determined. If the degradation reaction also obeyed the first-order kinetics, the reaction rate would be described with the following equation:

$$-d[\mathbf{2}]/dt = -k_2[\mathbf{2}] \quad (3)$$

It was also converted to equation (4):

$$ln[\mathbf{2}]/[\mathbf{2}]_0 = -k_2 t \quad (4)$$

Time-course plots of **4** for 293.15 K were drawn to determine the half-life period $\tau_4$ of **4**. The plots were fit by a line and the slope ($-k_4$) was calculated by least squares approximation to determine $5.82 \times 10^{-8}$ $sec^{-1}$. The half-life period $\tau_4$ of **4** was estimated from the following equation to be 3307 h:

$$\tau_4 = ln2/\,k_4 \quad (5)$$

In a similar way, time-course plots of **2** for 293.15 K were drawn to determine the half-life period $\tau_2$ of **2**. The plots were fit by a line and the slope ($-k_2$) was calculated by least squares approximation to determine $0.30 \times 10^{-6}$ $sec^{-1}$. The half-life period $\tau_2$ of **2** was estimated from the following equation to be 497 h:

$$\tau_3 = ln2/\,k_2 \quad (6)$$

In the same way, $k_4$, $k_2$, $\tau_4$, and $\tau_2$ were estimated for different temperatures 313.15 and 333.15 K.

**Table S3.** Kinetic parameters for degradation of **4**.

| temp. /K | $k_4$ /sec$^{-1}$ | $\tau_4$ /h |
|---|---|---|
| 293.15 | $5.82 \times 10^{-8}$ | 3307.4 |
| 313.15 | $0.80 \times 10^{-6}$ | 224.2 |
| 333.15 | $0.45 \times 10^{-5}$ | 42.7 |

**Table S4.** Kinetic parameters for degradation of **2**.

| temp. /K | $K_2$ /sec$^{-1}$ | $\tau_2$ /h |
|---|---|---|
| 293.15 | $0.30 \times 10^{-6}$ | 497.3 |
| 313.15 | $0.29 \times 10^{-5}$ | 66.1 |
| 333.15 | $1.40 \times 10^{-5}$ | 13.6 |

**Evaluation of activation energy for degradation.**

The activation energy for degradation was determined according to the following equation;

$$k = A\exp(-E/RT) \qquad (7)$$

It was converted to Arrhenius equation (5);

$$\ln k = -E/RT + \ln A \qquad (8)$$

$k$: dissociation kinetic constant

E: activation energy

R: gas constant (8.31 $m^2$ kg $s^{-2}$ $K^{-1}mol^{-1}$)

T: absolute temperature

A: frequency factor of Arrhenius equation

Inverse of temperature was plotted against *ln*k to determine the activation energy $E_4$. The plots for **4** were fit by a line and the slope ($-E_4/R$) was calculated by least squares approximation to determine $-10.6 \times 10^3$, which give the value of $E_4$ as 88 kJ/mol. The plots for **2** were fit by a line and the slope ($-E_2/R$) was calculated by least squares approximation to determine $-9.4 \times 10^3$, which give the value of $E_4$ as 78 kJ/mol.

**Table 2.5** Analysis of Arrhenius plots for degradation of **4**.

| T (K) | 1/T | ln $k_4$ |
|---|---|---|
| 293.15 | 0.003411 | - 16.6591 |
| 313.15 | 0.003193 | - 14.0386 |
| 333.15 | 0.003002 | - 12.3114 |

**Table 2.6** Analysis of Arrhenius plots for degradation of **2**.

| T (K) | 1/T | ln $k_2$ |
|---|---|---|
| 293.15 | 0.003411 | - 15.0195 |
| 313.15 | 0.003193 | - 12.7508 |
| 333.15 | 0.003002 | - 11.1765 |

**Evaluation of Gibbs' activation free energy, activation entropy, and activation enthalpy for degradation**

Gibbs' activation free energy for degradation was determined according to Eyring equation (9);

$$\Delta G^{\ddagger} = -RT\ln(k\,h/Tk_{B}) \quad (9)$$

$\Delta G^{\ddagger}$ : Gibbs' activation free energy

R: gas constant (8.31 $m^2\ kg{\cdot}s^{-2}\ K^{-1}\ mol^{-1}$)

T: absolute temperature

*k*: degradation kinetic constant

h: Plank constant ($6.63 \times 10^{-34}\ m^2 kg{\cdot}s^{-1}$)

$k_B$: Boltzmann constant ($1.38 \times 10^{-23}\ m^2\ kg{\cdot}s^{-2}K^{-1}$)

**Table S7.** Gibbs' activation free energy for degradation of **4**.

| temp. /K | $\Delta G^{\ddagger}_4$ (kJ/mol) |
|---|---|
| 293.15 | –112.300 |
| 313.15 | –113.314 |
| 333.15 | –115.940 |

**Table S8.** Gibbs' activation free energy for degradation of **2**.

| temp. /K | $\Delta G^{\ddagger}_2$ (kJ/mol) |
|---|---|
| 293.15 | −108.305 |
| 313.15 | −109.962 |
| 333.15 | −112.798 |

Eyring equation (9) was converted to following equation (10);

$$\ln (k/T) = \ln k_B / h + \Delta S^{\ddagger} / R - \Delta H^{\ddagger} / RT \qquad (10)$$

$\Delta S^{\ddagger}$ : activation entropy

$\Delta H^{\ddagger}$ : activation enthalpy

Inverse of temperature was plotted against $ln(k_4/T)$ to determine the activation entropy ($\Delta S^{\ddagger}_4$) and enthalpy ($\Delta H^{\ddagger}_4$) for **4**. The plots were fit by a line and the slope ($-\Delta H^{\ddagger}/R$) was calculated by least squares approximation to determine $-10.3 \times 10^3$, which gave the value of $\Delta H^{\ddagger}_4$ as 86 kJ/mol, while the intercept [$ln(k_B/h) + \Delta S^{\ddagger}/R$] was also calculated by least squares approximation to determine 13.05, which gave the value of $\Delta S^{\ddagger}_4$ as −31.5 J/K·mol.

In a similar way, the plots for **2** were fit by a line to give the value of slope to be $-9.1 \times 10^3$, which gave the value of $\Delta H^{\ddagger}_2$ as 75 kJ/mol. The intercept was 10.4, which gave the value of $\Delta S^{\ddagger}_2$ as −53.7 J/K·mol.

**Table S9.** Analysis of Eyring plots for degradation of **4**.

| temp. /K | 1/T | $lnk_4$ |
|---|---|---|
| 293.15 | 0.003411 | -22.3459 |
| 313.15 | 0.003193 | -19.7853 |
| 333.15 | 0.003002 | -18.1199 |

**Table S10.** Analysis of Eyring plots for degradation of **2**.

| temp. /K | 1/T | $lnk_2$ |
|---|---|---|
| 293.15 | 0.003411 | -20.7002 |
| 313.15 | 0.003193 | -18.4975 |
| 333.15 | 0.003002 | -16.9850 |

**Table S11.** Activation energy, activation entropy, and activation enthalpy for degradation.

| Compound | Activation energy ($\Delta G^{\ddagger}$) / kJ/mol | Activation entropy ($\Delta S^{\ddagger}$) / J/K·mol | Activation enthalpy ($\Delta H^{\ddagger}$) / kJ/mol |
|---|---|---|---|
| Cyclic sulfite **4** | 88 | –31 | 86 |
| Epoxide **2** | 78 | –53 | 75 |

**Anionic polymerization of cyclic sulfite**

Prior to the synthesis of nD-β-Glcp-(1-2), I investigated the synthesis of thioglycoside **5** as a monomeric unit in order to confirm a regio- and stereo-selectivity of nucleophilic addition of thiolate to the cyclic sulfite. Because the sulfite inherently has two reactive carbon centers, I investigated the reactivity using excess amount of potasium thiolate. As a result, the reaction of cyclic sulfite with 200 mol% of TolSK in DMF proceeded selectively to give thioglycoside **5**, along with a formation of hemi-

acetal degraded by humidity.

The structure of **5** was a β-thioglycoside as a single isomer, which was clearly evidenced by a big coupling constant between H-1 and H-2 protons to suggest the structure of 1,2-*trans*-substituents. I also confirmed a generation of alcohol at the 2 position by a removal of $SO_2$ group, which was determined by the IR spectrum. The structure of **5** clearly indicates a regio-selective addition to the anomeric center bearing weakened C–$OSO_2$ bond caused by a negative hyperconjugation to the oxygen of pyran, a stereo-selective reaction attributed to an $S_N2$ reaction, and efficient removal of $SO_2$ to generate the corresponding alkoxide as a propagation terminus, supporting the applicability of the nucleophilic reaction to polymerization reaction of cyclic sulfite. According to the model reaction condition, I investigated the polymerization of cyclic sulfite using 10 mol% of thiolate initiator (Scheme 2.4). The results are summarized in Table 2.12.

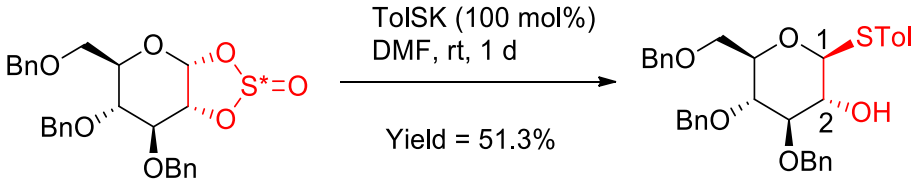


**4** **5**

**Scheme 2.3** Schematic illustration for synthesis of unit model

The polymerization using 10 mol% of initiator in the presence of drierite in DMF was performed at 100 - 120 °C. The product was purified by reperecipitation by hexane. But polymer is contaminated

by polymeric sulfur appeared as a brown gummy solid after the reaction, and found difficult to remove due to its gummy nature. The formation of gummy polymeric sulpfur implying the elimination of $SO_2$.

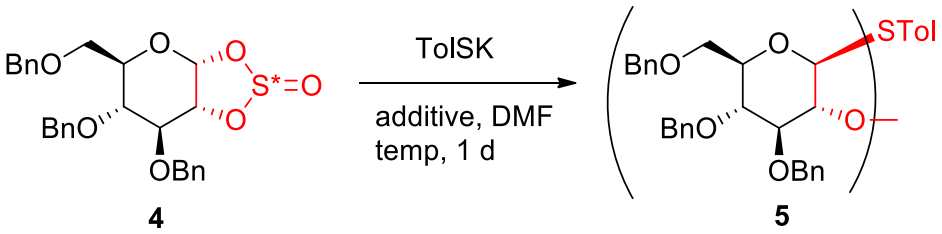


**Scheme 2.4** Scheme of anionic polymerization

**Table 2.12** Results of anionic polymerization

| entry | initiator amount (mol%) | additive | temp (°C) | hexane-insoluble yield (%) | $M_n$[a] | $M_w/M_n$[a] | hexane-soluble yield (%) |
|---|---|---|---|---|---|---|---|
| 1 | 10 | - | 100 | 11 | 990 | 4.1 | 34 |
| 2 | 10 | MS 4A | 100 | 58 | 510 | 1.5 | 29 |
| 3 | 10 | $CaSO_4$ | 100 | 85 | 730 | 2.5 | 19 |
| 4 | 10 | $CaSO_4$ | 80 | 63 | 780 | 1.5 | 25 |
| 5 | 10 | $CaSO_4$ | 120 | 55 | 890 | 3.2 | 9 |
| 6 | 10 | $CaSO_4$ | 140 | 44 | 9000 | 2.0 | 36 |
| 7 | 5 | $CaSO_4$ | 120 | 46 | 1200 | 4.0 | 6 |

[a] Estimated by SEC analyses on the basis of polystyrene standards.

The obtained polymer and unimer was analysed by $^1$H NMR, IR, and MALDI–TOF mass spectra and elemental analysis. The $^1$H NMR spectrum of polymer clearly supported the absence of

characteristic signals of cyclic sulfite at around 6.4 ppm. It was also found that the spectrum of polymer is in a good agreement with that of **5**, implying the formation of nD-β-Glcp(1,2) skeleton.

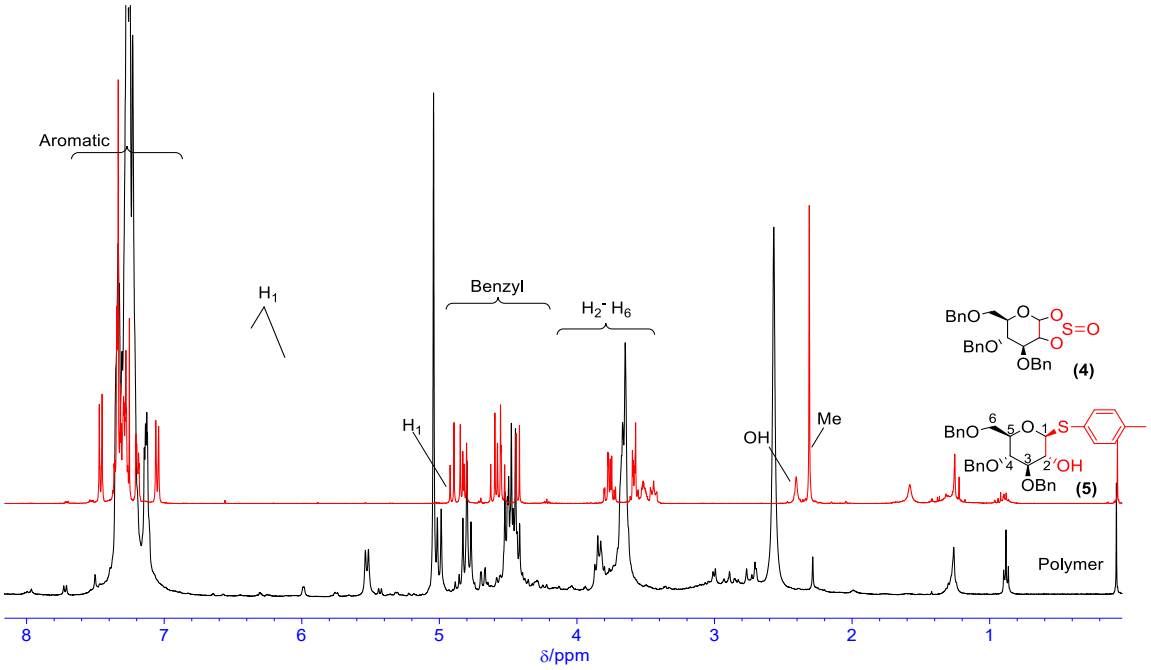


**Figure 2.1** $^{1}$H NMR spectra of **4**, **5** and polymer (entry-5) (400 MHz, $CDCl_3$, r.t.).

The IR spectra of cyclic sulfite and polymer is shown below. The IR spectrum of polymer clearly indicates the decrease in the characteristic absorption peak attributed to cyclic sulfite, suggesting that the polymer mainly consisting of polyether linkages. The remained small peak may be corresponds to some other sulfur containing impurities or remained $CaSO_4$ which I used as a dehydrator for the reaction.

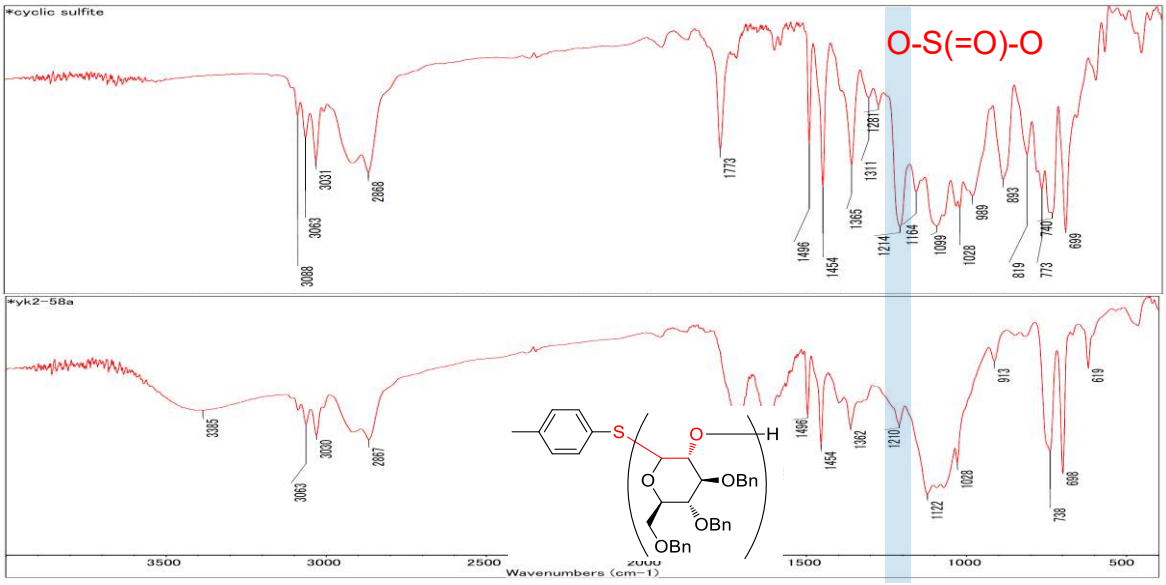


**Figure 2.2** IR spectra of cyclic sulfite and polymer (entry-5).

I also measured the MALDI–TOF MS spectrum of polymer. I found that the plural peaks in the spectrum were observed as peaks with even intervals corresponding to the monomeric unit and the observed peak values are in good accordance with those of expected values, strongly supporting that the sulfide-terminated desired polyether was formed.

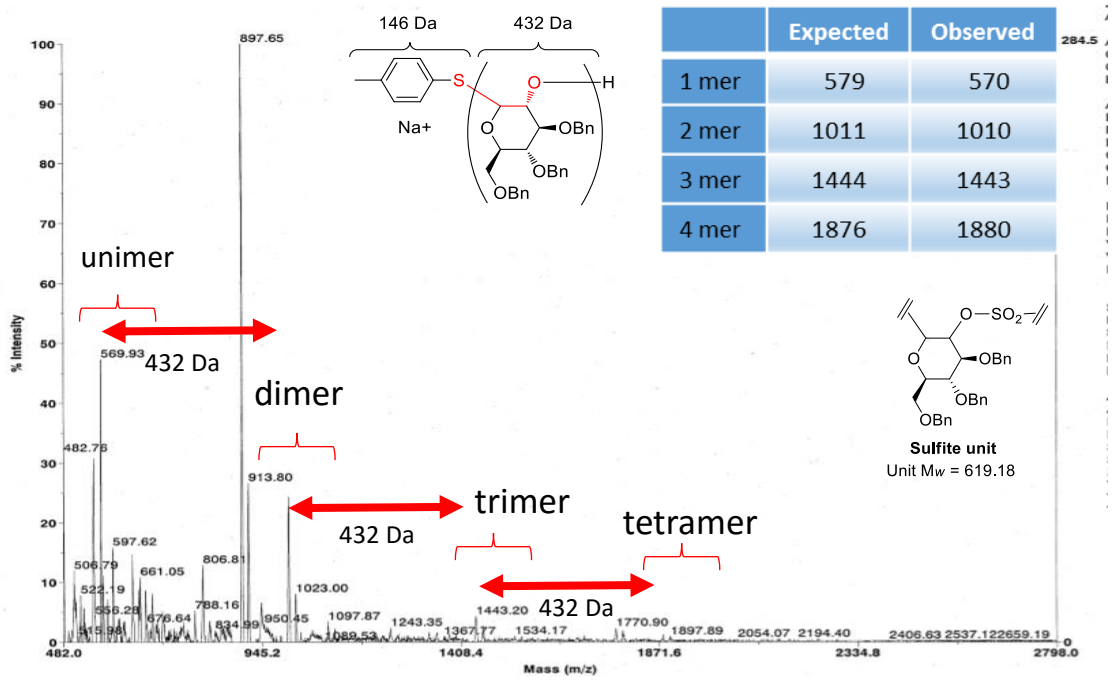


| | Expected | Observed |
|---|---|---|
| 1 mer | 579 | 570 |
| 2 mer | 1011 | 1010 |
| 3 mer | 1444 | 1443 |
| 4 mer | 1876 | 1880 |

**Figure 2.3** MALDI–TOF MS (matrix: CHCα) of polymer prepared at 120 °C

Despite of such agreements of spectral data with those of theoretical values, the elemental analysis data of the polymer was largely different from those for the proposed structure (calculated for nD-β-Glcp(1-2) is C= 74.98%, H= 6.53%, O= 18.50%, found (polymer entry 5): C= 61.03%, H= 6.23%, S= 4.69%). The observed value was much closer to that of cyclic sulfite (C= 65.31%, H= 5.68%, S= 6.46%). Such results suggested that the products could have a partial polysulfite structure or also be a mixture of nD-β-Glcp(1,2) and some S-atom based compound could be produced. Expected impurity is: $SO_2$ + 2DMF → $[(CH_3)_2NCO]_2SO$ + $H_2O$ → 1/8$S_8$ + X. Prof. Miyamoto reported that a mixing sulfur dioxide in DMF spontaneously generates $H_2O$ and sulfur, although the mechanism has not been clarified.[17]

## 2.3 Conclusion

In conclusion, I invented the usefulness of cyclic sulfite to use it as monomer also I evaluated the higher stability of cyclic sulfite than the glycal epoxide through kinetic studies for the degradation. The anionic ring-opening condensation polymerization of cyclic sulfite seems to lead to a mixture of structures including the proposed structure and some other impurities containing sulfur.

## 2.4 Experimental

**General methods:**

**Materials.** Tetrahydrofuran (THF) (Kanto Chemical Co., Inc.) was freshly distilled in the presence of sodium and benzophenone under nitrogen atromsphere before use. Dichloromethane was distilled over $CaH_2$ and stored with MS 4Å. MS 3Å as a dehydrator was activated by three times heating for 1 min in a microwave oven following careful heating by a heat gun under vacuum. The other chemicals were used without purification. Cyclic sulfite was prepared according to the literature: A. Benksim, D. Beaupère, A. Wadouachi, *Org. Lett.* **2004**, *6*, 3913-3915..

**Measurements.** $^{1}H$ NMR (400 MHz) and $^{13}C$ NMR (100 MHz) spectra were recorded on JEOL JNM-ESC400 and JNM-ESC600 spectrometers using $CDCl_3$ as the solvent, calibrated using residual undeuterated solvent and tetramethylsilane as the internal standard. FT-IR spectra were measured using a Thermo Fischer Scientific Nexus 870 spectrometer. Optical rotation was measured with a JASCO P-1030 digital polarimeter. SEC analyses were carried out using a chromatographic system

consisting of a JASCO PU-2080 plus pump with a JASCO UV-1570 (UV detector) equipped with Shodex Asahipak GF-310 HQ (30 x 0.75 (i.d.) cm) (eluent DMF with LiCl (30 mM), flow rate 1.0 mL/min). MALDI–TOF MS spectra were recorded on a Shimadzu Voyager-DE STR-H mass spectrometer (matrix: α– CHCA) at Instrumental Analysis Division, Equipment Management Center Creative Research Institution, Hokkaido University.

**Typical procedure for the preparation of cyclic sulfite 4[4, 11-13]**

To a solution of imidazole (5.59 g, 82.0 mmol) in THF (80 mL) was added dropwise $SOCl_2$ (1.49 mL, 20.5 mL) at 0 ºC. The mixture was warmed to room temperature, stirred for 30 min, and filtered. To the resulting *N*,*N*-thionyldiimidazole solution was added a solution of diol (1.54 g, 3.42 mmol) in THF (20 mL) at 0 ºC. The mixture was warmed to room temperature, stirred for 30 min, and carefully concentrated in vacuo below 30 ºC. The crude was purified by a florisil column chromatography (eluent: hexane : ethyl acetate = 9:1 → 3:1) to give the cyclic sulfite **4** (689.1 mg) as an *endo/exo* diastereo-mixture (2:1) on the sulfur atom; $[\alpha]_D^{25.2}$ +35.6 ($CHCl_3$, c. 1.00); $^1$H NMR (400 MHz, 298 K, $CDCl_3$) δ 7.37–7.14 (15H, m) 6.37 (0.63H, d, *J* = 4.8 Hz), 6.12 (0.37H, d, *J* = 6.0 Hz), 4.96–4.28 (7H, m), 4.14–3.57 (5H, m) ppm; $^{13}$C NMR (100 MHz, 298 K, $CDCl_3$) δ 138.0, 137.9, 137.79, 137.76, 137.4, 137.1, 128.8, 128.61, 128.58, 128.54, 128.49, 128.47, 128.24, 128.21, 128.1, 128.0, 127.94, 127.90, 105.9, 102.4, 83.8, 80.1, 75.8, 75.0, 74.8, 74.6, 74.3, 74.0, 73.7, 73.5, 72.8, 72.6, 71.4, 68.7, 68.6, 67.9 ppm; IR (NaCl) $\upsilon$ 3088, 3063, 3031, 2868, 1773, 1496, 1454, 1365, 1214 (OS(O)O), 1164,

1099, 1028, 989, 893, 819, 773, 740, 699 $cm^{-1}$; MALDI–TOF MS (matrix: CHCα) calc'd for $C_{27}H_{28}NaO_7S^+$ [M+$Na^+$] 519.14; found 519.59.

**Typical procedure for the preparation of glycal epoxide 2**

To a solution of **1** (100 mg, 0.24 mmol) in dichloromethane (1.98 ml) and acetone (0.72 ml) was added a saturated solution of $NaHCO_3$ at 0 $^0$C followed by the addition of oxone (885.4 mg, 1.44 mmol) solution in water (2 ml) slowly. The reaction mixture was stirred for 30 minute at 0 $^0$C and warmed to room temperature, stirred for 5 hours. TLC was checked. TLC showed the absence of starting material. Workup was then carried out by dilution with water and extracted with dichloromethane. The organic layer was separated and concentrated to get the product **2** (102 mg, 98.3%) The product obtained was characterized by $^1$H NMR.

The product from the reaction was characterized by $^1$H NMR. The analytical details are mentioned below. $^1$H NMR (400 MHz, $CDCl_3$, 293 K) δ 7.50-7.18 (m, 15 H, aromatic H), 4.98 (dd, 1H, $J_{1,2}$= 2.5 Hz, H-1), 4.88-3.45 (m, 11H), 3.05 (d, 1 H, H-2) ppm.

**Typical procedure for the preparation of unit model 5**

To a solution of **4** (35 mg, 0.07 mmol) in DMF (7.7 mL) under nitrogen atmosphere potassium salt of 4-methylbenzenethiolate (Initiator) was added (0.011 g, 0.0.070 mmol). The reaction mixture was allowed to stir gently at room temperature for 45 minutes. TLC was checked. TLC showed the absence

of starting material and the generation of single product. Workup was then carried out by dilution with water and extracted with diethyl ether. The organic layer was separated and concentrated to get the crude. The crude was purified by column chromatography using silica gel with the solvents hexane and ethyl acetate. The desired fraction was concentrated to get a white solid (20 mg, 51.3%). The product obtained was characterized by $^{1}$H NMR.

The product from the reaction was characterized by $^{1}$H NMR, 2D NMR, IR, $^{13}$C NMR, MALDI mass, melting range and optical rotation. By the calculation of coupling constant (*J*= 9.2 Hz) I found the obtained product is β-anomer, The analytical details are mentioned below. Off- white solid. $^{1}$H NMR (400 MHz, $CDCl_3$, 293 K) δ 7.45 (d, *J* = 8.2 Hz, 2H), 7.36-7.18 (m, 15 H, Ph), 7.05 (d, *J* = 8.2 Hz, 2H), 4.91 (d, *J* = 11.2 Hz, 1H, $CH_2Ph$), 4.83 (d, *J* = 11.2 Hz, 1H, $CH_2Ph$), 4.81 (d, *J* = 11.5 Hz, 1H, $CH_2Ph$), 4.61 (d, *J* = 12.4 Hz, 1H, $CH_2Ph$), 4.56 (d, *J* = 11.5 Hz, 1H, $CH_2Ph$), 4.54 (d, *J* = 12.4 Hz, 1H, $CH_2Ph$), 4.40 (d, *J* = 9.2 Hz, 1H, H-1), 3.78 (dd, *J* = 11.2, 1.8 Hz, 1H, H-6), 3.73 (dd, *J* = 11.2, 4.3 Hz, 1H, H-6), 3.59-3.55 (m, 2H, H-4,3), 3.51 (br, 1H, H-5), 3.44 (t, *J* = 9.2 Hz, 1H, H-2), 2.40 (br, 1H, OH), 2.31 (s,3H, $CH_3$) ppm. $^{13}$C NMR (100 MHz, $CDCl_3$, 293 K) δ 138.47, 138.42, 138.33, 138.06, 133.64, 129.73, 128.49, 128.40, 128.32, 127.98, 127.94, 127.78, 127.62, 127.53, 127.50, 88.06, 85.90, 79.44, 77.33, 75.31, 75.06, 73.41, 72.44, 68.98, 21.14 ppm. $[\alpha]_D^{22} = -31.1250$ (c.1.60, $CHCl_3$)

**Typical procedure of anionic polymerization of cyclic sulfite 4**

To a solution of **4** in DMF (0.8 M) was added potassium 4-methylbenzenethiolate (0.1 eq) and drierite (100 mg). The suspension was stirred for 24 h at 120 ˚C. Reaction was monitored by the SEC analysis. After 24 h, reaction mixture was diluted with acetone and then filtered to remove solid additive. Filtration was followed by evaporation to get the crude material as dark yellow syrup. The crude was purified by reprecipitation using chloroform and hexane. Both soluble and insoluble parts were dried under reduced pressure at 35 ˚C gave yellow syrup which were characterized by $^{1}$H NMR, IR, MALDI-TOF mass, elemental analysis and SEC. $^{1}$H NMR (400 MHz, $CDCl_3$, 293 K) δ 7.45-7.05 (m), 4.91-4.38 (m), 3.78-3.44 (m), 2.40 (br, 1H, OH), 2.31 (s, $CH_3$) ppm; IR (NaCl) $\upsilon$ 3385, 3063, 3030, 2921, 2867, 1496, 1454, 1362, 1210, 1122, 1028, 738, 698 $cm^{-1}$; Elemental analysis: calc'd for $C_{224.24}H_{237.36}O_{41.6}\cdot CHCl_3$ based on the polymerization degree (8.12) estimated by the $^{1}$H NMR spectrum (entry 5): C 72.77, H 6.46, Found: C 61.03, H 6.23; S 4.69%.

## Figures

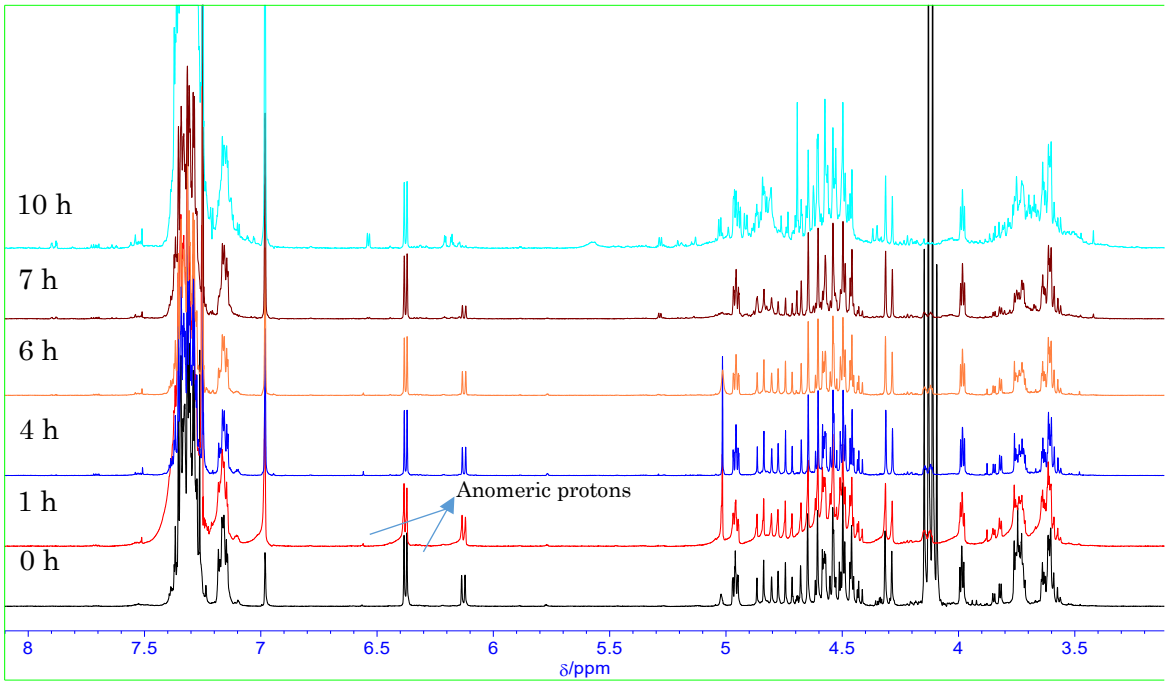


**Figure 2.4** Spectral change of $^{1}$H NMR spectrum of cyclic sulfite **4** (400 MHz, $CDCl_3$).

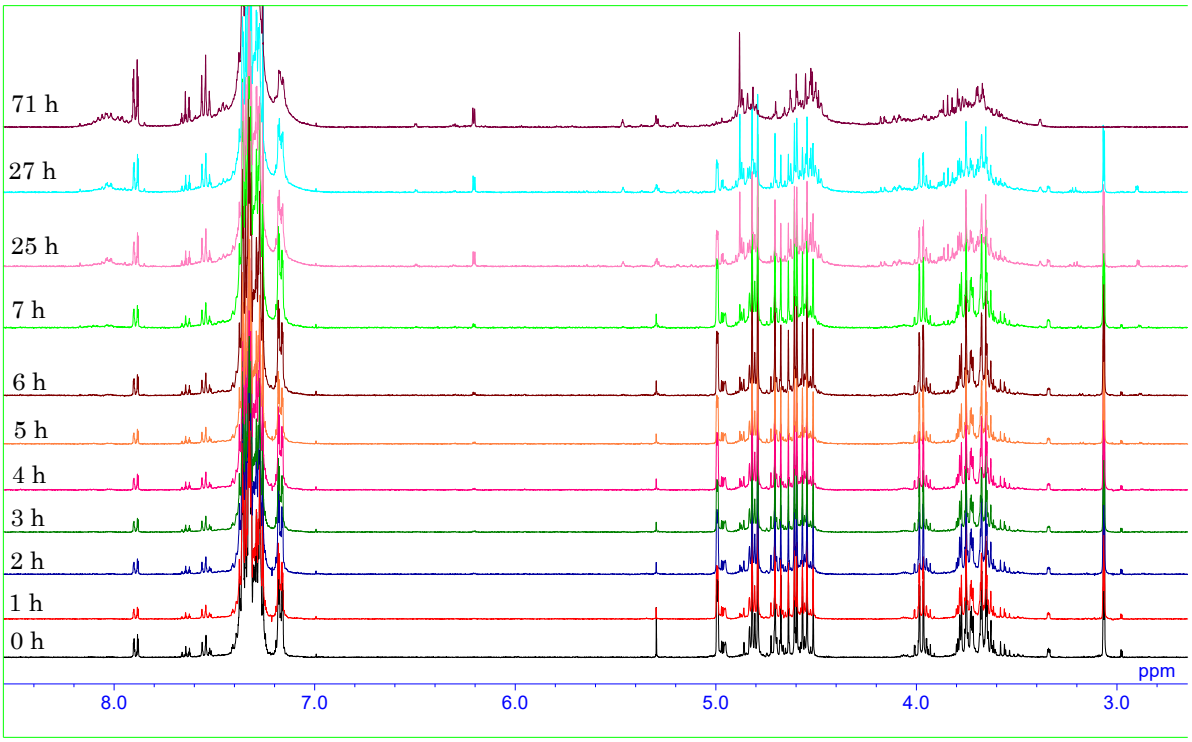


**Figure 2.5** Spectral change of $^{1}$H NMR spectrum of epoxide **2** (400 MHz, $CDCl_3$).

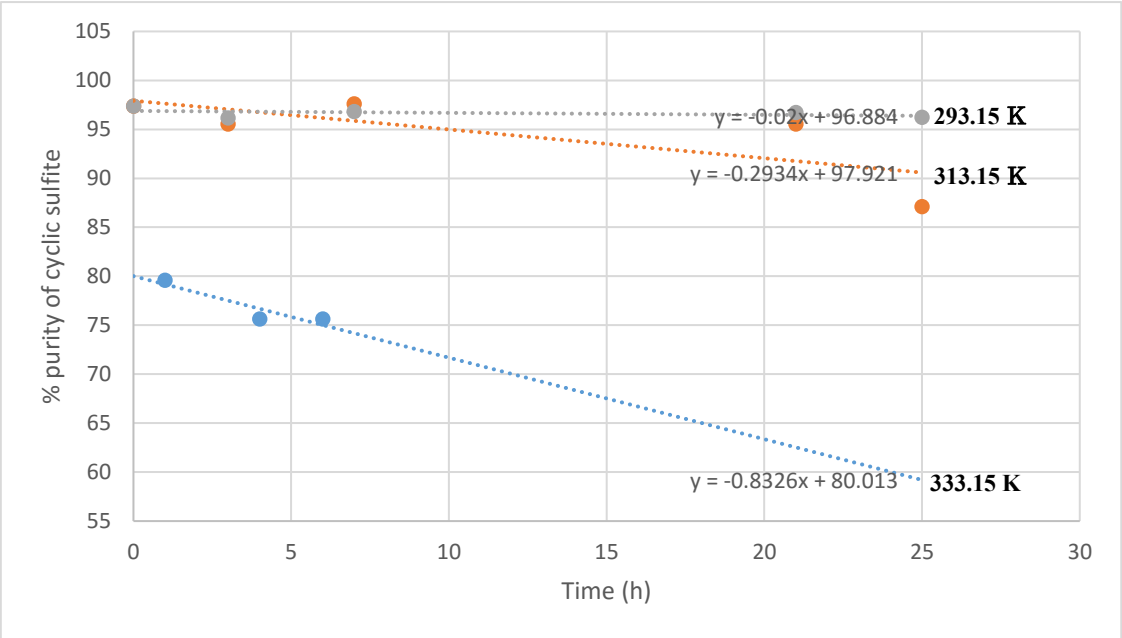


**Figure 2.6** First-order kinetic plots for dissociation of cyclic sulfite **4**

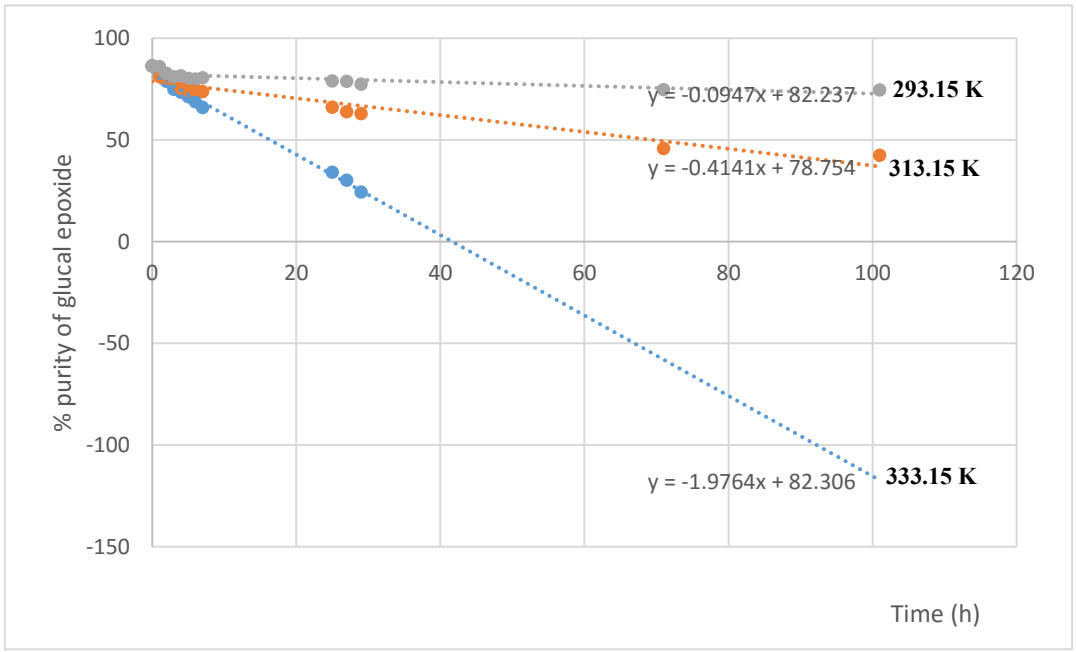


**Figure 2.7** First-order kinetic plots for dissociation of epoxide **2**.

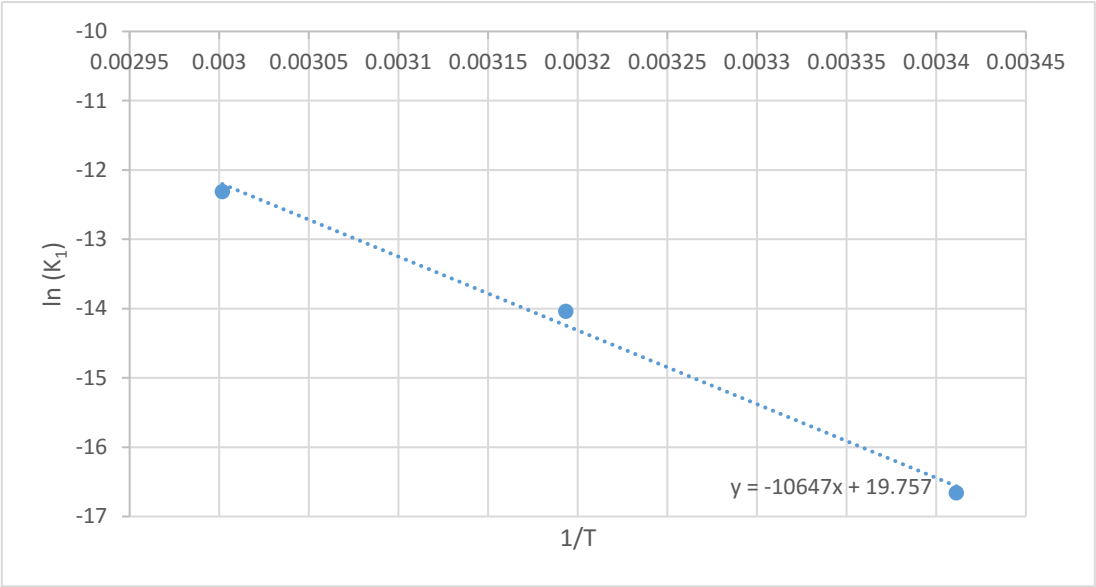


**Figure 2.8** Arrhenius plots for dissociation of cyclic sulfite **4**

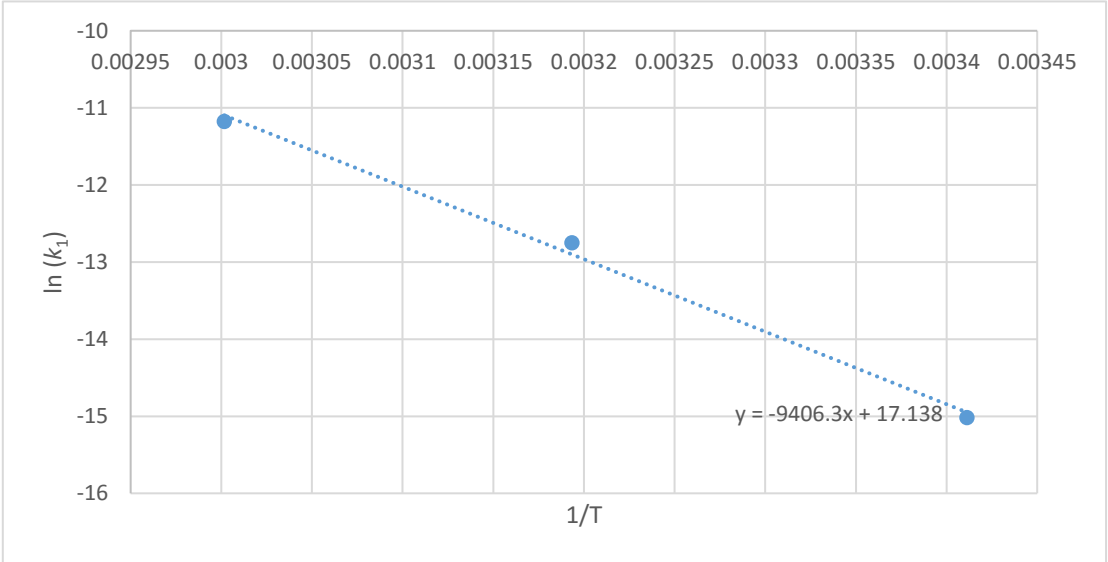


**Figure 2.9** Arrhenius plots for dissociation of epoxide **2**

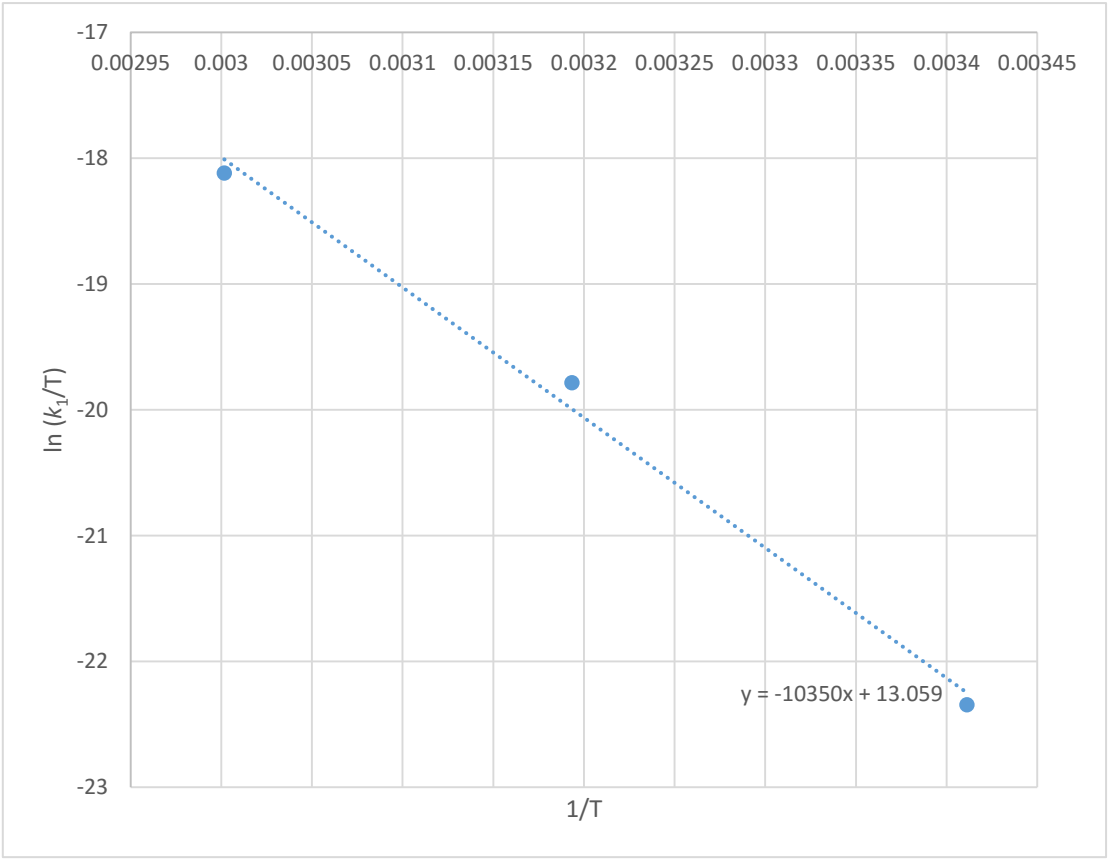


**Figure 2.10** Eyring plots for dissociation of cyclic sulfite **4**.

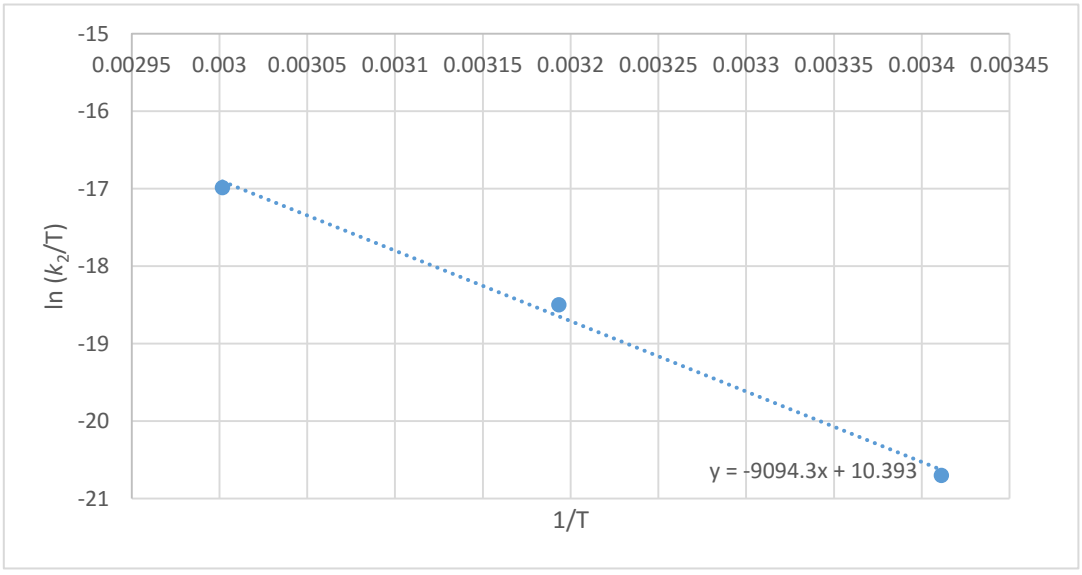


**Figure 2.11** Eyring plots for dissociation of epoxide **2**

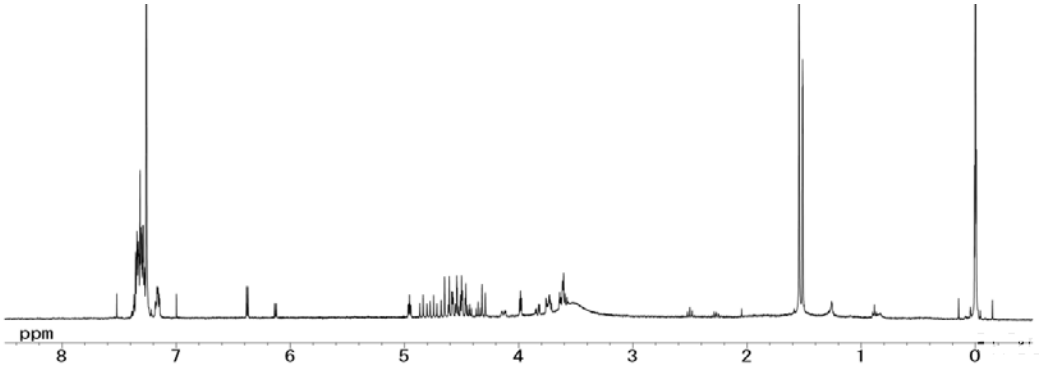


**Figure 2.12** $^{1}$H NMR spectrum of cyclic sulfite **4** (400 MHz, $CDCl_3$, 293 K).

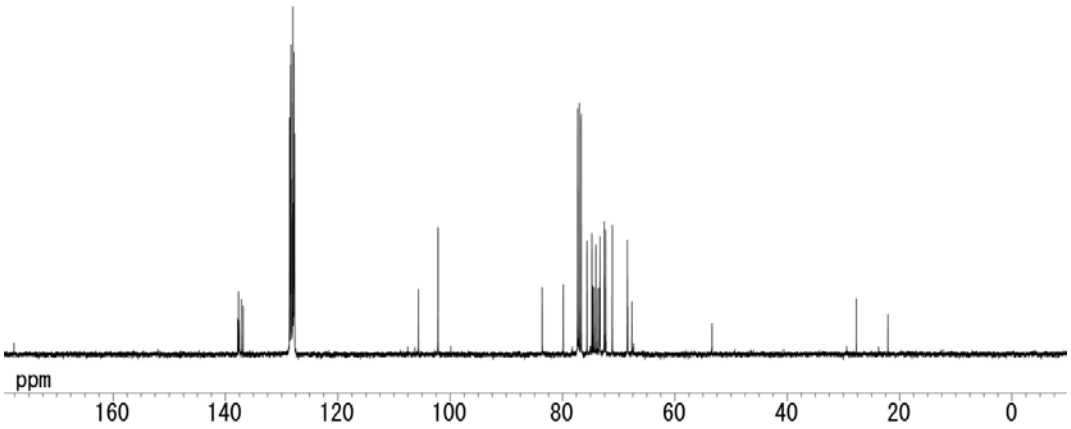


**Figure 2.13** $^{13}$C NMR spectrum of cyclic sulfite **4** (100 MHz, $CDCl_3$, 293 K).

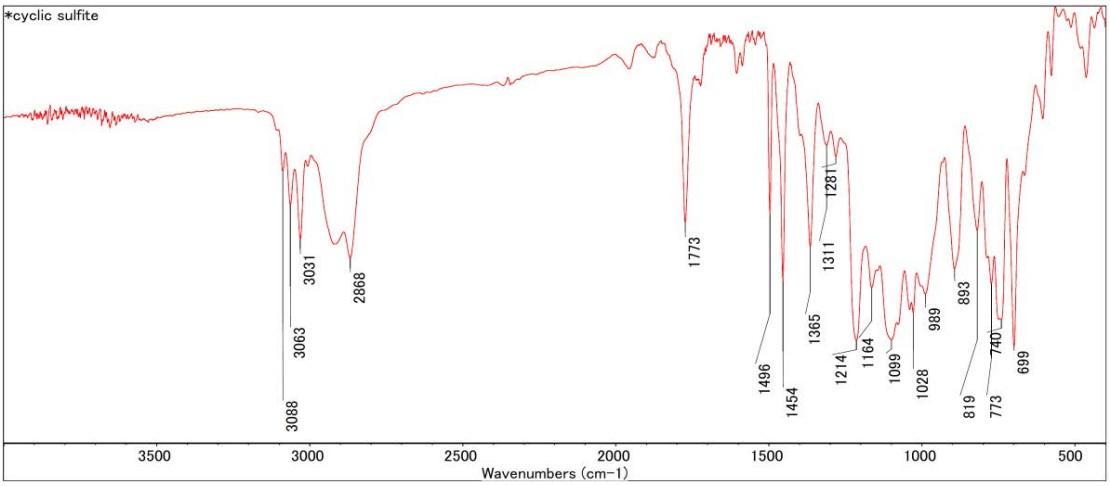


**Figure 2.14** IR spectrum of cyclic sulfite **4** (NaCl).

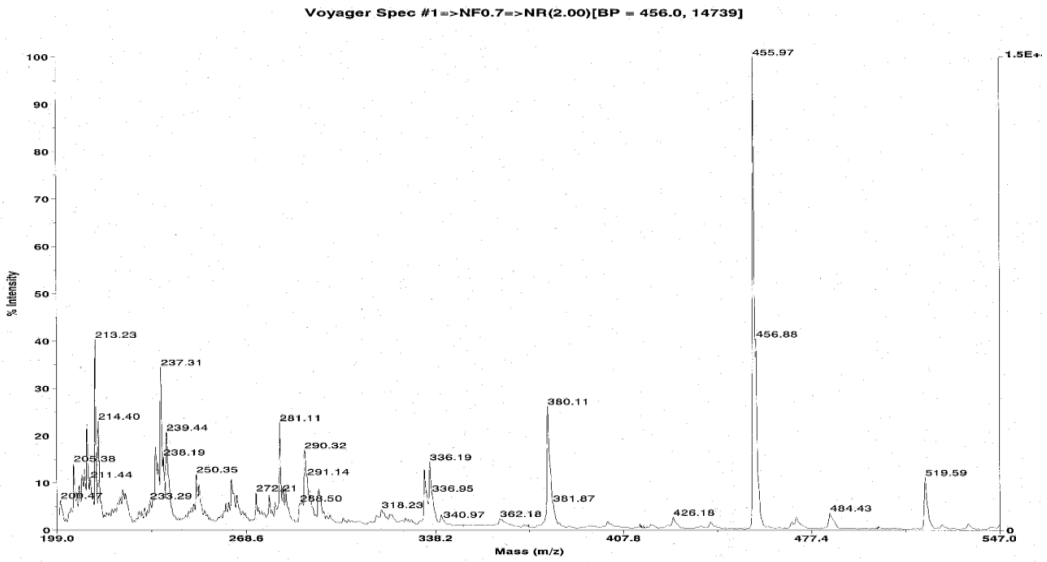


**Figure 2.15** MALDI–TOF MS spectrum of cyclic sulfite **4**.

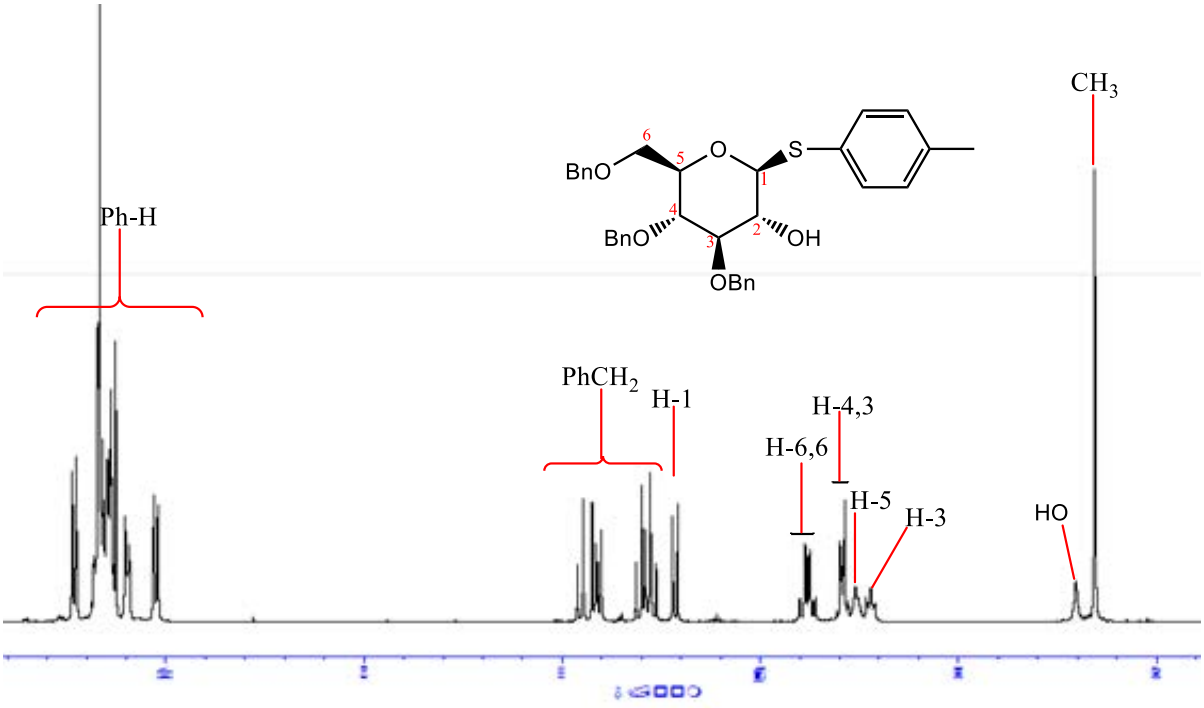


**Figure 2.16** $^{1}$H NMR spectrum of **5** (400 MHz, $CDCl_3$, r.t.).

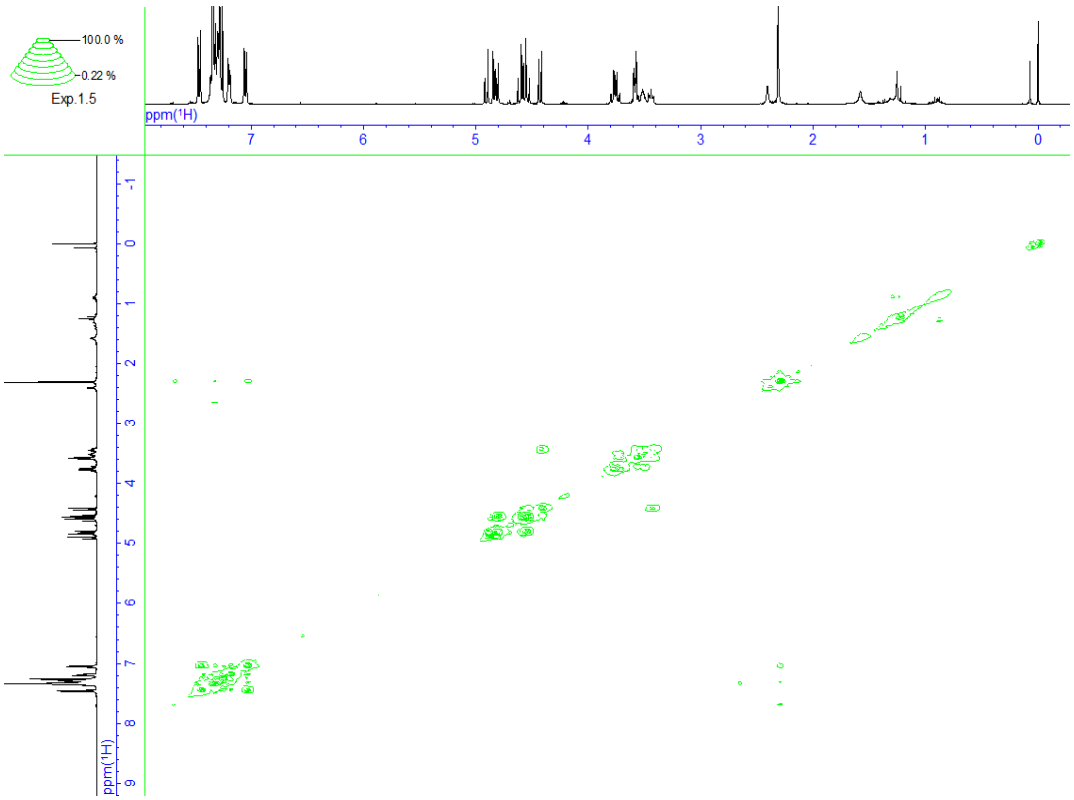


**Figure 2.17** 2D NMR spectrum of **5** (400 MHz, $CDCl_3$, r.t.).

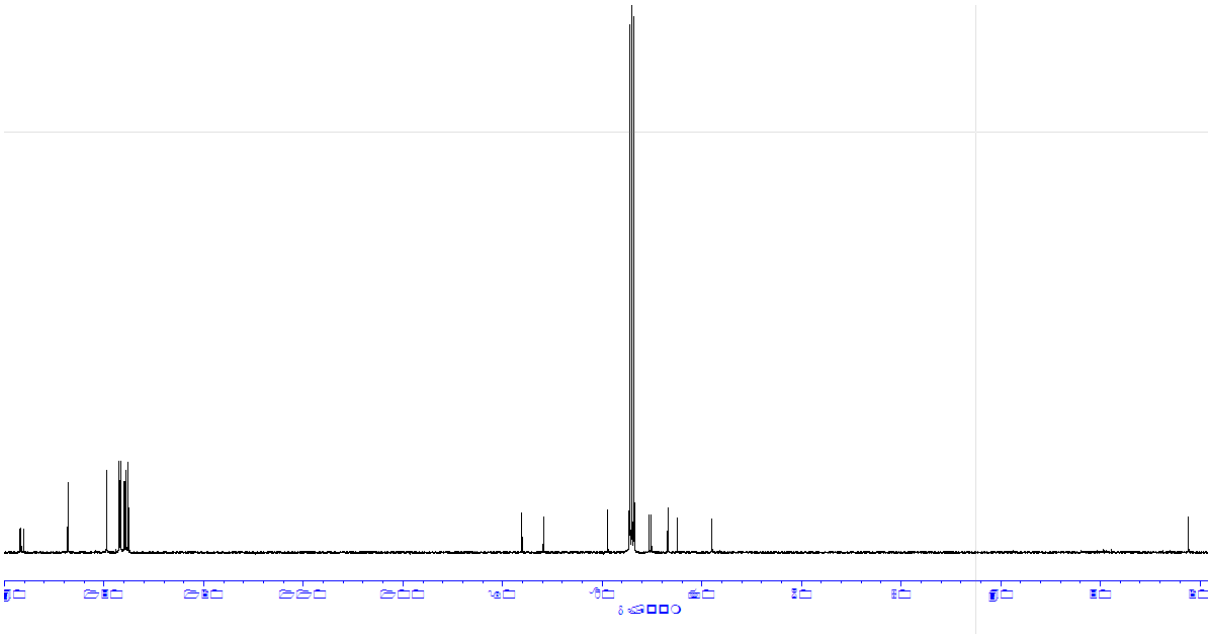

**Figure 2.18** $^{13}C$ NMR spectrum of **5** (400 MHz, $CDCl_3$, r.t.).

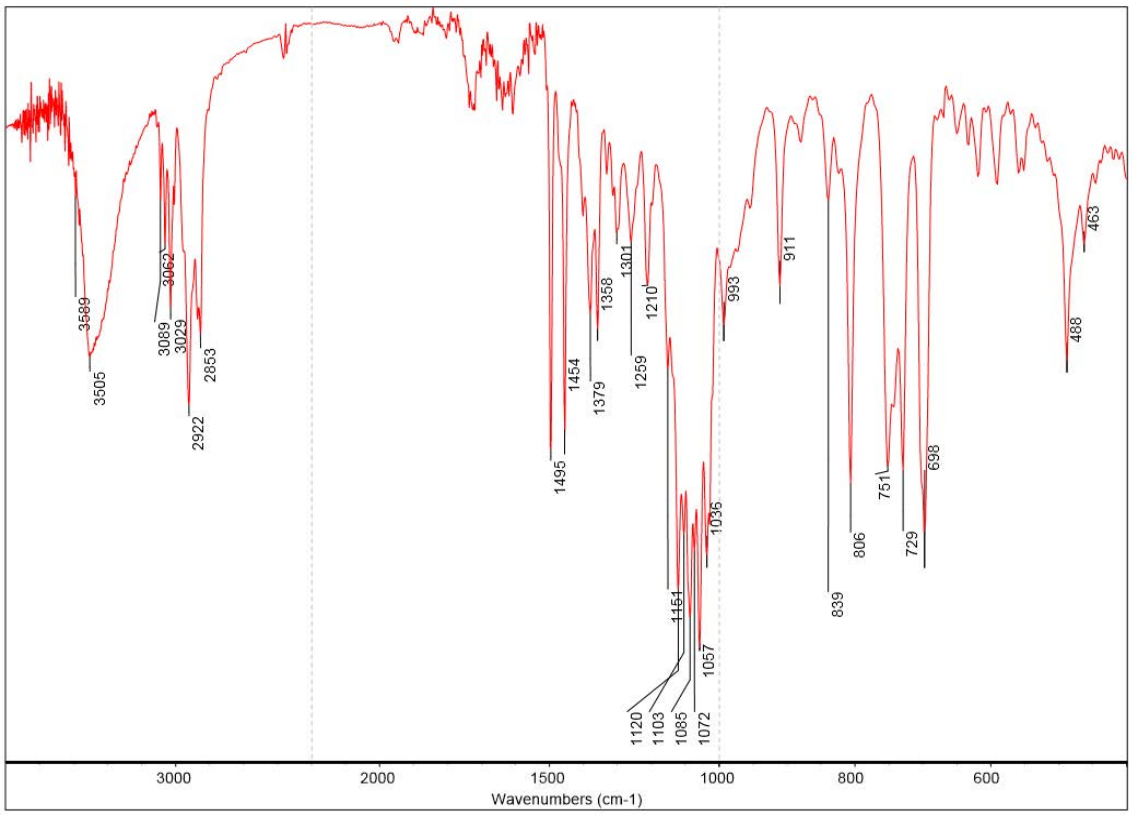


**Figure 2.19** $^{13}$C NMR spectrum of **5.**

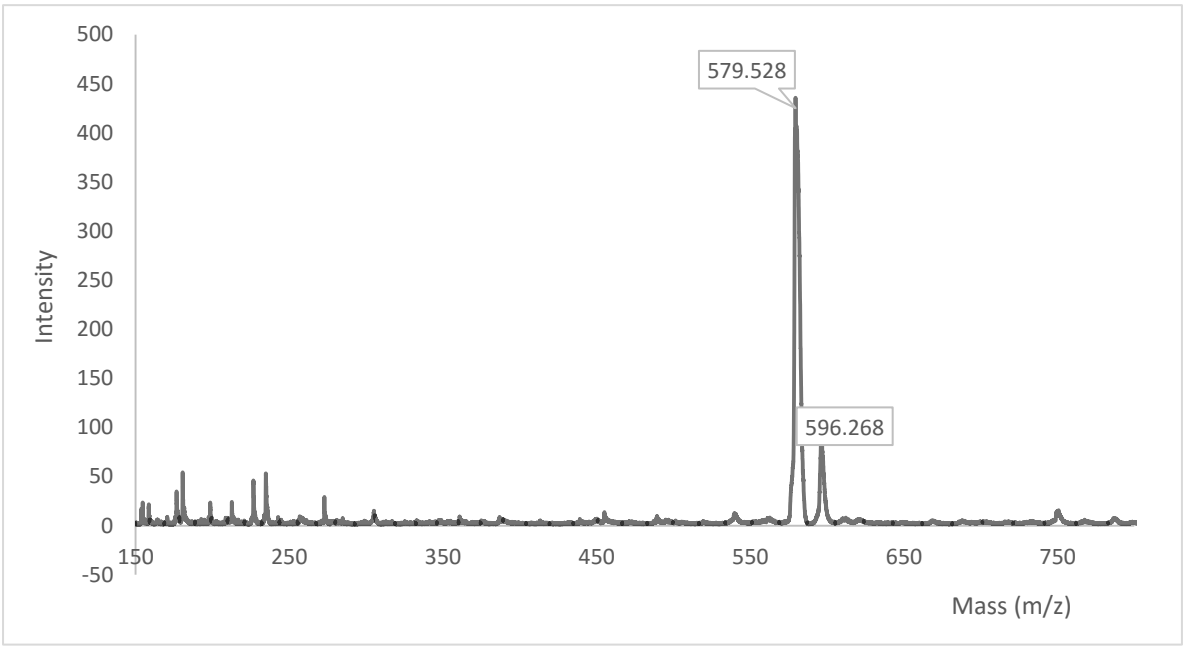


**Figure 2.20** MALDI-TOF MS of **5.**

## 2.5 References


1) (a) Goodall, D. M.; Norton, I. T. *Acc. Chem. Res.* **1987**, *20*, 59-65. (b) Rees, D. A. *Pure Appl. Chem.* **1981**, *53*, 1-14. (c) Latgé, J.-P. *Mol. Microbiol.* **2007**, *66*, 279-290.

2) (a) Ikai, T.; Okamoto, Y. *Chem. Rev.* **2009**, *109*, 6077-6101. (b) Yashima, E. *J. Chromatogr. A* **2001**, *906*, 105-125. (c) Yashima, E.; Yamamoto, C.; Okamoto, Y. *Synlett* **1998**, 344-360. (d) Okamoto, Y.; Yashima, E. *Angew. Chem., Int. Ed.* **1998**, *37*, 1020-1043.

3) (a) Kawabata, Y.; Tanaka, M.; Ogata, I. *Chem. Lett.* **1976**, *5*, 1213-1214. (b) Xue, L.; Zhou, D.-J.; Tang, L.; Ji, X.-F.; Huang, M.-Y.; Jiang, Y.-Y. *React. Funct. Polym.* **2004**, *58*, 117-121. (c) Ricci, A.; Bernardi, L.; Gioia, C.; Vierucci, S.; Robitzer, M.; Quignard, F. *Chem. Commun.* **2010**, *46*, 6288-6290. (d) Ikai, T.; Moro, M.; Maeda, K.; Kanoh, S. *React. Funct. Polym.* **2011**, *71*, 1055-1058.

4) (a) Sata, H.; Murayama, M.; Shimamoto, S. *Macromol. Symp*. **2004**, *208*, 323-333. (b) Mori, H. *J. Display Technol.* **2005**, *1*, 179-186. (c) Nakayama, H.; Fukagawa, N.; Nishiura, Y.; Yasuda, T.; Ito, T.; Mihayashi, K. *J. Photopolym. Sci. Technol.* **2006**, *19*, 169-173.

5) (a) Yoshida, T. *Prog. Polym. Sci.* **2001**, *26*, 379-441. (b) Uryu, T. *Kobunshi*, **1986**, *35*, 120-123.

6) (a) Kobayashi, S.; Kashiwa, K.; Kawasaki, T.; Shoda, S. *J. Am. Chem. Soc.* **1991**, *113*, 3079-3084. (b) Kaneko, Y.; Kadokawa, J. *Chem. Rec.* **2005**, *5*, 36-46.

7) (a) York, W. S. ; McNeil, M.; Darvill, A. G.; Albersheim, P. *J. Bacteriol.* **1980**, *142*, 243-248. (b) Puvanesarajah, V.; Schell, F. M.; Stacey, G.; Douglas, C. J.; Nester, E. W. *J. Bacteriol.* **1985**, *164*, 102-106. (c) Zorreguieta, A.; Ugalde, R. A. *J. Bacteriol.* **1986**, *167*, 947-951.

8) For a related report concerning cyclic (1-2)-β-D-glucan, see: Choma, A.; Komaniecka, I. *Acta Biochim. Pol.* **2003**, *50*, 1273-1281.

9) (a) Kissel, T.; Li, Y.; Unger, F. *Adv. Drug Deliv. Rev.* **2002**, *54*, 99-134. (b) Mangold, C.; Wurm, F.; Frey, H. *Polym. Chem.* **2012**, *3*, 1714-1721. (c) Parker, J. M.; Wright, P. V.; Lee, C. C. *Polymer*, **1981**, *22*, 1305-1307. (d) Wei, L.; Liu, Q.; Gao, Y.; Yao, Y.; Hu, B.; Chen, Q. *Macromolecules* **2013**, *46*, 4447-4453.

10) Sharkey, P. F.; Eby, R. C. Schuerch, *Carbohydr. Res.* **1981**, *96*, 223-229.

11) Meslouti, A. E.; Beaupère, D.; Demailly, G.; Uzan, R. *Tetrahedron Lett.* **1994**, *35*, 3913-3916.

12) Benksim, A.; Massoui, M.; Beaupère, D.; Wadouachi, A. *Tetrahedron Lett.* **2007**, *48*, 5087-5089.

13) Benksim, A.; Beaupère, D.; Wadouachi, A. *Org. Lett.* **2004**, *6*, 3913-3915.

14) Loharay, B. B. *Synthesis*, **1992**, *11*,1035-1052.

15) Leshch, Y.; Waschke, D.; Thimm, J.; Thiem, J. *Synthesis*, **2011**, *23*, 3871-3877.

16) For selected reviews, see: (a) Zhu, X.; Schmidt, R. R. *Angew. Chem., Int. Ed.* **2009**, *48*, 1900-1934. (b) Codée, J. D. C.; Litiens, R. E. J. N.; van den Bos, L. J.; Overkleeft, H. S.; van der Marel, G. A. *Chem. Soc. Rev.* **2005**, *34*, 769-782. (c) Fairbanks, A. J. *Synlett* **2003**, *13*, 1945-1958. (d)

Demchenko, A. V. *Synlett* **2003**, *9*, 1225-1240. (e) Sinaÿ, P. *Pure Appl. Chem.* **1991**, *63*, 519-528. (f) Fügedi, P.; Garegg, P. J.; Lönn, H.; Norberg, T. *Glycoconjugate* **1987**, *4*, 97-108.

17) Yoshimura, C.; Miyamoto, K.S. *Bunseki Kagaku.*, **1980**, *29*, 40-44.

18) Cheshev, P.; Marra, A.; Dondoni, A. *Carbohydr. Res.,* **2006**, *341*, 2741–2716.

19) For our previous reports concerning the determination of thermodynamic parameters, see: (a) Akae, Y.; Koyama, Y.; Kuwata, S.; Takata, T. *Chem. Eur. J.*, **2014**, *20*, 17132–17136. (b) Akae, Y.; Okamura, H.; Koyama, Y.; Arai, T.; Takata, T. *Org. Lett.*, **2012**, *14*, 2226–2229.

# Chapter 3

# Synthesis and Structure of (1→2)-D-Glucopyranan via Cationic Ring-Opening Condensation Polymerization of Cyclic Sulfite

### 3.1. Introduction

As I discussed in the chapter 2, the anionic polymerization seems to lead to a mixture of structures including proposed structure and some other impurities containing sulphur. However the polymerization enables selective introductions of stereogenic centers to the anomeric positions with thioglycoside terminus, the product was contaminated with sulfur. I am unable to purify in any method. Therefore, I next focused on the cationic polymerization of the sugar based cyclic sulfite.

It has been reported that the polymerizability of cyclic sulfites under cationic conditions are strongly dependent on the ring size and strain: The cationic polymerization of 7-membered sulfite efficiently gives polysulfite without a lack of sulfite linkage, while that of 6-membered sulfite partially accompanies with elimination of $SO_2$.[1] Whereas, the both copolymerization[2,3] with cyclic anhydrides and homopolymerization[3] of 5-membered sulfite results in perfect elimination of $SO_2$ to afford the corresponding polyesters. Therefore, I expected that 5-membered cyclic sulfite **I** could work as a surrogate of the epoxy monomer to give 1,2-glycosidic polymer through cationic polymerization.

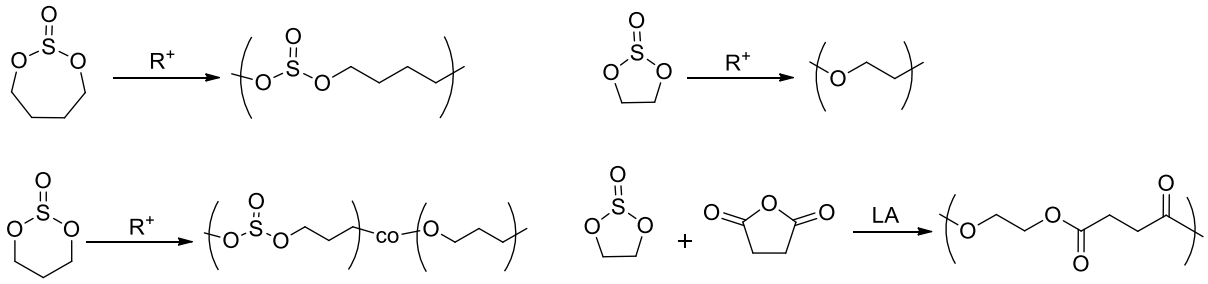


**Scheme 3.1** Cationic ring-opening polymerization of 5, 6 and 7- membered cyclic sulfites.

In this work, I selected 4-pentenol as an initiator (R'OH) for the polymerization, because both glycosidation and glycosylation reactions using pentenoyl glycosides have been well established.[4] 4-Pentenol would attack to the anomeric center in the presence of acid to give monomeric alcohol **II** accompanying with a removal of $SO_2$. If the glycosydation reaction of the generated secondary alcohol to the other monomer proceeded to furnish **III** at the stereo-selective manner attributed to an $S_N2$ reaction, the successive propagation would give nD-β-Glcp-(1-2) skeleton with pentenoyl group at the polymer terminus.

### 3.2 Results and Discussion

#### Cationic polymerization of cyclic sulfite

Scheme 3.2 shows the schematic illustration for the synthesis of nD-β-Glcp-(1-2) via cationic ring-opening condensation polymerization of the cyclic sulfite.

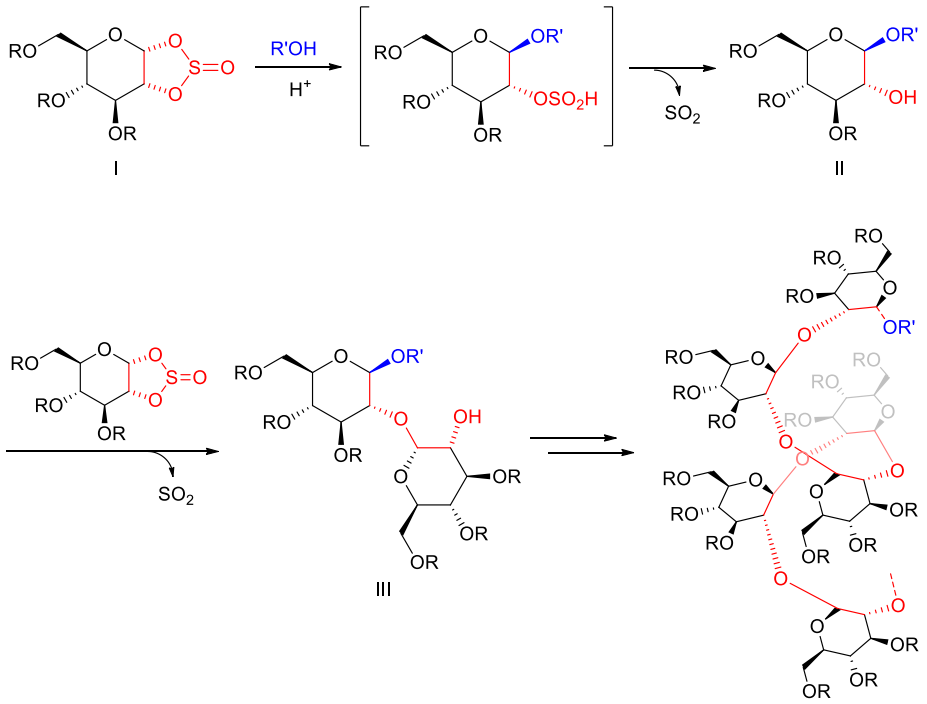


**Scheme 3.2** Schematic illustration for a cationic ring-opening condensation polymerization of cyclic sulfite to prepare nD-β-Glcp-(1-2) framework.

I investigated the polymerization of **I** using 10 mol% of 4-pentenol initiator in the presence of a dehydrator in $CH_2Cl_2$ (0.6 M). The results are summarized in Table 3.1.

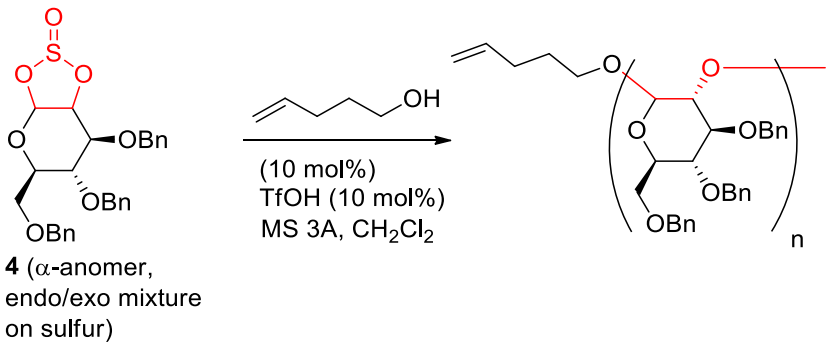


**Scheme 3.3** Cationic polymerization of cyclic sulfite

I also investigated the effects of reaction temperature and feed ratio of initiator on the yields and $M_n$ as summarised in the below table. From the results of entries 4–9, I found that the conversions of **4** decrease as the temperature decrease. $M_n$ was moderately controllable by prolonging the reaction time (entries 8 and 9) and changing [M]/[I] (entries 4, 5, 6, 11, and 12).

**Table 3.1** Results of cationic polymerization.

| entry | initiator (mol%) | acid | dehydrator[c] | temp (°C) | time (h) | yield (%) | $M_n$[d] (Da) | $M_w/M_n$[e] | $[\alpha]_D$[f] |
|---|---|---|---|---|---|---|---|---|---|
| 1 | 10 | $CF_3COOH$ | $CaSO_4$ | rt | 24 | 0 | – | – | – |
| 2 | 10 | TfOH | $CaSO_4$ | rt | 24 | 85 | 4500 | 1.8 | +109 |
| 3 | 10 | TfOH | $CaSO_4$ | 0 | 24 | 83 | 4800 | 1.2 | +61 |
| 4 | 10 | TfOH | MS 3Å[g] | rt | 24 | 61 | 1800 | 1.4 | +52 |
| 5 | 5 | TfOH[h] | MS 3Å | rt | 41 | 85 | 4200 | 2.4 | +61 |
| 6 | 10 | TfOH | MS 3Å | –10 | 24 | 73 | 5000 | 1.2 | +55 |
| 7 | 10 | TfOH | MS 3Å | –20 | 41 | 55 | 3000 | 1.3 | +37 |
| 8 | 10 | TfOH | MS 3Å | –40 | 41 | 56 | 2900 | 1.3 | +35 |
| 9 | 10 | TfOH | MS 3Å | –40 | 100 | 42 | 10900 | 1.3 | +56 |
| 10 | 10 | TfOH | MS 3Å | –60 | 41 | 28 | 1900 | 1.2 | +8.7 |
| 11 | 5 | TfOH | MS 3Å | –20 | 41 | 80 | 4300 | 1.4 | +49 |
| 12 | 20 | TfOH | MS 3Å | –20 | 41 | 91 | 1700 | 1.3 | +39 |

[a] The reaction was performed by using **4** (0.30–0.40 mmol), initiator (10 mol%), and acid (10 mol%) in the presence of a dehydrator in $CH_2Cl_2$ (0.6 M). [b] Monomer conversion ratio was determined by $^1H$ NMR spectra of the crude mixture. [c] 50 wt% of dehydrator per **4** was used. [d] Number-

average molecular weights ($M_n$) were estimated by the integral ratio in the $^1$H NMR spectra. [e] Polydispersity indices ($M_w/M_n$) were determined by a size exclusion chromatography (SEC) using DMF as an eluent. [f] Specific optical rotation ($[\alpha]_D$) was measured in $CHCl_3$ at 25–28 ºC. [g] 150 wt% of MS 3Å was used. [h] 5.0 mol% of TfOH was used.

Polymerization using $CF_3COOH$ (pKa −0.25) resulted in no reaction (entry 1), the use of TfOH (pKa −14) in the presence of $CaSO_4$ as a dehydrator efficiently facilitated the polymerization at room temperature and 0 ºC to afford high yields of polymers (entries 2 and 3). The polymerization reaction was also performed in the presence of acetonitrile in place of dichloromethane at – 20 $^0$C, RT and 80 $^0$C. But the result was unfruitful, there was no product formation. The structures of the obtained polymers were evaluated by IR, $^1$H NMR, and MALDI−TOF MS spectra.

In the IR spectra, the absence of the characteristic signal of sulfite at around 1200 $cm^{-1}$ was observed, implying that the polymerization of **4** efficiently eliminates $SO_2$ to form polyoxyethylene main chain (Figures 3.14, 3.17, 3.20, 3.21, 3.22, 3.23). Elemental analysis of the polymer finally evidenced the absence of sulphur atom in the obtained polymer skeleton. The appearance of olefinic proton signals in the $^1$H NMR spectra supports the introduction of pentenoyl group to the polymer terminus. The number average of molecular weights ($M_n$) were determined on the basis of the integral ratio between the internal olefinic proton of pentenoyl group and the other aliphatic protons in the $^1$H NMR spectra. The distributions ($M_w/M_n$) were estimated by a size exclusion chromatography (SEC)

using *N*,*N*-dimethylformamide (DMF) based on polystyrene standards. Matrix associated laser desorption/ionization time-of-flight mass (MALDI–TOF MS) with the theoretical values corresponding to the polymer, supporting the formation of pentenoyl-group terminated nD-Glcp-(1-2) skeleton. However, I also found the additional minor peaks attributed to the formation of OH-terminated polymers and cyclic polymer in the MS spectra. After considerable efforts, I found that MS 3Å works as a good dehydrator efficiently to suppress the formation of OH-terminated polymers (entries 4 and 5). The MALDI–TOF MS spectrum of the polymer exhibited a simple pattern assignable to the pentenoyl group-terminated polymers excluding the peaks from OH-terminated polymer, strongly suggesting the good dehydrating capability of MS 3Å under the polymerization condition.

I also investigated the effects of reaction temperature and feed ratio of initiator on the yields and $M_n$ (entries 4–11 in Table 3.1). From the results of entries 4–9, I found that the conversions of cyclic sulphite decrease as the temperature decrease. $M_n$ was moderately controllable by prolonging the reaction time (entries 8 and 9) and changing [M]/[I] (entries 4, 5, 6, 11, and 12).

For the purpose to determine the stereochemistry at the anomeric centers of polymer, unit models **5β** and **5α** were prepared as a reference material (Scheme 3.4). Treatment of cyclic sulphite with 1.2 equivalent of 4-pentenol in the presence of a catalytic amount of TfOH (10 mol%) at room temperature for 13 h in diluted $CH_2Cl_2$ (0.05 M) gave a 1:1 mixture of **5β** and **5α** in good yields. The stereochemistry of **5β** and **5α** were determined by the coupling constants between the 1 and 2 protons in the $^1$H NMR spectra.

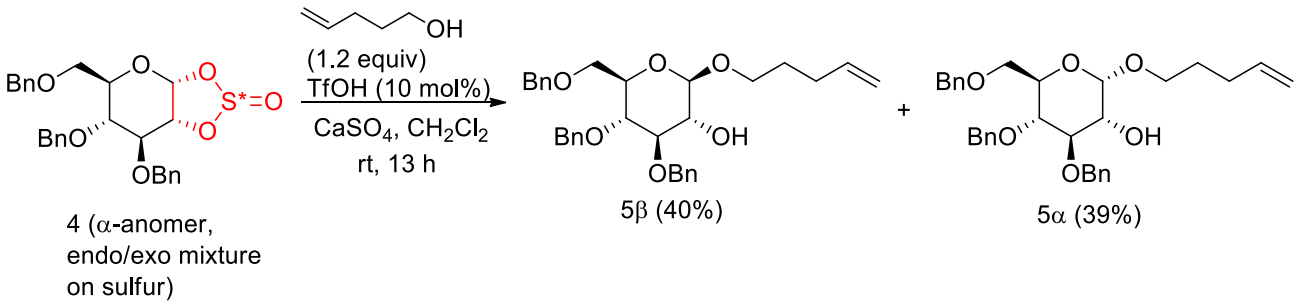


**Scheme 3.4** Synthesis of unit model

To estimate roughly the anomeric stereochemistry of the polymer, I first measured the specific optical rotations ($[\alpha]_D$) of polymers and unit models (Table 1). As a result, it was found that polymer prepared at lower temperature exhibits a smaller positive $[\alpha]_D$ value compared with the polymer prepared at higher temperature. The reported $[\alpha]_D$s of branched, cyclic nD-β-Glcp-(1-2), and its dimer were −12, −5, and +15, while that of α-kojibiose as a glucose dimer consisting of an α-glycosidic linkage is +162.[10] In addition, the $[\alpha]_D$s of **5β** and **5α** consisting of β- and α-pentenoly group are −5 and +69, respectively. Therefore, it is expected that the presence of α-glycosidic linkage could lead the $[\alpha]_D$ of polymer to remarkably big positive value. Therefore, the polymers obtained at room temperature (entries 4 and 5) seem to be consisting of much more α-glycosidic linkages than the other polymers, whereas the polymer from entry 10 could mainly include β-glycosidic centers.

I next measured and compared $^{13}C$ NMR spectra of unit models and polymers. Figure 3.1 shows the partial $^{13}C$ NMR spectra of unit models (**5β** and **5α**) and the synthetic polymers in Table 1. In the spectra of unit models (A) and (B), the chemical shifts of anomeric carbon with pentenoly group were

102.9 ppm for **5β** and 98.6 ppm for **5α**. On the other hand, the signals assignable to anomeric carbons in the spectra (C) of polymer obtained at room temperature (entry 5) appeared as multiple peaks, indicating the presence of both α- and β-anomeric centers. The spectra of (D) and (E) from entries 7 and 10 were mainly consisting of two intense signals: The sharp signal at 103 ppm should be a terminal anomeric carbon containing a pentenoyl group, because the chemical shift is similar to that of **5β** (A). The other broad signal at around 104 ppm would be assignable to β-anomeric carbons originating from the glycosidic linkages in the main chain, whose chemical shifts are in good accordance to those of reported natural[11,12] and synthetic polymers.[10] Therefore, I concluded that (i) the peaks in a range from 90 to 97 ppm in the spectrum (C) could be attributed to the presence of α-anomeric centers in the main chain and (ii) the polymerization at low temperature from −20 ºC to −60 ºC sufficiently suppresses the formation of α-anomeric center to give nD-β-Glcp-(1-2) skeleton.

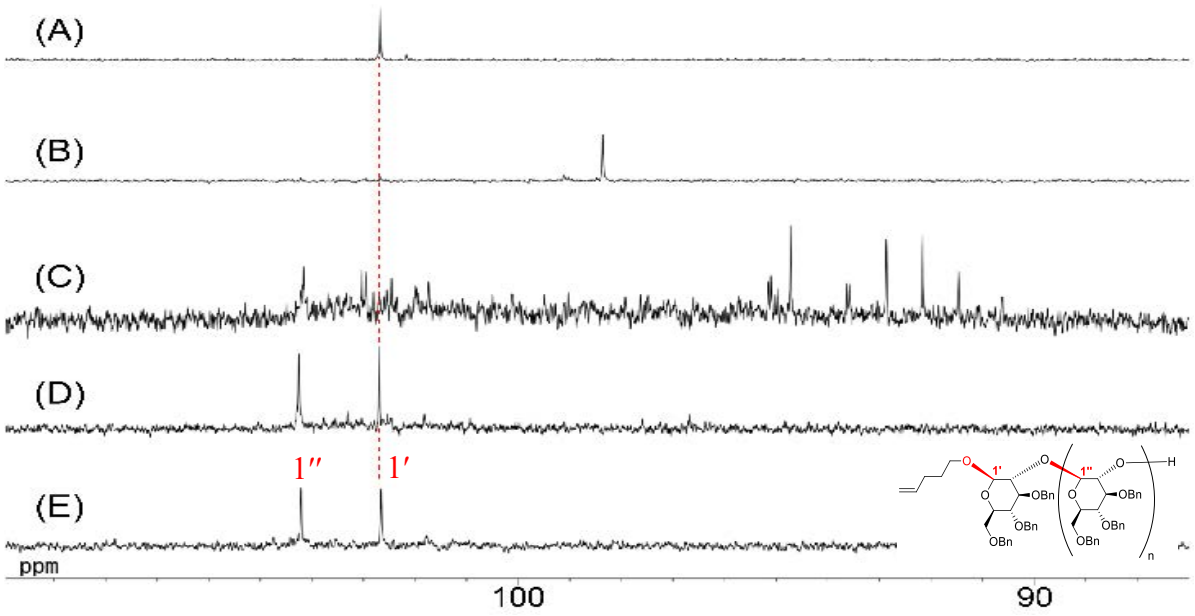


**Figure 3.1** Partial $^{13}C$ NMR spectra of unit model **5β** (A) and **5α** (B) and synthetic polymers of entry 5 (C), entry 7 (D), and entry 10 (E) (150 MHz, $CDCl_3$ 293 K).

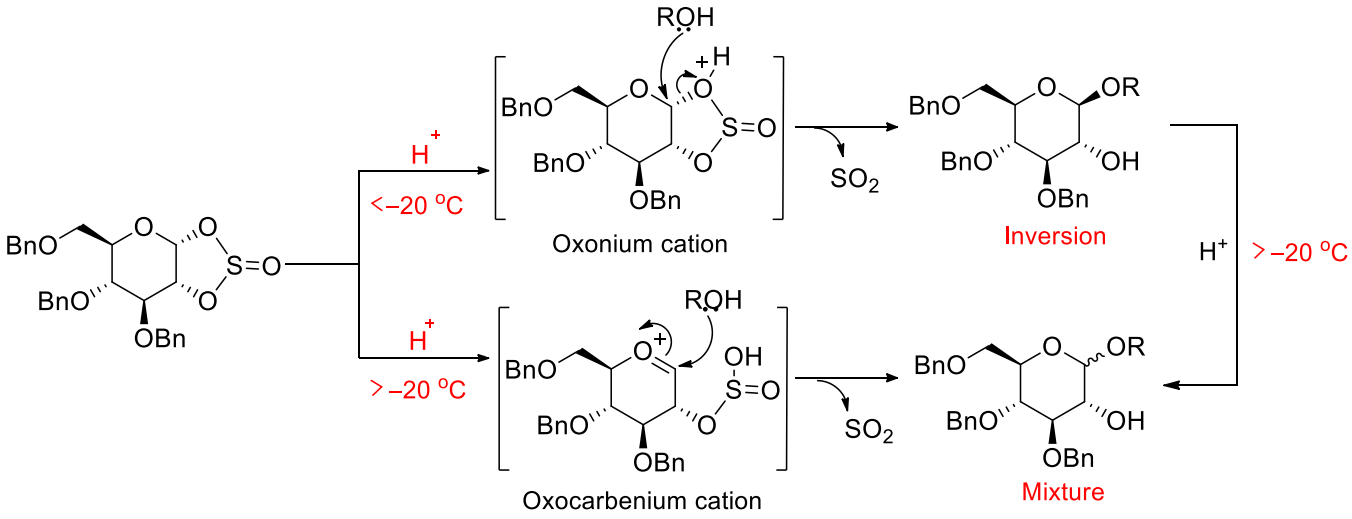


**Scheme 3.5** Plausible reaction mechanism for cationic polymerization of cyclic sulfite.

On the basis of the related mechanism for the ring-opening polymerization of anhydro sugar,[13] the plausible reaction mechanism for the cationic polymerization of cyclic sulfite is shown in the scheme 3.5. At low temperature, the polymerization would occur in $S_N2$ inversion manner through the formation of oxonium cation as intermediate, which results in the formation of β-anomeric center.[13] In the case of high temperature, the reaction would afford the formation of oxocarbenium cation which results in the formation of anomeric mixture.[13] In addition, the anomerization from β-anomeric compound could be also possible to give the mixture.

To confirm the chemical structure of the polymer, the benzyl groups of the synthesized polymer (entry 7) was deprotected by Birch reduction. By comparision of $^{13}C$ NMR between the reported[10] and the obtained polymers, it was found that the anomeric carbon signals of the synthetic polymer appeared as multiple peaks (Figure 3.2), probably because of the difference in the terminal structure and the chain length to those of the reported polymer. The appearance of pentenoyl group carbons clearly support the formation of pentenoyl-terminated polymer. The anomeric stereochemistry of the polymer was roughly estimated to be β:α = ca. 3:1.

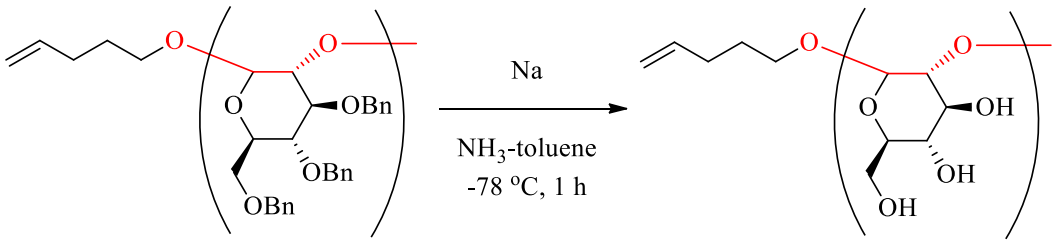


**Scheme 3.6** Debenzylation of polymer prepared by cationic polymerization.

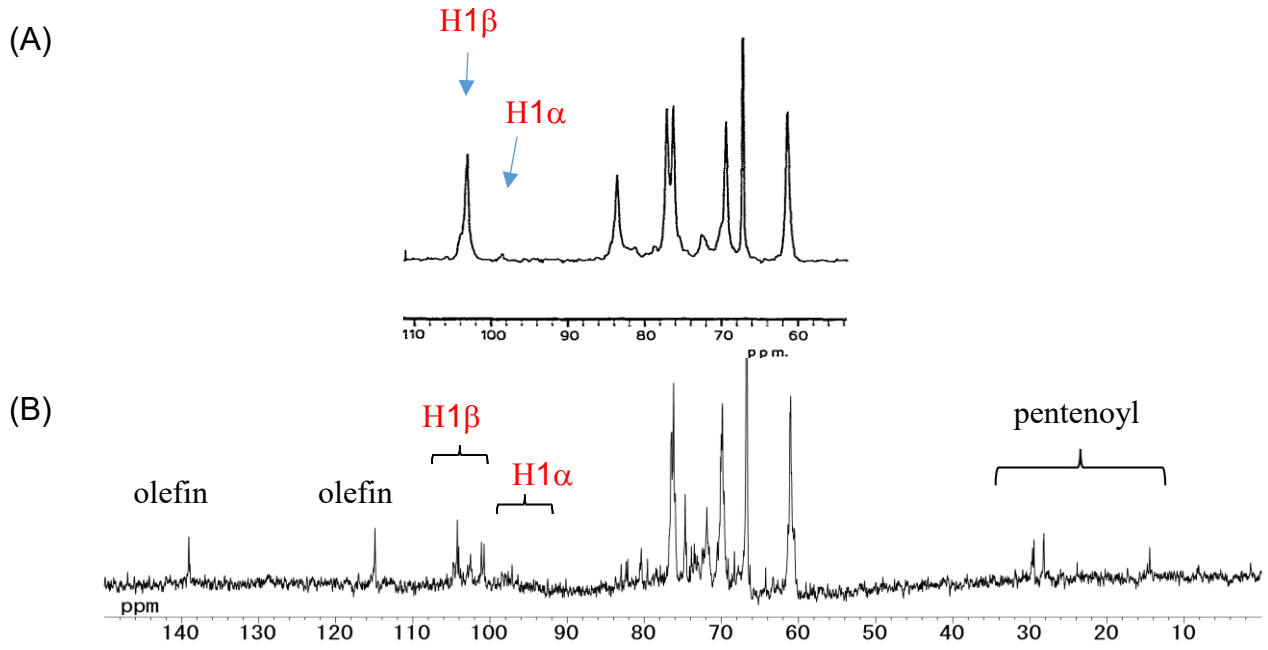


**Figure 3.2** $^{13}C$ NMR spectra (125 MHz, $D_2O$, rt) of reported nD-β-Glcp(1-2) (A) and the obtained polymer (B).

**Effects of monomer structure on the cationic ring-opening condensation polymerization**

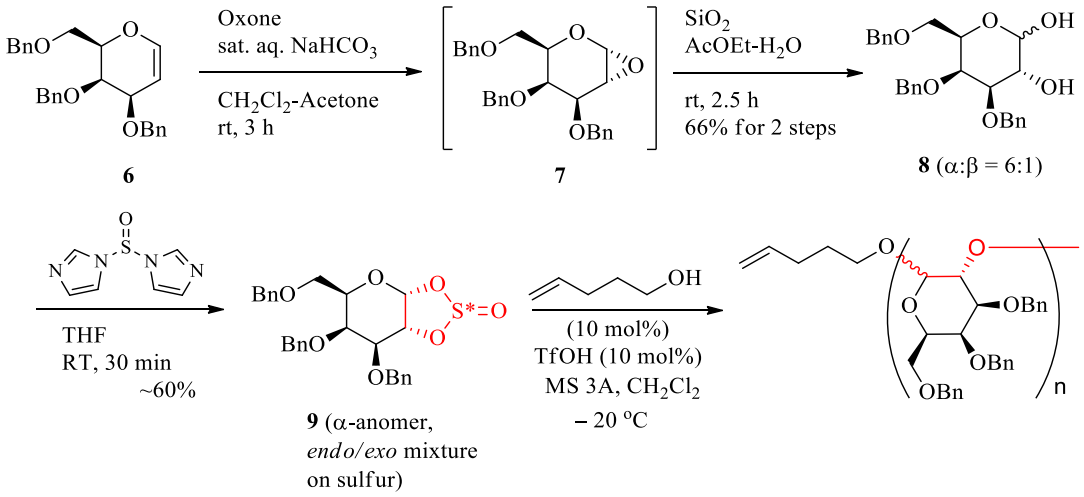


**Scheme 3.7** Synthesis of (1→2)-D-galactopyranan

To clarify the effects of monomer structure on the polymerization, I also examined the polymerization of cyclic sulfite **9** as a D-galactal derivative. The results are shown in the Table 3.2.

**Table 3.2** Effects of monomer structure on the polymerization.

| monomer | initiator (mol%) | acid | dehydrator[c] | temp (°C) | time (h) | Conv. (%) | $M_n$[d] (Da) | $M_w/M_n$[e] | $[\alpha]_D$[f] |
|---|---|---|---|---|---|---|---|---|---|
| **4** | 10 | TfOH | MS 3Å | –20 | 41 | 55 | 3000 | 1.3 | +37 |
| **9** | 10 | TfOH | MS 3Å | –20 | 41 | 99 | 4150 | 3.2 | +75 |

[a] The reaction was performed by using **9** (0.33 mmol), initiator (10 mol%), and acid (10 mol%) in the presence of a dehydrator in $CH_2Cl_2$ (0.6 M). [b] Monomer conversion ratio was determined by $^1$H NMR spectra of the crude mixture. [c] 50 wt% of dehydrator per **I** was used. [d] Number-average molecular weights ($M_n$) were estimated by the integral ratio in the $^1$H NMR spectra. [e] Polydispersity indices ($M_w/M_n$) were determined by a size exclusion chromatography (SEC) using DMF as an eluent. [f] Specific optical rotation ($[\alpha]_D$) was measured in $CHCl_3$ at 25–28 °C.

The polymerization of **9** was performed at the same manner that of **4**, which afforded a quantitative yield of the polymer. The yield is in a good contrast to that from **4**, clearly indicating the higher reactivity of **9**. The reason might be attributed to the stereochemistry of –OBn groups at C3, C4, and C6 positions projecting the β plane, which facilitates the attack of pentenol initiator at C1 position from the α plane. As a result, the resulting polymer would have higher ratio of α-anomeric center than that of β-anomeric center, because of the steric hindrance of the β plane. In this case, the reaction could

form the oxocarbenium cation intermediate. The structures of the obtained polymer were evaluated by IR, $^{1}$H NMR, $^{13}$C NMR, and MALDI–TOF mass spectra.

In the IR spectrum, the absence of the characteristic signal of sulfite at around 1200 $cm^{-1}$ was observed, implying that the polymerization of **9** efficiently eliminates $SO_2$ to form polyoxyethylene main chain (Figure 3.35). The appearance of olefinic proton signals in the $^{1}$H NMR spectrum supports the introduction of pentenoyl group to the polymer terminus. The number average of molecular weight ($M_n$) was determined on the basis of the integral ratio between the internal olefinic proton of pentenoyl group and the other aliphatic protons in the $^{1}$H NMR spectrum. The distribution ($M_w/M_n$) was estimated by a size exclusion chromatography (SEC) using *N*,*N*-dimethylformamide (DMF) based on polystyrene standards. In the MALDI–TOF mass spectrum, the observed values were agreed with the theoretical values corresponding to the polymer, supporting the formation of pentenoyl group-terminated polymers.

I also measured the specific optical rotations ($[\alpha]_D$) of the polymer. As a result, it was found that polymer exhibits a higher positive $[\alpha]_D$ value compared with the polymer prepared from **4**. Therefore, the polymer obtained from **9** seem to be consisting of much more α-glycosidic linkages than the other polymer from **4**.

CD and UV spectra of the polymer prepared at –20 °C and the β-unimer were measured (Figure 3.3). In the UV spectra, the signal of the polymer exhibits hypochromicity (lower intensity) compared with that of unimer, which implies that aromatic groups in the polymer have π-stacked conformation.

In the CD spectrum of the polymer, the positive signal around 205 nm is larger and the negative signal around 194 nm is smaller than those of unimer. Such results suggest that the polymer has a chiral higher-order-structure like a helical structure.

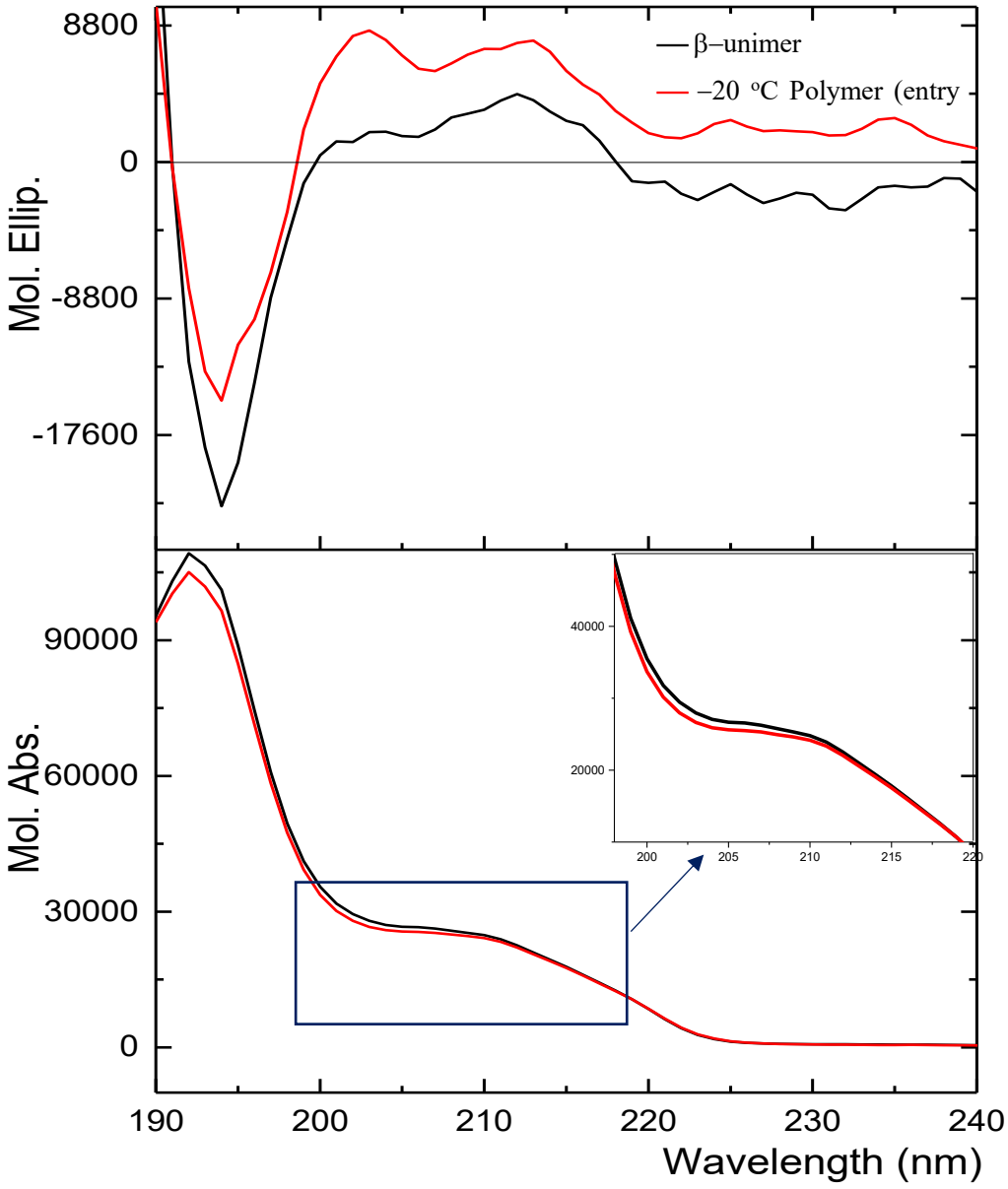


**Figure 3.3** CD and UV spectra of β-unimer and polymer (entry 7) at room temperature (cyclohexane, $10^{-4}$ μM).

**Application of glycosylation-active terminal group to the synthesis of oligosaccharide-containing glycoside.**

The importance of glycosylation-active terminal group of the obtained polymers was demonstrated by using cinnayl alcohol as a glycosyl acceptor. The reaction was performed in the presence of 10 equivalent of cinnamyl alcohol and bis(2,4,6-trimethylpyridine)iodonium hexafluorophosphate as a catalyst at 0 °C.[14] The conversion was estimated by $^1$H NMR analysis to be 70%. The observed mass values in the MALDI–TOF MS spectra showed a simple pattern, which agreed with the theoretical values of the structure with cinnamyl alcohol group at the terminus. These results indicate that our synthesized polymer can be grafted onto the materials bearing an alcohol.

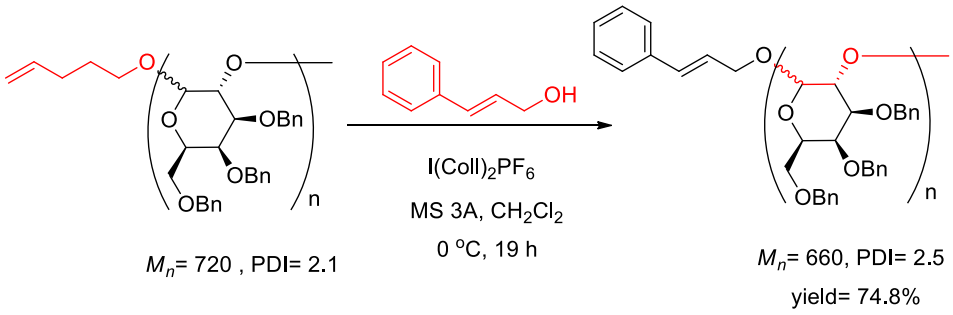


**Scheme 3.8** Glycosyl activity of terminal pentenoyl group of (1→2)-β-D-glucopyranan.

### 3.3 Conclusion

In conclusion, I first discovered the usefulness of cyclic sulfite **4** monomer for 1,2-glycosidic polymer as a surrogate of glycal epoxide. I achieved the creation of glycosylation-active polymer with

terminal pentenoyl group via cationic ring-opening condensation polymerization of cyclic sulfite. The anomeric stereocenters of polymer were moderately controllable by changing the reaction temperature. As an application, I demonstrated the glycosylation using the terminal group of the synthetic polymer to cinnamyl alcohol to give the corresponding glycoside.

### 3.4 Experimental

**General methods:**

**Materials.** Tetrahydrofuran (THF) (Kanto Chemical Co., Inc.) was freshly distilled in the presence of sodium and benzophenone under nitrogen atromsphere before use. Dichloromethane was distilled over $CaH_2$ and stored with MS 4Å. MS 3Å as a dehydrator was activated by three times heating for 1 min in a microwave oven following careful heating by a heat gun under vacuum. The other chemicals were used without purification. Cyclic sulfite was prepared according to the literature: A. Benksim, D. Beaupère, A. Wadouachi, *Org. Lett.* **2004**, *6*, 3913-3915.

**Measurements.** $^{1}H$ NMR (400 and 600 MHz) and $^{13}C$ NMR (100 and 150 MHz) spectra were recorded on JEOL JNM-ESC400 and JNM-ESC600 spectrometers using $CDCl_3$ as the solvent, calibrated using residual undeuterated solvent and tetramethylsilane as the internal standard. FT-IR spectra were measured using a Thermo Fischer Scientific Nexus 870 spectrometer. Optical rotation was measured with a JASCO P-1030 digital polarimeter. SEC analyses were carried out using a

chromatographic system consisting of a JASCO PU-2080 plus pump with a JASCO UV-1570 (UV detector) equipped with Shodex Asahipak GF-310 HQ (30 x 0.75 (i.d.) cm) (eluent DMF with LiCl (30 mM), flow rate 1.0 mL/min). UV-VIS absorption spectra were measured at room temperature with a JASCO V-570 spectrophotometer. CD spectra were taken on a JASCO J-820 spectrometer. MALDI–TOF MS spectra were recorded on a Shimadzu Voyager-DE STR-H mass spectrometer (matrix: α–CHCA) at Instrumental Analysis Division, Equipment Management Center Creative Research Institution, Hokkaido University.

**Typical procedure for the preparation of cyclic sulfite**[7,8,9] (For scheme and spectra, chapter 2)

To a solution of imidazole (5.59 g, 82.0 mmol) in THF (80 mL) was added dropwise $SOCl_2$ (1.49 mL, 20.5 mL) at 0 ºC. The mixture was warmed to room temperature, stirred for 30 min, and filtered. To the resulting *N*,*N*-thionyldiimidazole solution was added a solution of diol (1.54 g, 3.42 mmol) in THF (20 mL) at 0 ºC. The mixture was warmed to room temperature, stirred for 30 min, and carefully concentrated in vacuo below 30 ºC. The crude was purified by a florisil column chromatography (eluent: hexane : ethyl acetate = 9:1 → 3:1) to give the cyclic sulfite (689.1 mg) as an endo/exo diastereo-mixture (2:1) on the sulfur atom; In case of **D-glucal**; $[\alpha]_D^{25.2}$ +35.6 ($CHCl_3$, c. 1.00); $^1$H NMR (400 MHz, 298 K, $CDCl_3$) δ 7.37–7.14 (15H, m) 6.37 (0.63H, d, *J* = 4.8 Hz), 6.12 (0.37H, d, *J* = 6.0 Hz), 4.96–4.28 (7H, m), 4.14–3.57 (5H, m) ppm; $^{13}$C NMR (100 MHz, 298 K, $CDCl_3$) δ 138.0, 137.9, 137.79, 137.76, 137.4, 137.1, 128.8, 128.61, 128.58, 128.54, 128.49, 128.47, 128.24, 128.21,

128.1, 128.0, 127.94, 127.90, 105.9, 102.4, 83.8, 80.1, 75.8, 75.0, 74.8, 74.6, 74.3, 74.0, 73.7, 73.5, 72.8, 72.6, 71.4, 68.7, 68.6, 67.9 ppm; IR (NaCl) $\upsilon$ 3088, 3063, 3031, 2868, 1773, 1496, 1454, 1365, 1214 (OS(O)O), 1164, 1099, 1028, 989, 893, 819, 773, 740, 699 $cm^{-1}$; MALDI–TOF MS (matrix: α–CHCA) calc'd for $C_{27}H_{28}NaO_7S^+$ [M+$Na^+$] 519.14; found 519.59. In case of **D-galactal**; $^1H$ NMR (400 MHz, 298 K, $CDCl_3$) δ 7.37–7.14 (15H, m) 6.37 (0.48H, d, *J* = 4.4 Hz), 6.12 (0.50H, d, *J* = 5.4 Hz), 4.96–4.28 (7H, m), 4.14–3.57 (5H, m) ppm.

**Typical procedure for the preparation of unimer**

To a solution of cyclic sulfite (157.6 mg, 0.317 mmol) and 4-pentene-1-ol (38.6 μL, 0.381 mmol) in $CH_2Cl_2$ (3.0 mL) was added $CaSO_4$ (100 mg) at room temperature. After stirring for 30 min, trifluoromethanesulfonic acid (2.8 μL, 0.032 mmol) was added to the mixture and the mixture was stirred for 14 h. The reaction was quenched by the addition of sat. aq. $NaHCO_3$. The products were extracted with $CHCl_3$, repeatedly. The combined organic layer was dried over $MgSO_4$, filtered, and concentrated in vacuo to give a crude material (160.8 mg). The crude was purified by a preparative silica gel column chromatography (eluent: hexane : ethyl acetate = 5:1) to give β-anomeric compound **5β** (65.0 mg, 40%) and α-anomeric compound **5α** (64.3 mg, 39%) as a colorless oil.

**5β**: $[\alpha]_D^{26.7}$ –5.07 ($CHCl_3$, c. 1.00); $^1H$ NMR (400 MHz, 298 K, $CDCl_3$) δ 7.40–7.18 (15H, m), 5.85 (1H, ddd, *J* = 11.2, 7.2, 4.4 Hz), 5.06 (1H, dbrd, *J* = 11.2 Hz), 5.00 (1H, dbrd, *J* = 7.2 Hz), 4.96 (1H, d, *J* = 7.4 Hz), 4.86 (2H, d, *J* = 8.4 Hz), 4.64 (1H, d, *J* = 8.0 Hz), 4.57 (1H, d, *J* = 8.0 Hz), 4.56 (1H,

d, $J$ = 7.4 Hz), 4.27 (1H, d, $J$ = 5.2 Hz), 3.97 (1H, dt, $J$ = 6.4, 4.4 Hz), 3.78 (1H, dd, $J$ = 7.2, 1.2 Hz), 3.72 (1H, dd, $J$ = 7.2, 3.2 Hz), 3.65–3.54 (4H, m), 3.51 (1H, brd), 2.43 (1H, brd), 2.17 (2H, q, $J$ = 4.4 Hz), 1.77 (2H, sext, $J$ = 4.4 Hz) ppm; $^{13}$C NMR (100 MHz, 298 K, $CDCl_3$) δ 138.8, 138.27, 138.26, 138.2, 128.6, 128.53, 128.49, 128.11, 128.07, 127.93, 127.91, 127.84, 127.75, 115.1, 102.9, 84.6, 77.7, 75.3, 75.2, 75.1, 74.9, 73.6, 69.5, 69.0, 30.3, 28.9 ppm; IR (NaCl) $\upsilon$ 3453, 3087, 3064, 3030, 2920, 2868, 1496, 1453, 1361, 1311, 1270 1209, 1114, 1063, 1028, 913, 736, 698 cm$^{-1}$; MALDI–TOF MS (matrix: α– CHCA) calc'd for $C_{32}H_{38}NaO_6^+$ [M+Na$^+$] 541.26; found 541.89.

**5α**: $[\alpha]_D^{26.5}$ +69.22 ($CHCl_3$, c. 1.00); $^1$H NMR (400 MHz, 298 K, $CDCl_3$) δ 7.42–7.18 (15H, m), 5.86–5.79 (1H, m), 5.05 (1H, dbrd, $J$ = 11.2 Hz), 5.00 (1H, dbrd, $J$ = 7.2 Hz), 4.98 (1H, d, $J$ = 7.6 Hz), 4.89 (1H, d, $J$ = 10.0 Hz), 4.85 (1H, d, $J$ = 7.2 Hz), 4.65 (1H, d, $J$ = 7.6 Hz), 4.53 (1H, d, $J$ = 10.0 Hz), 4.52 (1H, brd), 3.80–3.65 (7H, m), 3.50 (1H, brd), 2.15 (2H, brd), 1.74 (2H, brd) ppm; $^{13}$C NMR (100 MHz, 298 K, $CDCl_3$) δ 138.9, 138.3, 138.09, 138.06, 128.52, 128.51, 128.08, 128.03, 127.93, 127.87, 127.84, 127.77, 127.7, 115.2, 98.6, 83.7, 77.7, 75.5, 75.2, 73.6, 73.2, 70.7, 68.6, 67.7, 30.5, 28.7 ppm; IR (NaCl) $\upsilon$ 3385, 3064, 2921, 2871, 1496, 1453, 1361, 1312, 1276, 1208, 1067, 915, 737, 698 cm$^{-1}$; MALDI–TOF MS (matrix: CHCα) calc'd for $C_{32}H_{38}NaO_6^+$ [M+Na$^+$] 541.26; found 541.52.

### 3.3d Typical procedure for cationic ring-opening condensation polymerization of cyclic sulfite (Table 3.1, entry 4)

To a solution of cyclic sulfite (143.0 mg, 0.288 mmol) and 4-pentene-1-ol (2.9 μL, 0.029 mmol)

in $CH_2Cl_2$ (0.58 mL) was added a freshly activated MS 3Å (ca. 200 mg) as a dehydrator at room temperature. After stirring for 2.5 h at room temperature, trifluoromethanesulfonic acid (TfOH, 2.9 μL, 0.029 mmol) was added to the mixture. The mixture was stirred for 1 d at the same temperature. The reaction was quenched by the addition of $Et_3N$ (ca. 200 μL) and the following addition of sat. aq. $NaHCO_3$. The products were extracted with $CHCl_3$, repeatedly. The combined organic layer was dried over $MgSO_4$, filtered, and concentrated in vacuo to give a crude material. The crude dissolved in $CHCl_3$ was reprecipitated into hexane to remove the remaining organic salts as an yellow oil. The filtrate was concentrated in vacuo to give a crude polymer including unreacted monomer (124.1 mg) as a colorless amorphous. The remaining monomer was separated by a gel permeation column chromatography (eluent: $CHCl_3$) to give the polymer (76.0 mg, 61%) as a colorless oil. The number average molecular weight ($M_n$) was estimated by integral ratio between the internal olefinic proton at around 5.8 ppm and protons in a range from 5.2 ppm to 3.2 ppm to be $M_n$ 1800 Da. The polydispersity index ($M_w/M_n$) was estimated by a size exclusion column chromatography analysis (SEC, eluent: DMF) on the basis of polystyrene standards to be $M_w/M_n$ 1.42: $[\alpha]_D^{26.1}$ +52.44 ($CHCl_3$, c. 1.00); $^1$H NMR (400 MHz, 298 K, $CDCl_3$) δ 7.36-6.84 (m) 5.68 (brd), 5.00-3.10 (m), 2.08-1.88 (m), 1.76-1.52 (m) ppm; $^{13}$C NMR (100 MHz, 298 K, $CDCl_3$) δ 138.8-137.2 (m), 128.6-127.0 (m), 115.0-92.0 (m), 85.0-68.0 (m), 30.0-28.0 (m) ppm; IR (NaCl) $\upsilon$ 3486, 3063, 3030, 2921, 2866, 1496, 1454, 1361, 1209, 1068, 1028, 736, 698 $cm^{-1}$; Elemental analysis: calc'd for $C_{224.24}H_{237.36}O_{41.6}\cdot CHCl_3$ based on the polymerization degree (8.12) estimated by the $^1$H NMR spectrum (entry 5): C 72.77, H 6.46, Found:

C 72.58, H 6.24; No sulfur atom was detected.

**Typical procedure for glycosylation using pentenoyl group of (1→2)-β-D-glucopyranan to cinnamyl alcohol**

To a solution of polymer (entry 7, table 3.1) (50.0 mg, 0.016 mmol) and cinnamyl alcohol (21.6 mg, 0.016 mmol) in $CH_2Cl_2$ (1.5 mL) was added a freshly activated MS 3Å (ca. 75 mg) as a dehydrator at room temperature. After stirring for 1 h at room temperature, $I(Coll)_2PF_6$ (12.4 mg, 0.024 mmol) was added to the mixture at 0 °C. The mixture was stirred for 19 h at the same temperature (0 °C). The % conversion of cyclic sulfite was estimated on the basis of $^1$H NMR of reaction mass in $CDCl_3$ by integral ratio between olefinic at around 5.8 ppm and protons in a range from 5.2- 3.2 ppm. The reaction was quenched by the addition of $Et_3N$ (ca. 0.1 mL) and the following addition of sat. aq. $Na_2S_2O_3$. The products were extracted with $CHCl_3$, repeatedly. The combined organic layer was washed with $NaHCO_3$ and separated organic was dried over $MgSO_4$, filtered, and concentrated in vacuo to give a crude material. The crude material was purified by GPC preparative (eluent: $CHCl_3$) to give the polymer (38.0 mg, 74.8%) as a colorless oil as a mixture of compound having both α- end pentenoyl and cinnamyl alcohol. The number average molecular weight ($M_n$) and The polydispersity index ($M_w/M_n$) was estimated by a size exclusion column chromatography analysis (SEC, eluent: DMF) on the basis of polystyrene standards to be $M_n$ 660 Da and $M_w/M_n$ 2.5 respectively: $^1$H NMR (400 MHz, 298 K, $CDCl_3$) δ 7.36-6.84 (m), 6.60 (brd), 6.25 (brd), 5.68 (brd), 5.00-3.10 (m), 2.08-1.20

(m) ppm; $^{13}$C NMR (100 MHz, 298 K, $CDCl_3$) δ 138.8-137.2 (m), 128.6-127.0 (m), 105.0-92.0 (m), 85.0-68.0 (m), 30.0-28.0 (m), 22.5 (s), 14.5(s) ppm; IR (NaCl) $\upsilon$ 3476, 3088, 3063, 2920, 2866, 1952, 1879, 1813, 1748, 1605, 1496, 1453, 1361, 1210, 1068, 1028, 751, 736, 699 $cm^{-1}$.

**Figures**

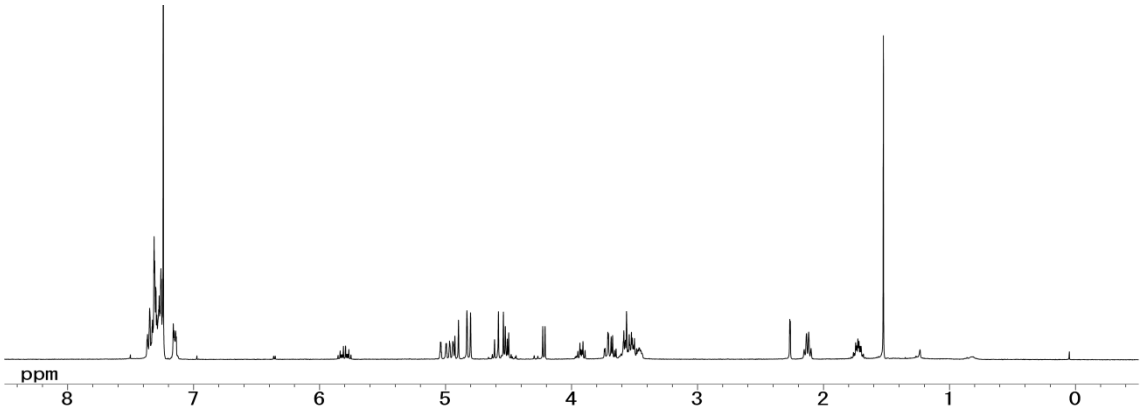


**Figure 3.4** $^1$H NMR spectrum of **5β** (400 MHz, $CDCl_3$, 293 K).

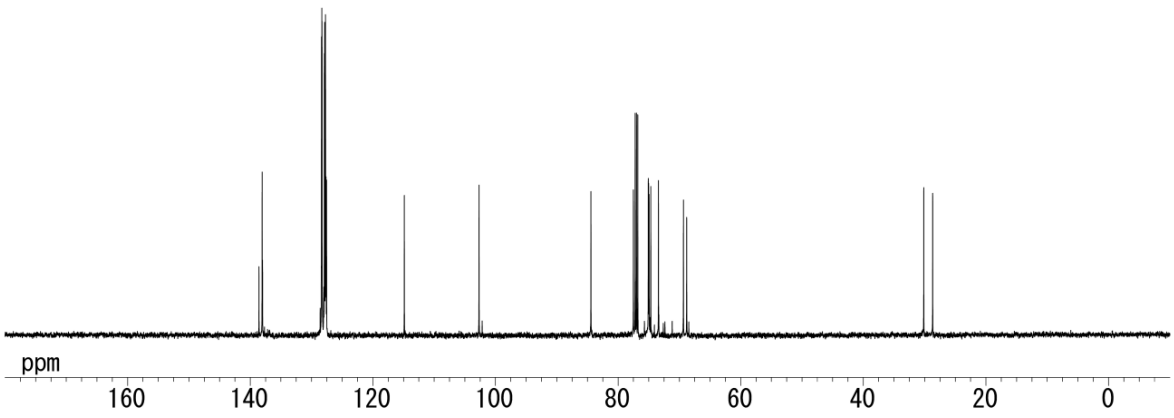


**Figure 3.5** $^{13}$C NMR spectrum of **5β** (150 MHz, $CDCl_3$, 293 K).

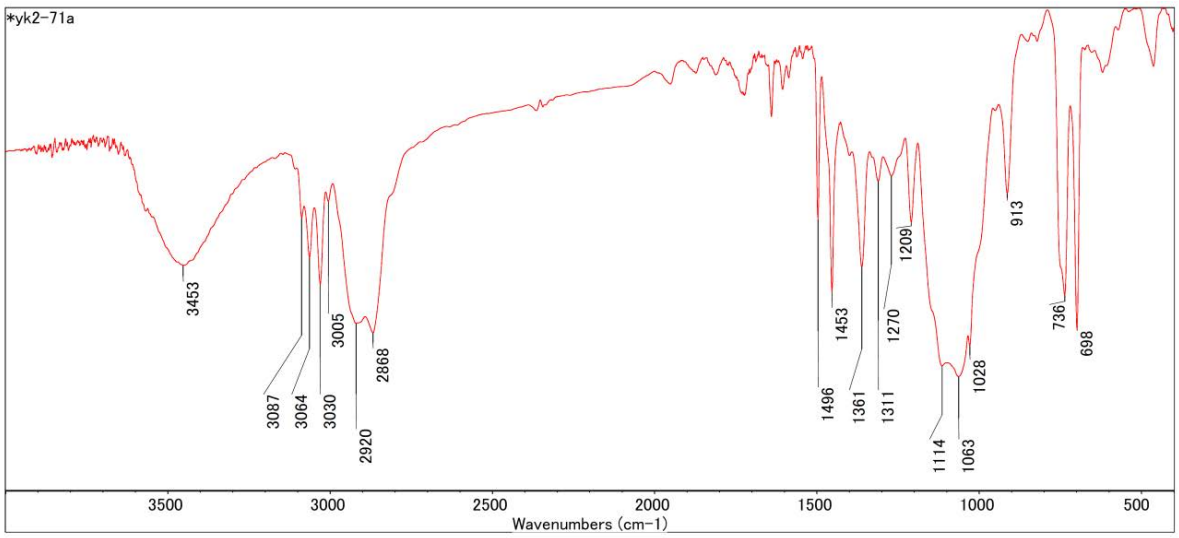


**Figure 3.6** IR spectrum of **5β** (NaCl).

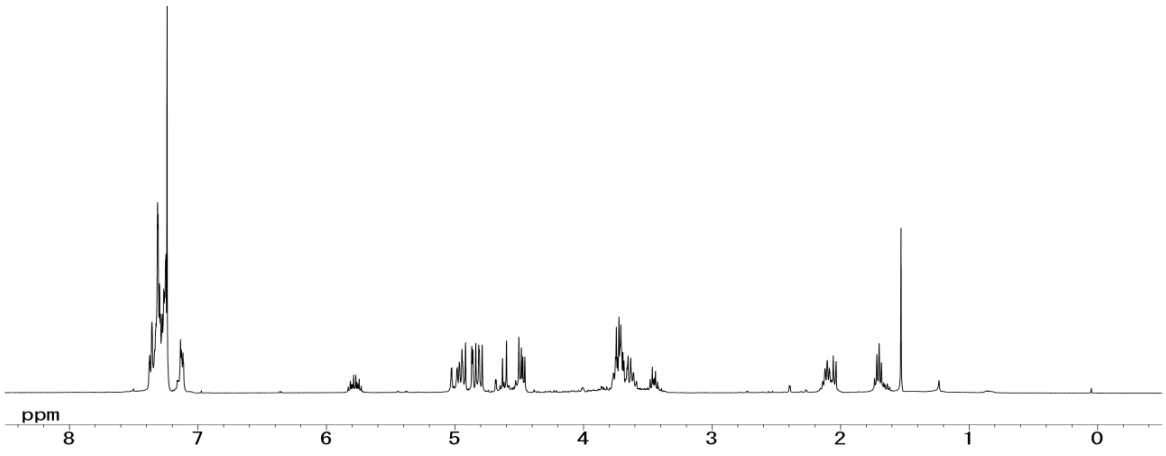


**Figure 3.7** $^{1}$H NMR spectrum of **5α** (400 MHz, $CDCl_3$, 293 K).

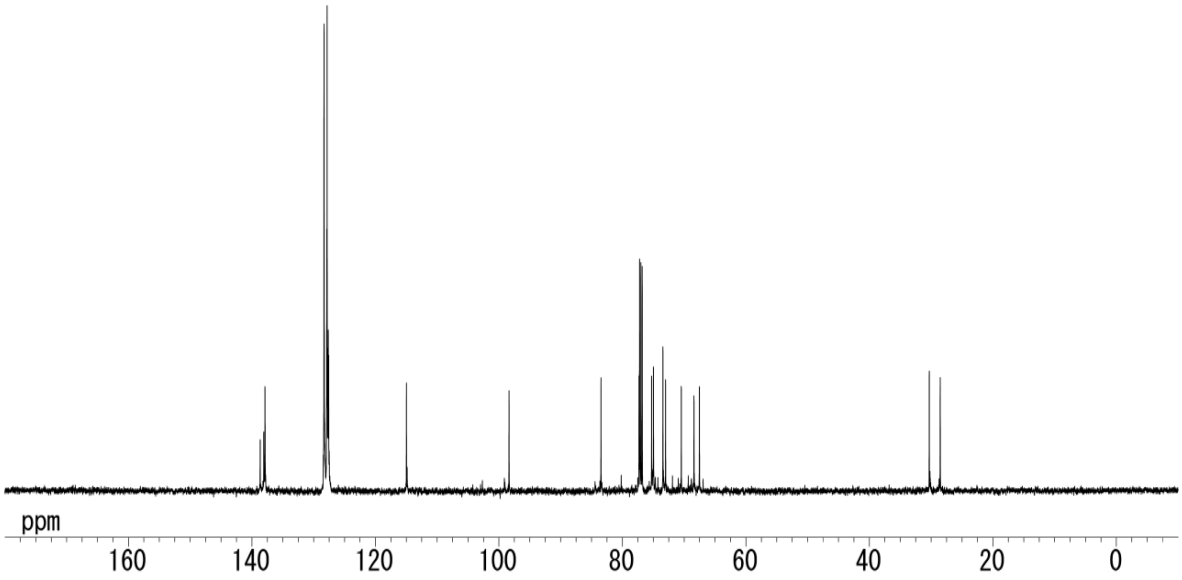


**Figure 3.8** $^{13}C$ NMR spectrum of **5α** (150 MHz, $CDCl_3$, 293 K).

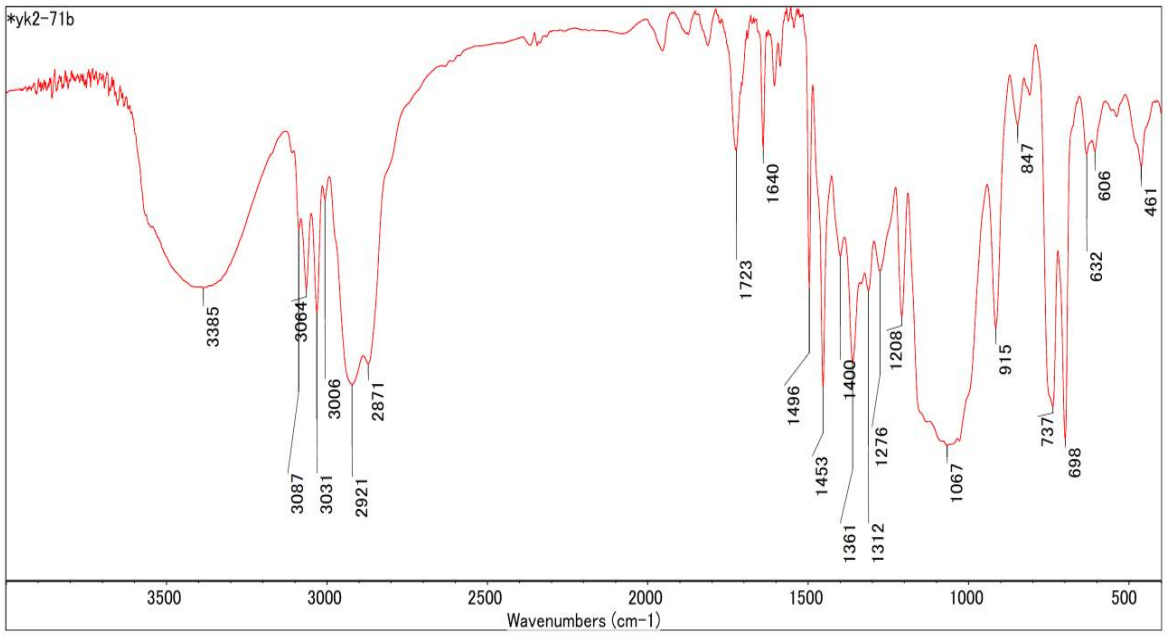


**Figure 3.9** IR spectrum of **5α** (NaCl).

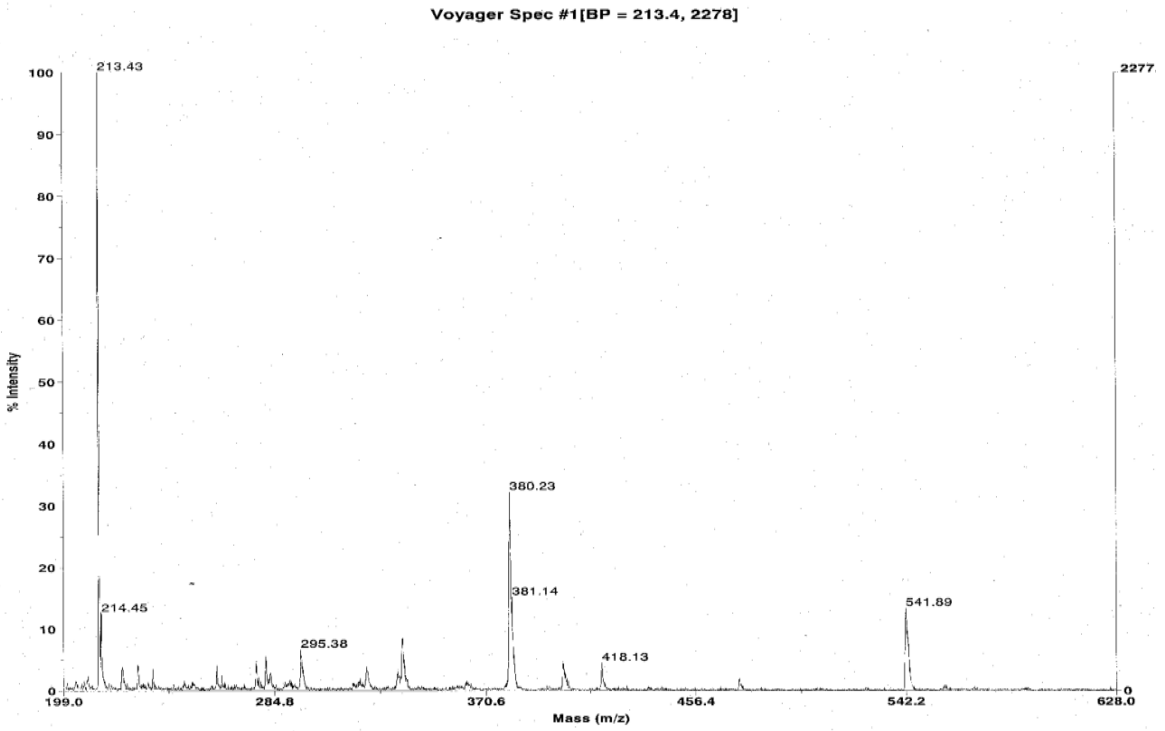


**Figure 3.10** MALDI–TOF MS spectrum of **5β**.

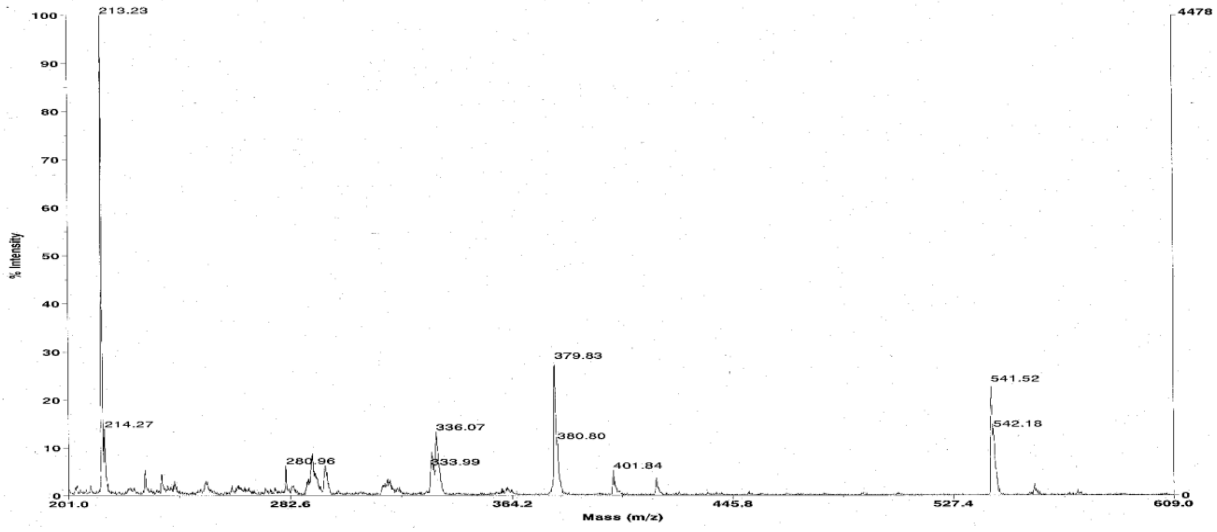


**Figure 3.11** MALDI–TOF MS spectrum of **5α**.

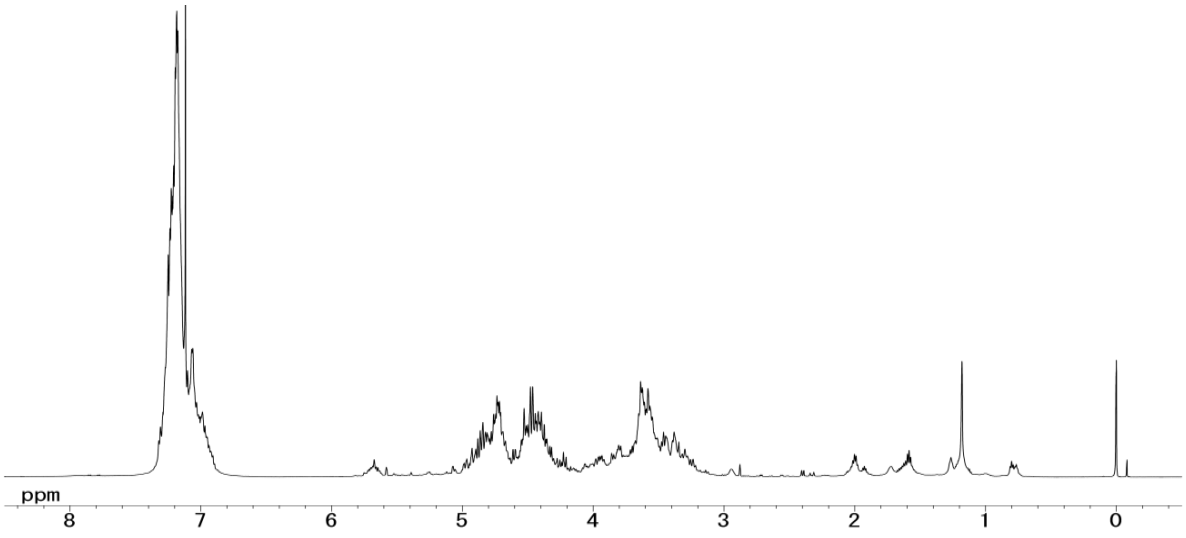


**Figure 3.12** $^{1}H$ NMR spectrum (100 MHz, $CDCl_3$, 293 K) of polymer obtained by the reaction at room temperature (Table 3.1, entry 4).

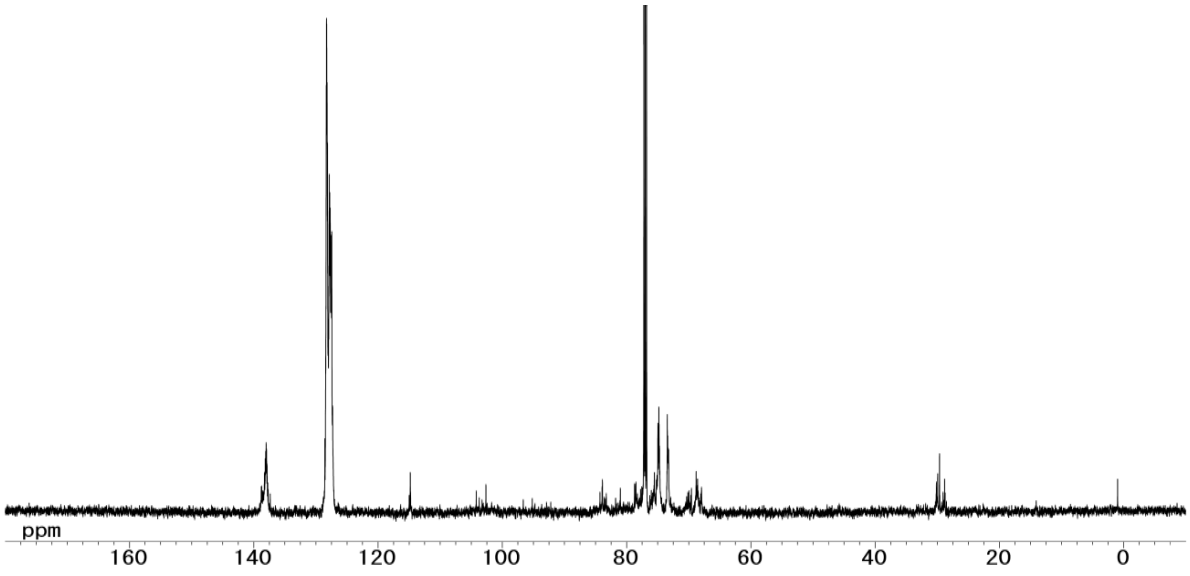


**Figure 3.13** $^{13}C$ NMR spectrum (150 MHz, $CDCl_3$, 293 K) of polymer obtained by the reaction at room temperature (Table 3.1, entry 4).

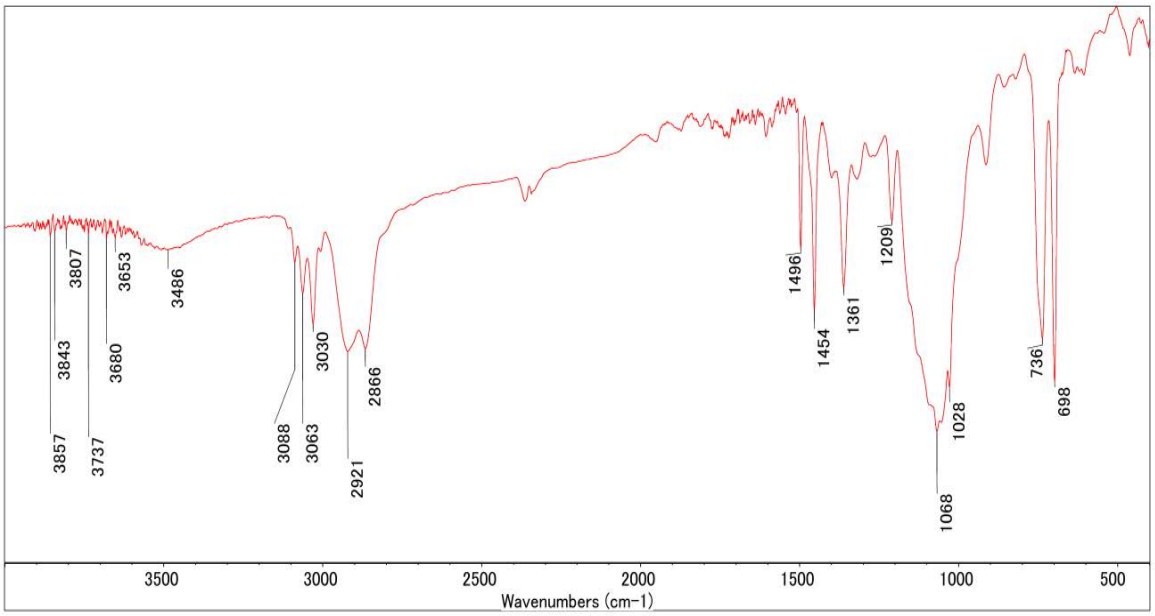


**Figure 3.14** IR spectrum (NaCl) of polymer obtained by the reaction at room temperature (Table 3.1, entry 4).

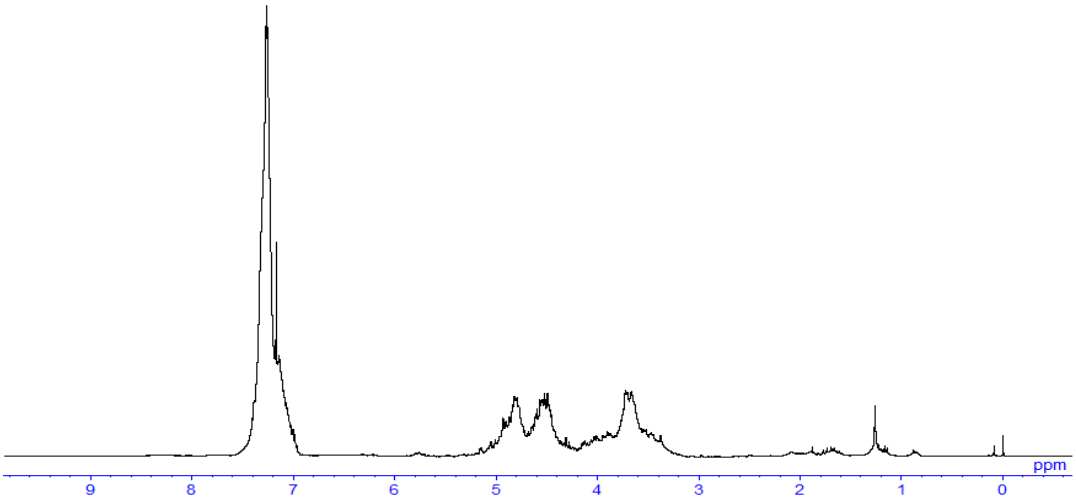


**Figure 3.15** $^{1}$H NMR spectrum (100 MHz, $CDCl_3$, 293 K) of polymer obtained by the reaction using 5 mol% of TfOH at room temperature (Table 3.1, entry 5).

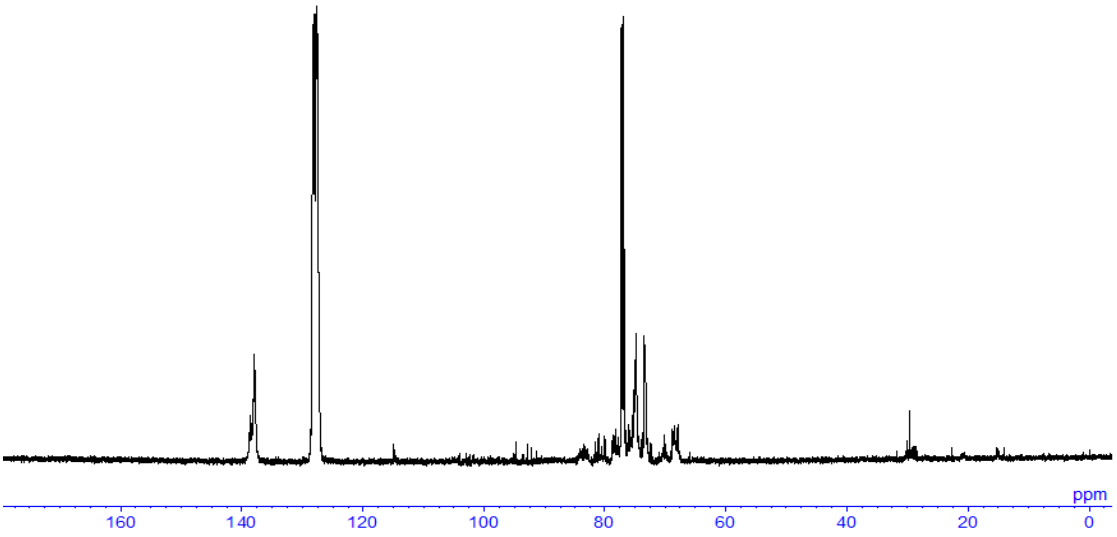


**Figure 3.16** $^{13}C$ NMR spectrum (150 MHz, $CDCl_3$, 293 K) of polymer obtained by the reaction using 5 mol% of TfOH at room temperature (Table 3.1, entry 5).

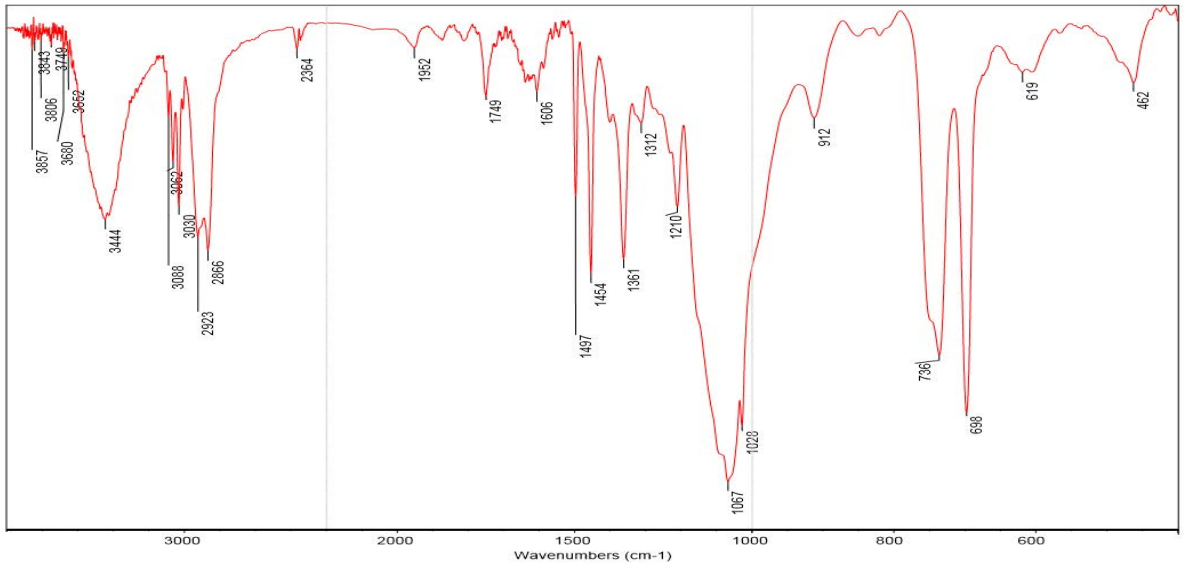


**Figure 3.17** IR spectrum (KBr) of polymer obtained by the reaction using 5 mol% of TfOH at room temperature (Table 3.1, entry 5).

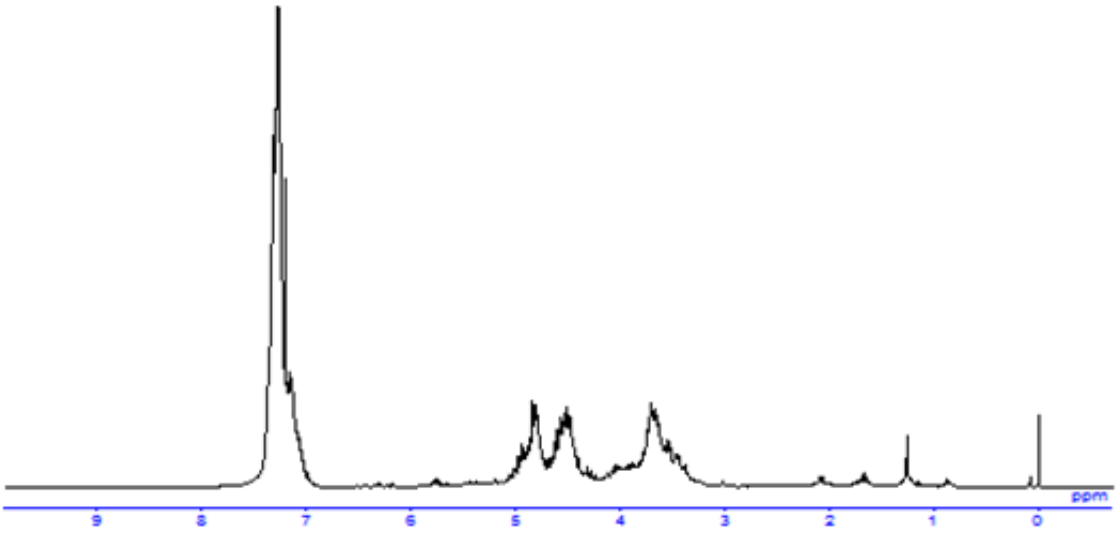


**Figure 3.18** $^{1}$H NMR spectrum (100 MHz, $CDCl_3$, 293 K) of polymer obtained by the reaction at −10 ºC (Table 3.1, entry 6).

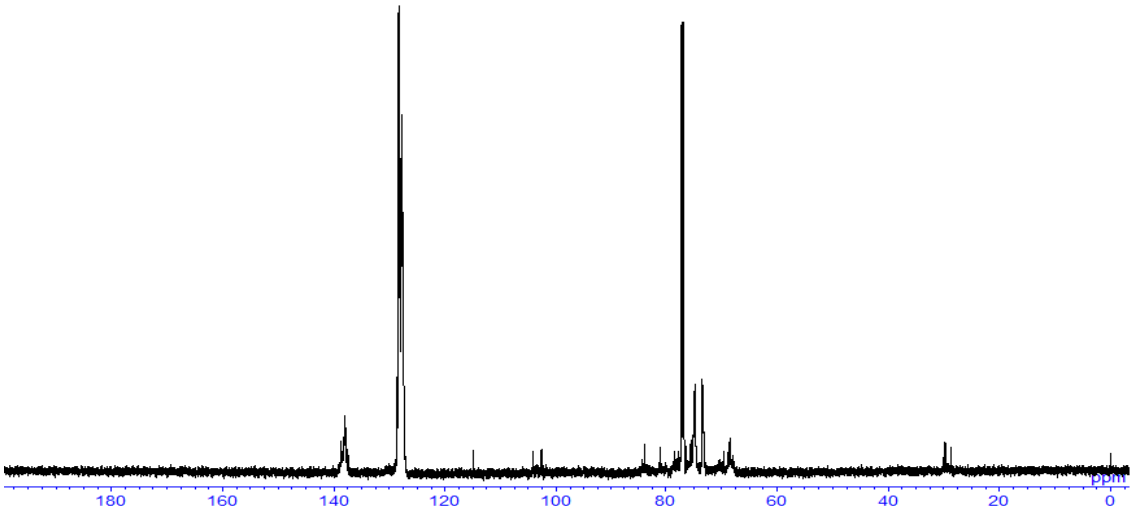


**Figure 3.19** $^{13}$C NMR spectrum (150 MHz, $CDCl_3$, 293 K) of polymer obtained by the reaction at −10 ºC (Table 3.1, entry 6).

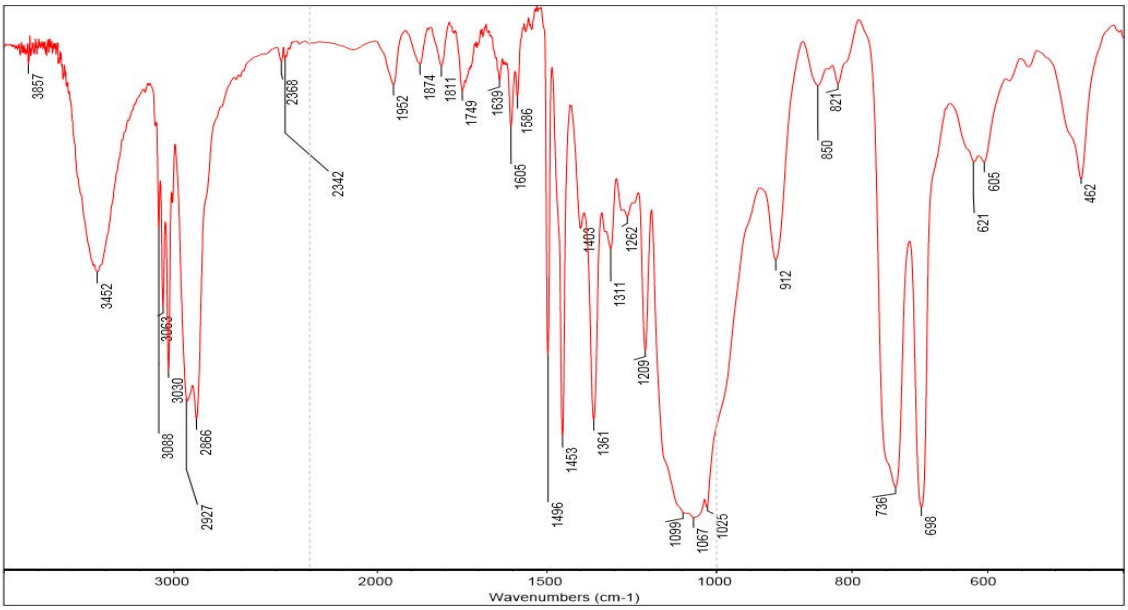


**Figure 3.20** IR spectrum of polymer obtained by the reaction at −10 ºC (Table 3.1, entry 6).

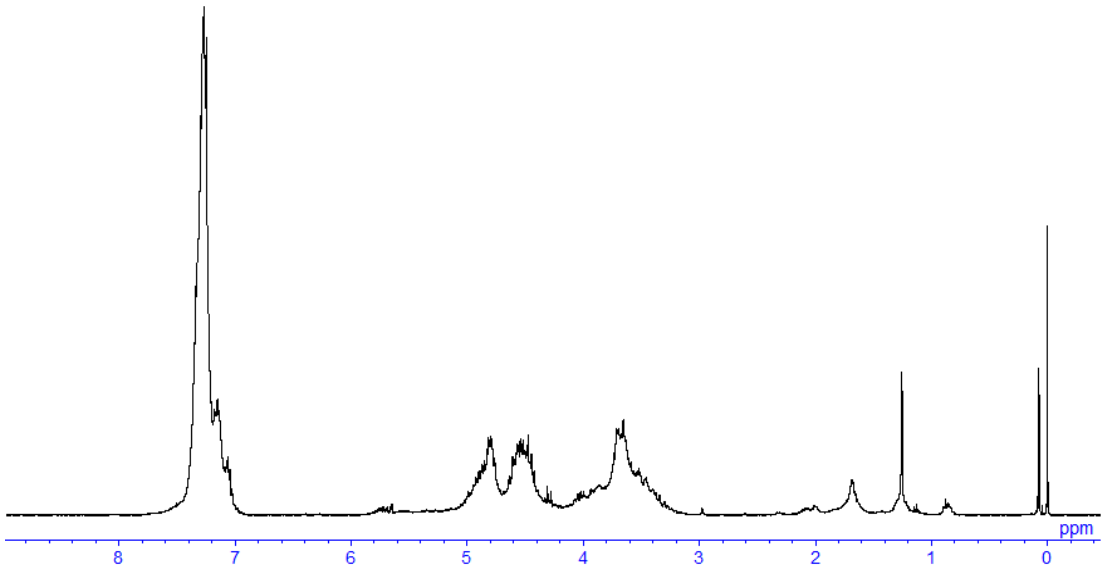


**Figure 3.21** $^{1}$H NMR spectrum (100 MHz, $CDCl_3$, 293 K) of polymer obtained by the reaction at −20 ºC (Table 3.1, entry 7).

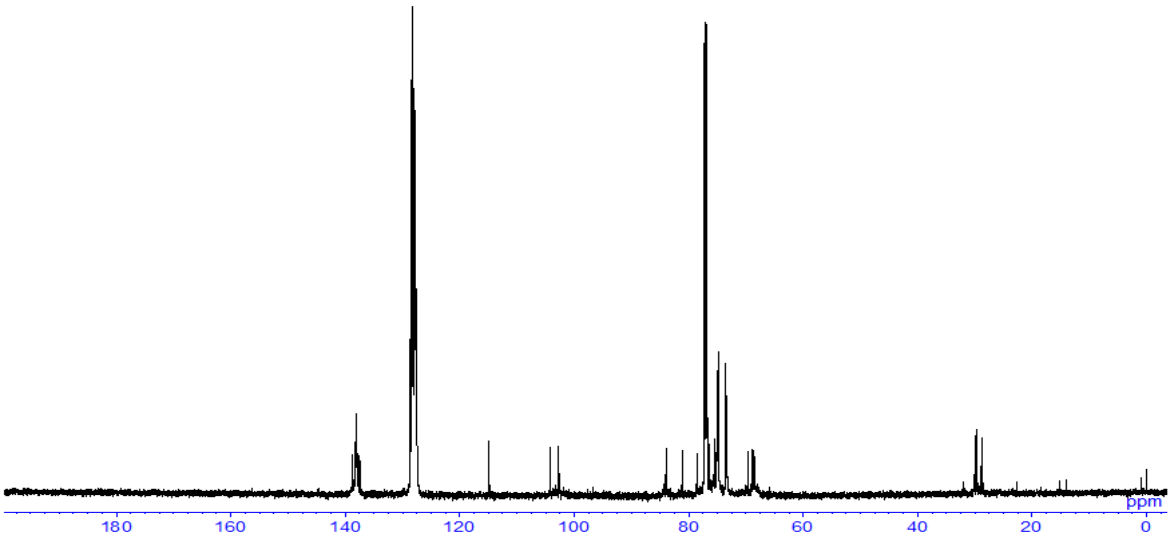


**Figure 3.22** $^{13}C$ NMR spectrum (150 MHz, $CDCl_3$, 293 K) of polymer obtained by the reaction at –20 ºC (Table 3.1, entry 7).

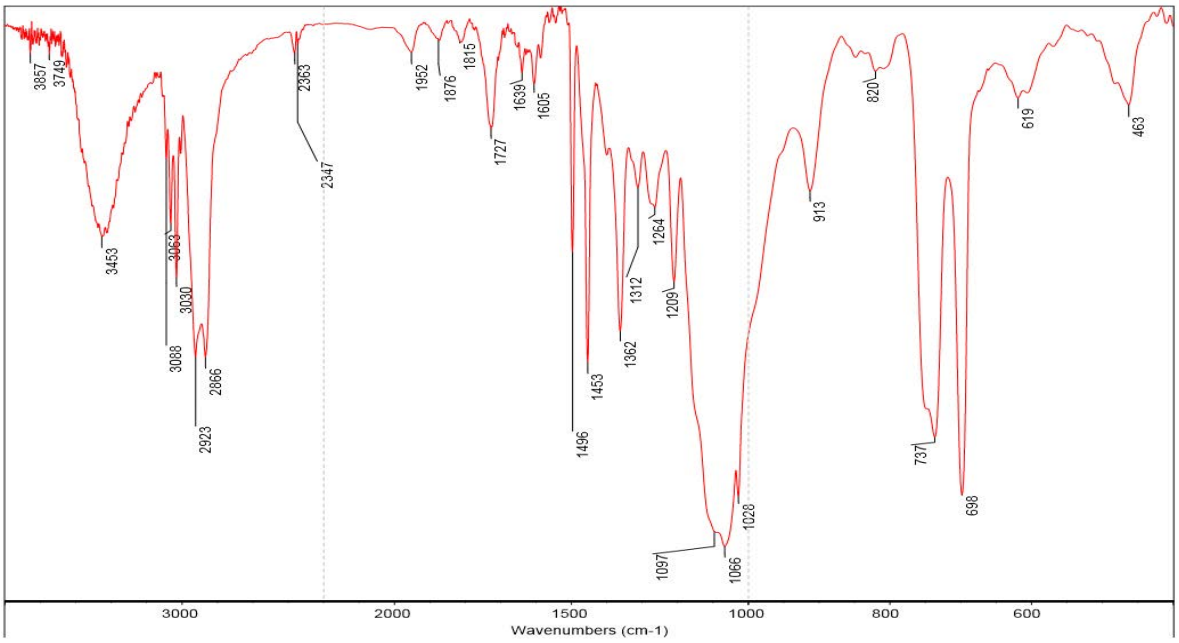


**Figure 3.23** IR spectrum of polymer obtained by the reaction at –20 ºC (Table 3.1, entry 7).

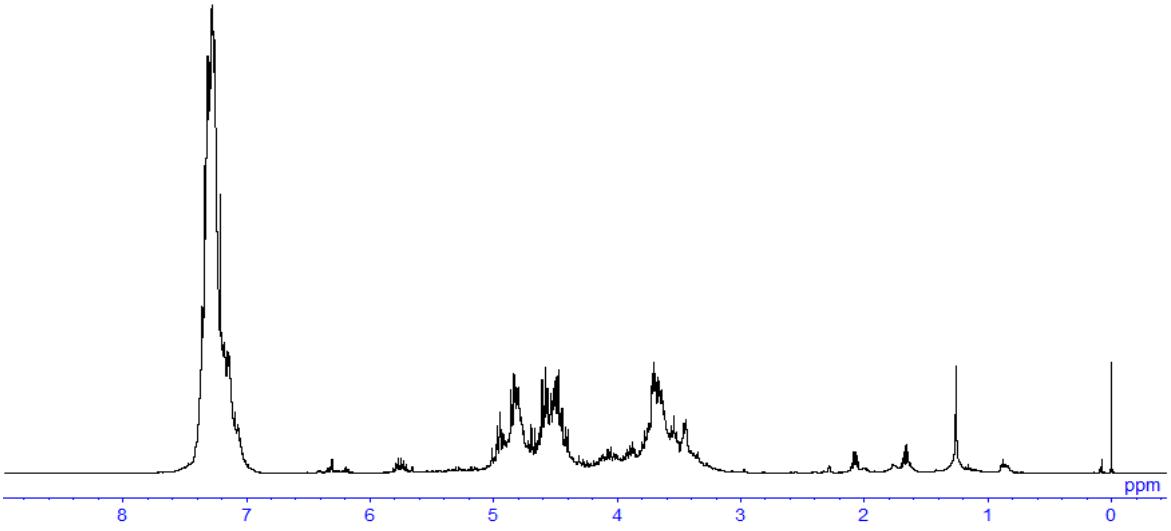


**Figure 3.24** $^{1}$H NMR spectrum (100 MHz, $CDCl_3$, 293 K) of polymer obtained by the reaction at –40 ºC (Table 3.1, entry 8).

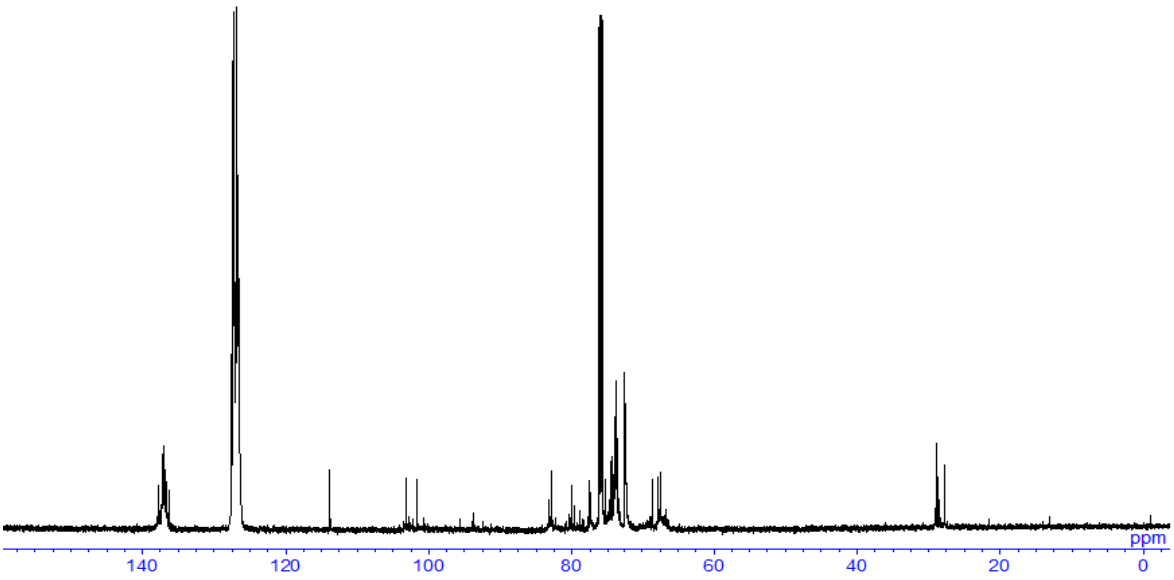


**Figure 3.25** $^{13}$C NMR spectrum (150 MHz, $CDCl_3$, 293 K) of polymer obtained by the reaction at –40 ºC (Table 3.1, entry 8).

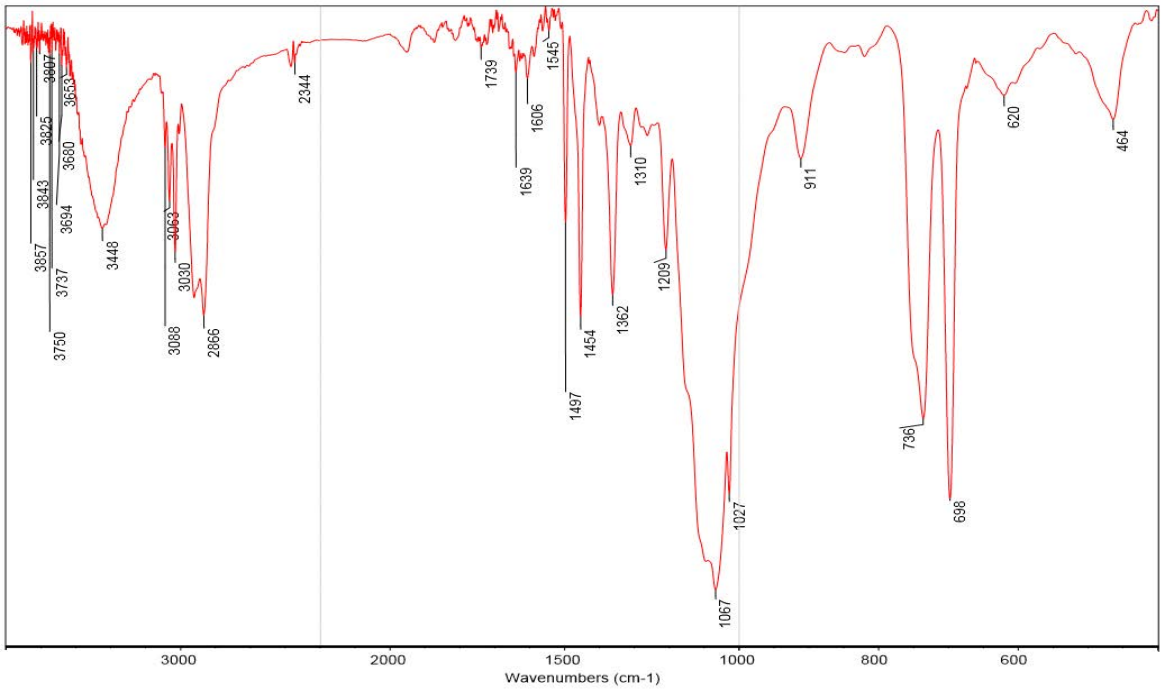


**Figure 3.26** IR spectrum of polymer obtained by the reaction at –40 ºC (Table 3.1, entry 8).

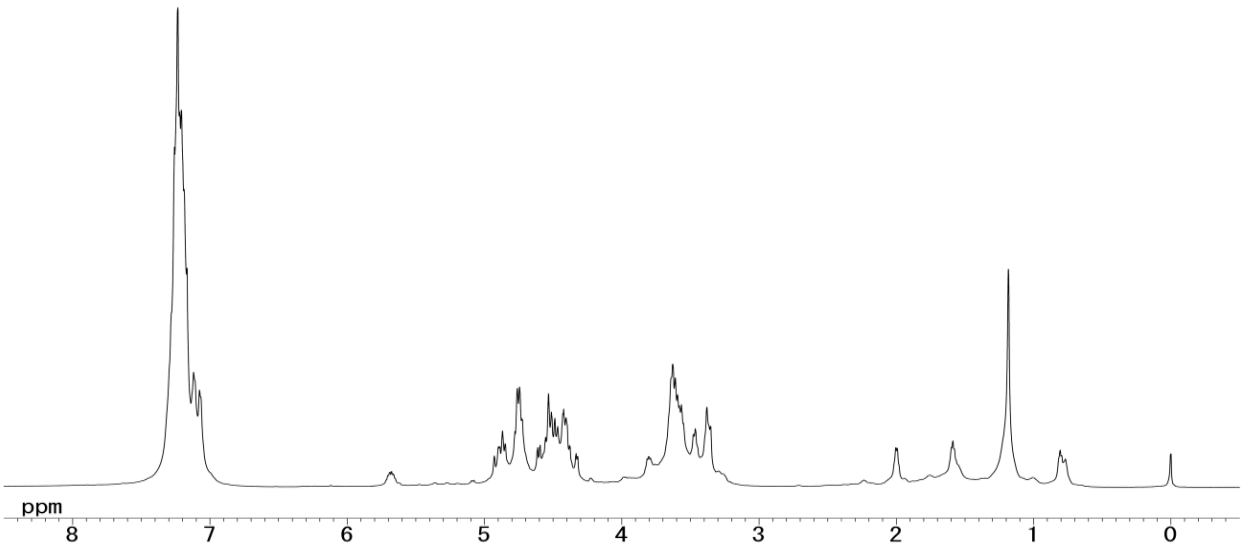


**Figure 3.27** $^{1}$H NMR spectrum (100 MHz, $CDCl_3$, 293 K) of polymer obtained by the reaction at –60 ºC (Table 3.1, entry 10).

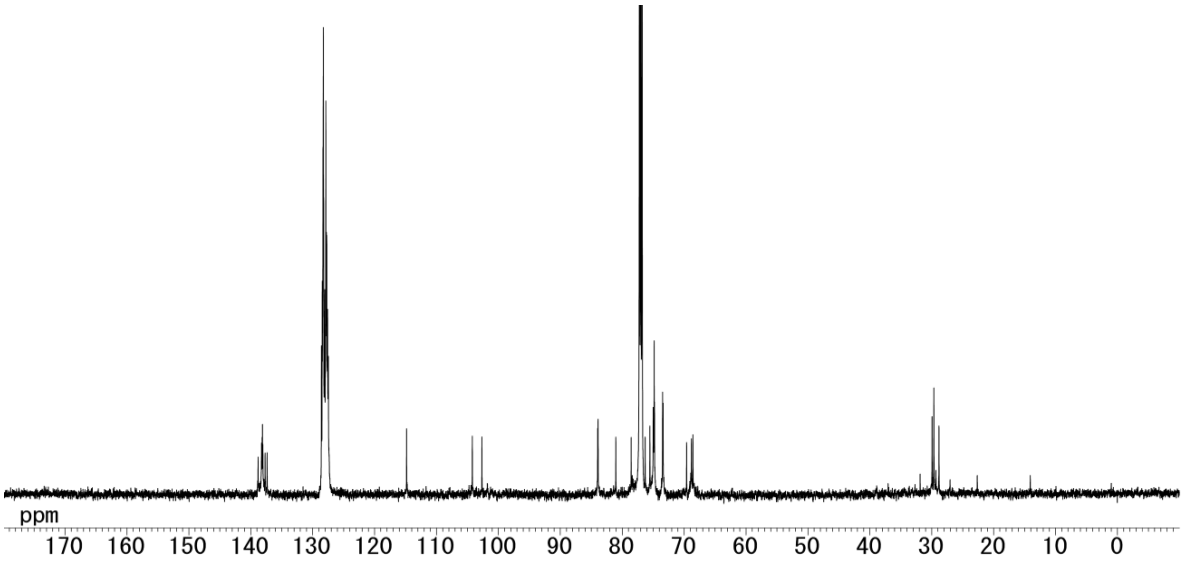


**Figure 3.28** $^{13}C$ NMR spectrum (150 MHz, $CDCl_3$, 293 K) of polymer obtained by the reaction at −60 ºC (Table 3.1, entry 10).

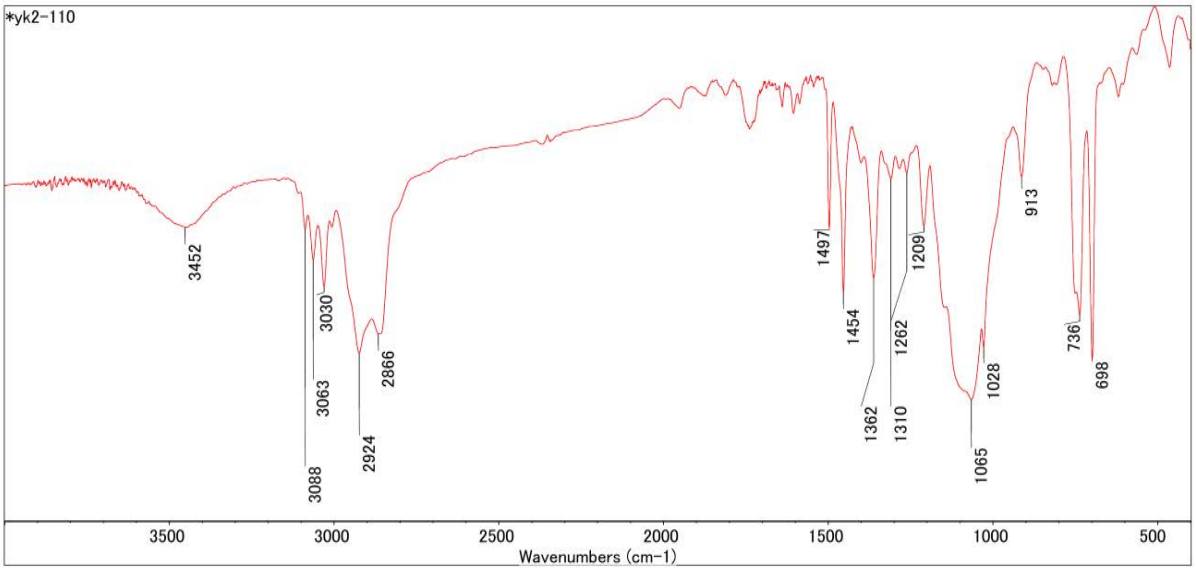


**Figure 3.29** IR spectrum (NaCl) of polymer obtained by the reaction at −60 ºC (Table 3.1, entry 10).

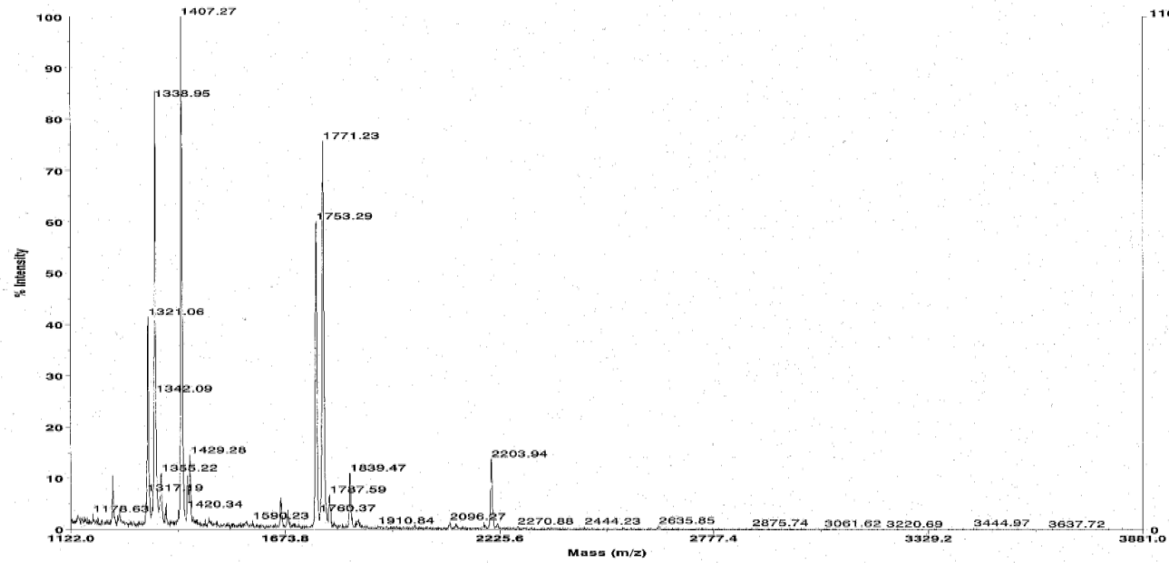


**Figure 3.30** MALDI–TOF MS spectrum of polymer obtained by the reaction in the presence of $CaSO_4$ at rt (Table 3.1, entry 10).

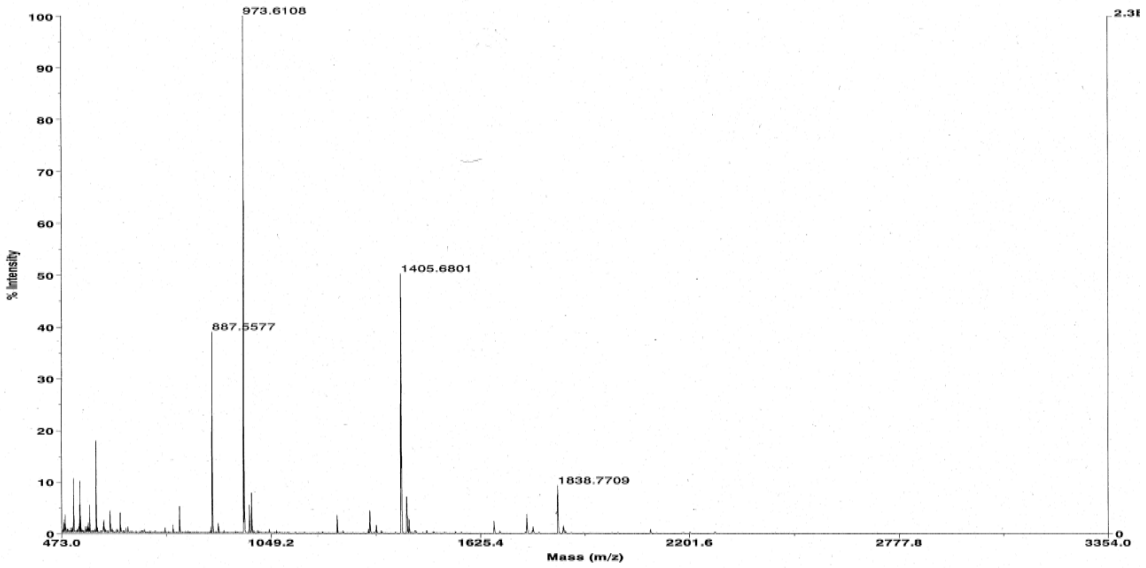


**Figure 3.31** MALDI–TOF MS spectrum of of polymer obtained by the reaction in the presence of MS 3Å at rt (Table 3.1, entry 10).

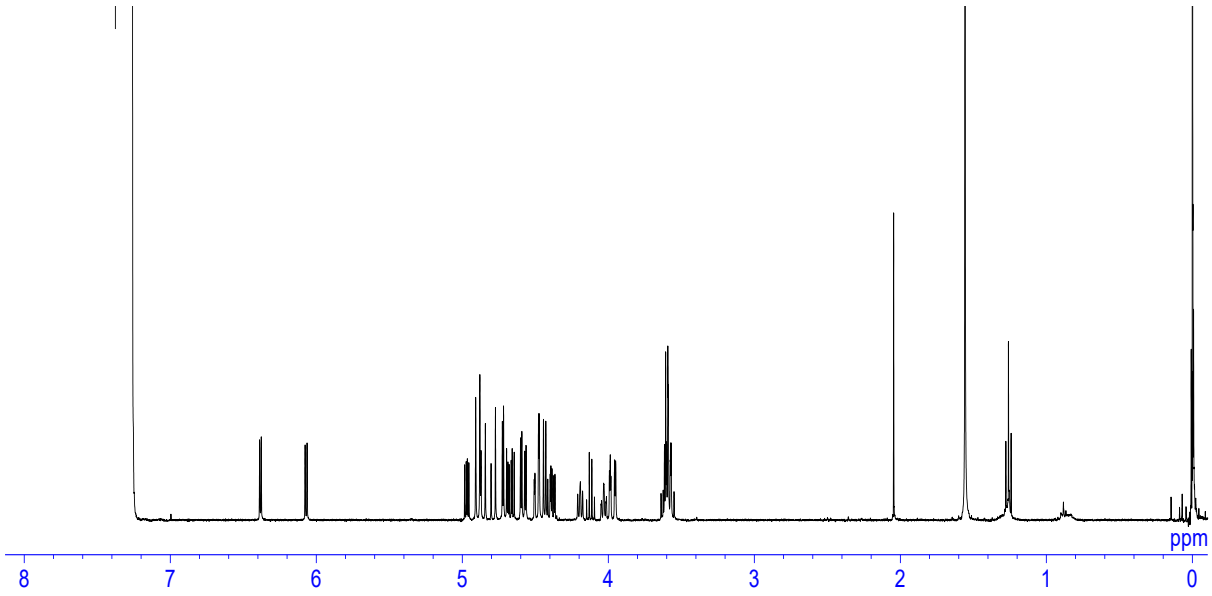


**Figure 3.32** $^{1}$H NMR spectrum (100 MHz, $CDCl_3$, 293 K) of D-galactal cyclic sulphite (Table 3.2)**.**

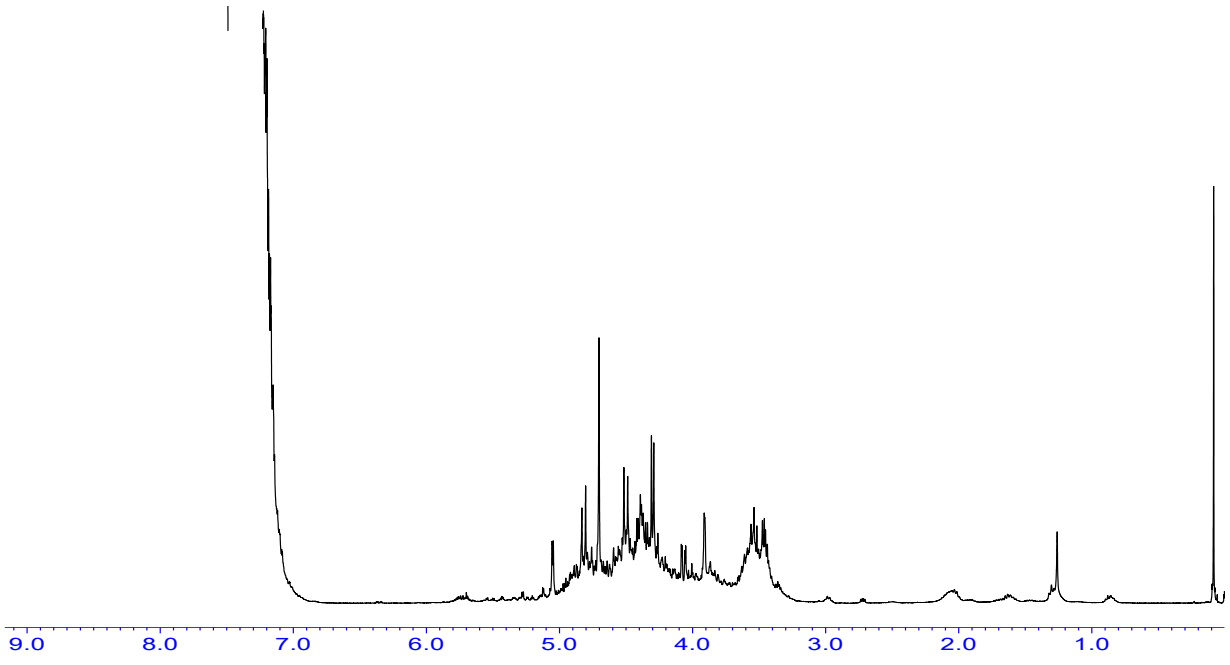


**Figure 3.33** $^{1}$H NMR spectrum (100 MHz, $CDCl_3$, 293 K) of D-galactal polymer obtained by the reaction at –20 ºC (Table 3.2).

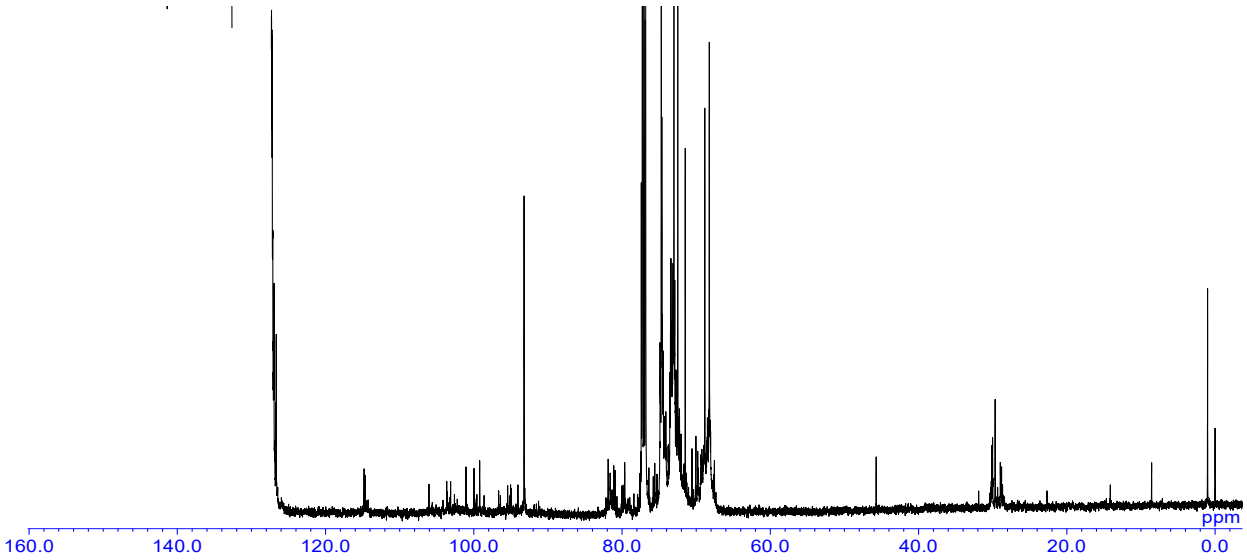


**Figure 3.34** $^{13}C$ NMR spectrum (150 MHz, $CDCl_3$, 293 K) of D-galactal polymer obtained by the reaction at –20 ºC (Table 3.2).

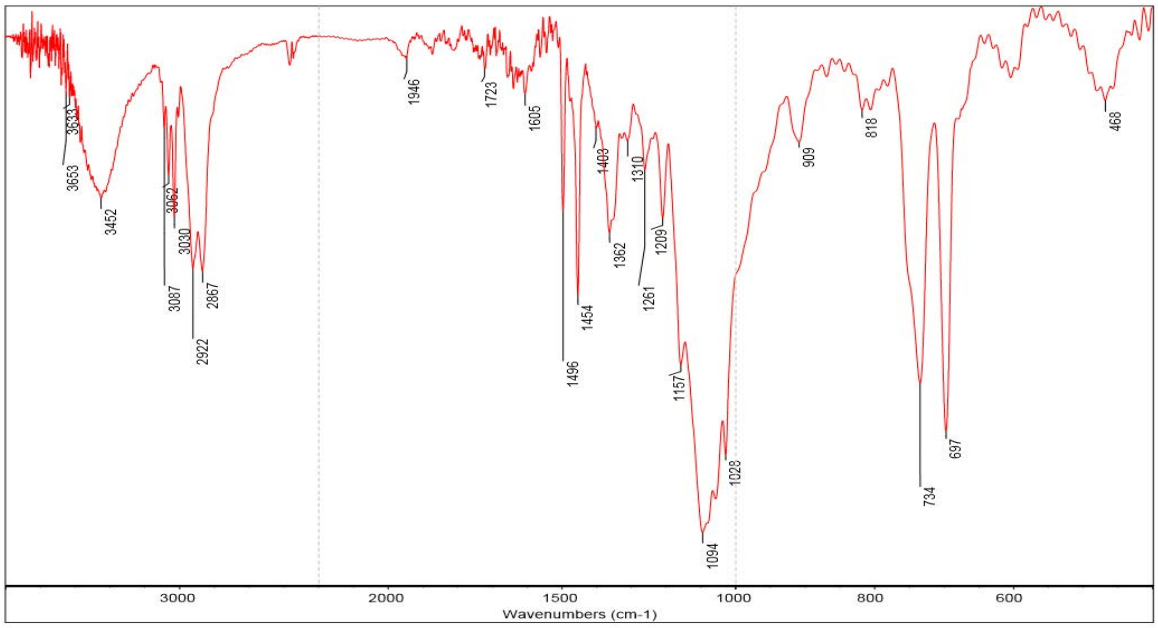


**Figure 3.35** IR spectrum (NaCl) of D-galactal polymer obtained by the reaction at –20 ºC (Table 3.2).

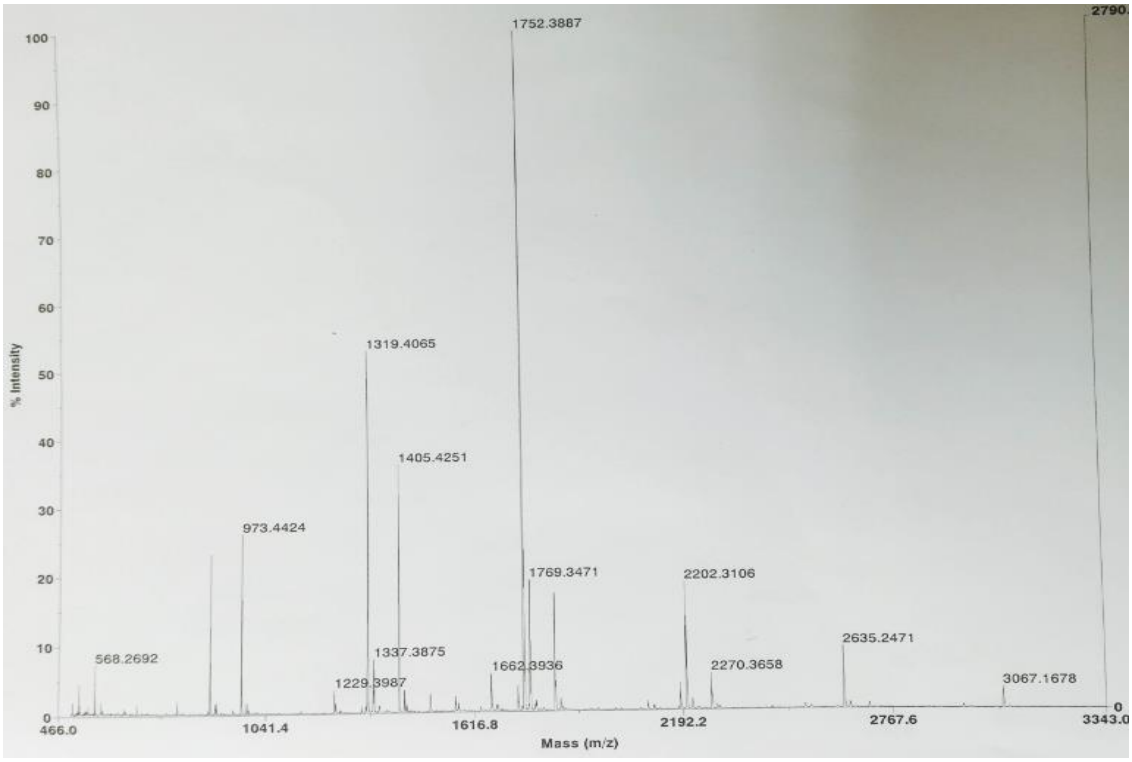


**Figure 3.36** MALDI–TOF MS spectrum of D-galactal polymer obtained by the reaction at –20 ºC (Table 3.2).

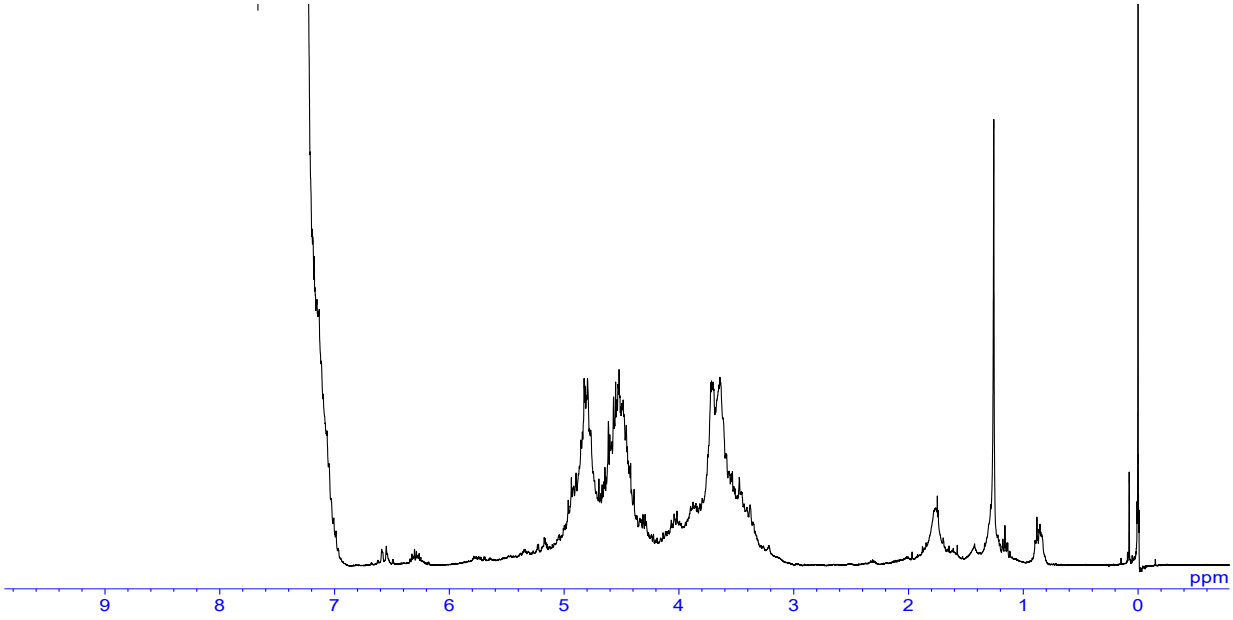


**Figure 3.37** $^{1}$H NMR spectrum (100 MHz, $CDCl_3$, 293 K) of polymer with cinnamyl alcohol terminal.

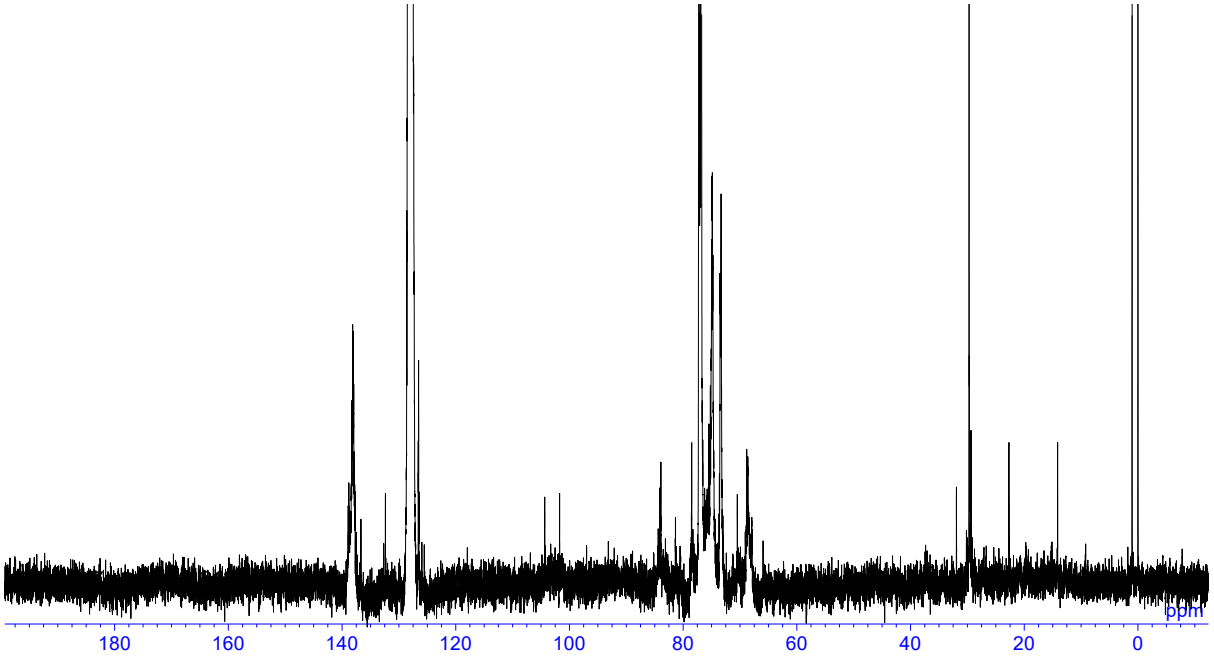


**Figure 3.38** $^{13}C$ NMR spectrum (150 MHz, $CDCl_3$, 293 K) of polymer with cinnamyl alcohol terminal.

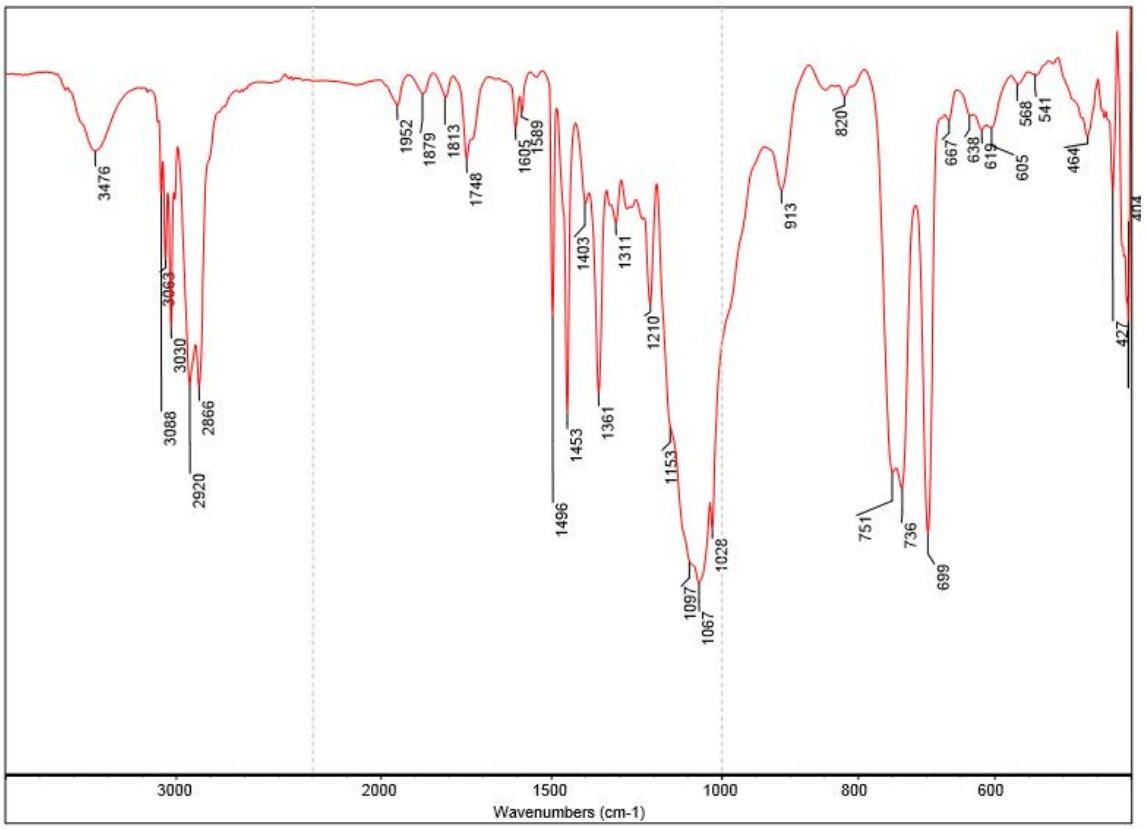


**Figure 3.39** IR spectrum (NaCl) of polymer with cinnamyl alcohol terminus.


**Figure 3.40** MALDI–TOF MS spectrum of polymer with cinnamyl alcohol terminal.

**References**


1) Azuma, N.; Sanda, F.; Takata, T.; Endo, T. *J. Polym. Sci. Part A: Polym. Chem.* **1997**, *35*, 3235-3240.

2) Kricheldorf, H. R.; Petermann, O. *Macromolecules* **2001**, *34*, 8841-8846.

3) Azuma, N.; Sanda, F.; Takata, T.; Endo, T. *Macromol. Chem. Phys.*. **1998**, *199*, 1785-1789.

4) For selected reports, see: (a) Mootoo, D. R.; Konradsson, P.; Udodong, U.; Fraser-Reid, B. O. *J. Am. Chem. Soc.* **1988**, *110*, 5583-5584. (b) Fraser-Reid, B. O.; Wu, Z.; Andews, C. W. Skowronski, E.; Bowen, J. P. *J. Am. Chem. Soc.* **1991**, *113*, 1435-1437.

5) Roset, M. S.; Ciocchini, A. E.; Ugalde, R. A.; de Iannino, N. I. *J. Bacteriol*. **2006**, *188*, 5003-5013.

6) Yoshimura, M.; Miyamoto, K. S. *Bunseki Kagaku.*, **1980**, *29*, 40-44.

7) Meslouti, A. E.; Beaupère, D.; Demailly, G.; Uzan, R. *Tetrahedron Lett.* **1994**, *35*, 3913-3916.

8) Benksim, A.; Massoui, M.; Beaupère, D.; Wadouachi, A. *Tetrahedron Lett.* **2007**, *48*, 5087-5089.

9) Benksim, A.; Beaupère, D.; Wadouachi, A. *Org. Lett.* **2004**, *6*, 3913-3915.

10) Sharkey, P. F.; Eby, R.; Schuerch, C. *Carbohydr. Res.* **1981**, *96*, 223-229.

11) (a) York, W. S.; McNeil, M.; Darvill, A. G.; Albersheim, P. *J. Bacteriol.* **1980**, *142*, 243-248. (b) Puvanesarajah, V.; Schell, F. M.; Stacey, G.; Douglas, C. J.; Nester, E. W. *J. Bacteriol.* **1985**, *164*, 102-106. (c) Zorreguieta, A.; Ugalde, R. A. *J. Bacteriol.* **1986**, *167*, 947-951.

12) For a related report concerning cyclic (1-2)-β-D-glucan, see: Choma, A.; Komaniecka, I. *Acta Biochim. Pol.* **2003**, *50*, 1273-1281.

13) Demchenko, A. V. *Synlett* **2003**, *9*, 1225-1240.

14) Fraser-Reid, B.; Ganney, P.; Ramamurty, C. V. S.; Gomez, A. M.; Lopez, J. C. *Chem. Comm.* **2013**, *49*, 3251-3253.

# Chapter 4

# One-Pot Synthesis of Glycyrrhetic Acid Polyglycosides Based on Grafting-from Method using Cyclic Sulfite.

## 4.1 Introduction

Natural saponins are a representative member of bioactive natural products.[1] Glycyrrhizin (**1**) is a triterpenoid saponin consisting of glycyrrhetic acid as an aglycon and (1→2)-β-bis(glucoronic acid) (Figure 4.1), which was isolated from extracts of licorice *Glycyrrhiza glabra* root.[2] The synthetic studies of the structural analogues have been considerably investigated from the viewpoint of structure-activity relationship, because the compound **1** exhibits unique bioactivities including anti-inflammatory,[3] antiulcer,[4] hypolipidemic,[5] antiviral against human immunodeficiency virus type 1 (HIV-1) and severe acute respiratory syndrome (SARS)-associated coronavirus,[6] and interferon-inducing activities.[7]

The previous syntheses were mainly focused on the change of oligosaccharide structure based on the stepwise glycosidations,[8] which required time-consuming multi-step reactions and purification processes. Therefore, the development of simple preparation method for the derivatives such as glycyrrhetic acid polyglycosides (**2**) has been strongly urged. Although the powerful polymerization methods to give (1→3)-, (1→4)-, and (1→6)-linked polysaccharides have been constructed to date,[9] that for (1→2)-linked polysaccharides has not been sufficiently developed yet. On the other hand, it is known that glycal epoxide is a potentially useful glycosyl donor for the synthesis of (1→2)-linked oligosaccharide-containing glycosides (Figure 2). Danishefsky *et al.* demonstrated the simple stepwise glycosidation of saccharide via ring-opening nucleophilic addition of alcohol to the epoxide.[10] Several processes concerning protection-deprotection can be shortened by using epoxide because the

nucleophilic addition to epoxide accompanies with the generation of a free secondary alcohol. However, the applications of epoxide to graft polymerization techniques were difficult due to the high unstability of epoxide.

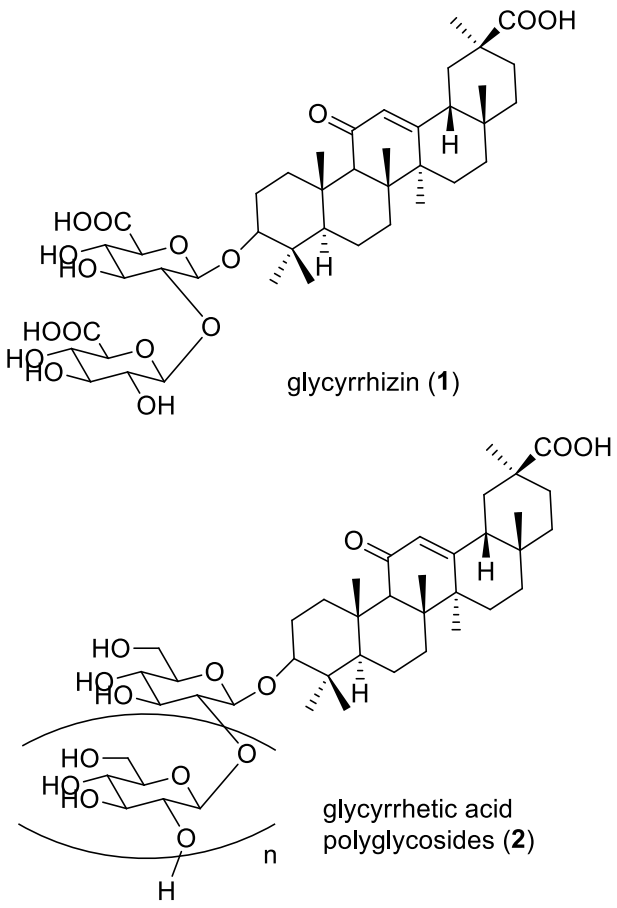


**Figure 4.1** Structures of glycyrrhizin (**1**) and glycyrrhetic acid polyglycosides (**2**).

In chapters 2 and 3, I discovered that shelf-stable cyclic sulfite **4** works as a practical monomer for the preparation of (1→2)-linked polysaccharide skeletons. The cationic ring-opening condensation

polymerization of **4** resulted in a perfect elimination of $SO_2$ linkages to afford the corresponding (1→2)-linked glucopyranan.[11,12]

Herein, I describe the synthesis of glycyrrhetic acid polyglycosides **(2)** as the application of our previous work to a grafting polymerization. The cationic ring-opening condensation polymerization of **4** was performed in the presence of glycyrrhetic acid **5** as an initiator and trifluoromethane sulfonic acid (TfOH) as a catalyst.[13] This method enables not only the one-pot synthesis of **2** but also the control of polymerization degree of (1→2)-linked oligosaccharide skeleton.

## 4.2 Results and Discussion

### Cationic ring-opening condensation polymerization of 4 initiated by glycyrrhetic acid (5)

Cyclic sulfite **4** was prepared according to the literature[14]. I investigated the grafting reaction of **4** from glycyrrhetic acid **(5)** to give the benzyl-protected skeleton of **2**, as shown in Scheme 4.1.

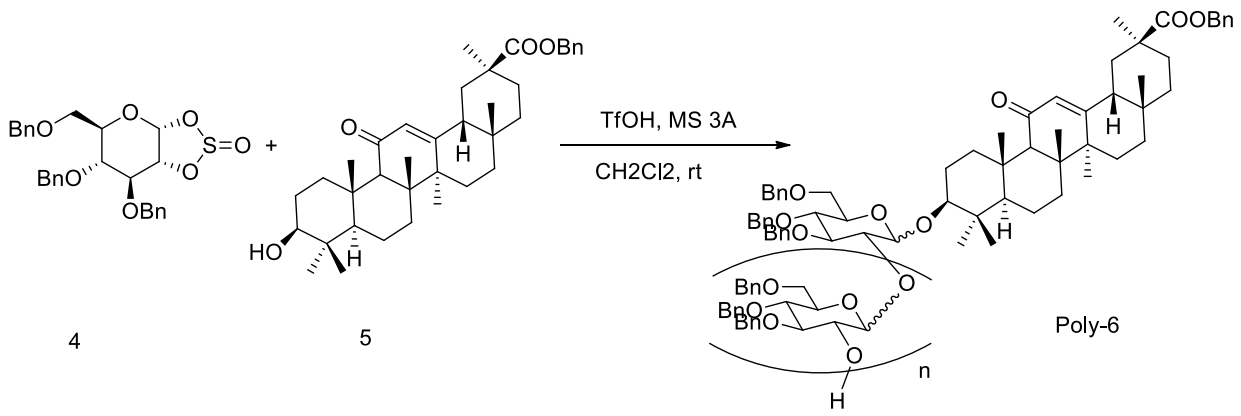


**Scheme 4.1** Cationic ring-opening condensation polymerization of **4** initiated by **5**.

Initiator **(5)** was prepared from commercially available glycyrrhetic acid via benzyl protection of carboxylic acid. The grafting polymerization of **4** from **5** were performed in $CH_2Cl_2$ in the presence of TfOH and molecular sieves 3Å (MS 3Å) at room temperature. The results are summarized in Table 4.1. The conversion of **4**, the polymerization degree, and the number average molecular weight ($M_n$) were determined by the $^1H$ NMR analysis of crude mixture. The conversion of **5** and the polydispersity index ($M_w/M_n$) were estimated by a size exclusion chromatography (SEC) using THF on the basis of polystyrene standards. At first, I used the stoichiometric amount of both **5** and TfOH to that of **4**.

**Table 4.1** Effects of the feed ratio on the conversions and $M_n$[a]

| Entry | Initiator (**5**) mol% | TfOH mol% | Time h | Conv. of **4** %[d] | Conv. of **5** %[e] | Polymerization Degree[d] | $M_n$[c] | $M_w/M_n$[f] |
|---|---|---|---|---|---|---|---|---|
| 1 | 100 | 100 | 1 | 100 | 45.8 | 2.9 | 1,800 | 1.1 |
| 2 | 150 | 100 | 1 | 100 | 30.8 | 2.5 | 1,700 | 1.1 |
| 3 | 50 | 50 | 2 | 100 | 63.7 | 4.7 | 2,600 | 1.6 |
| 4 | 20 | 20 | 94 | 76.1 | 98.5 | 4.6 | 2,600 | 1.1 |
| 5 | 10 | 10 | 94 | 46.8 | 100 | 4.0 | 2,300 | 1.1 |
| 6[b] | 10 | 10 | 94 | 71.1 | 100 | 8.0 | 4,000 | 1.1 |
| 7 | 5 | 5 | 137 | 14.6 | 100 | 3.0 | 1900 | 1.1 |
| 8[c] | 5 | 5 | 137 | 45.2 | 100 | 8.9 | 4400 | 1.1 |

[a]The reaction was performed by using cyclic sulfite **4** (0.18 mmol) in the presence of TfOH, glycyrrhetic acid, and MS 3Å (50 wt%) in $CH_2Cl_2$ (0.6 M per **4**) at room temperature. [b]MS 3Å (25 wt%) was used. [c]MS 3Å (12.5 wt%) was used. [d]Determined by $^1$H NMR analysis of the crude mixture. [e]Determined by size exclusion chromatography (SEC) analysis of the crude mixture. [f]Determined by SEC on the basis of polystyrene standards.

Contrary to our expectation that the reaction would mainly give the monosaccharide-containing glycoside, the conversion of **5** was middle (45.8%) and that of **4** was quantitative (entry 1, Table 4.1). The average polymerization degree was 2.9, indicating that $M_n$ of **Poly-6** is 1,800 Da. The $M_w/M_n$ of **Poly-6** was a relatively narrow value (1.1). Such results indicate that the bulky alcohol of **(5)** as a

neopentyl alcohol would slowly initiate the glycosylation reaction of **4** along with the elimination of $SO_2$ to generate a free alcohol at the 2 position of the sugar. The resultant secondary alcohol could exhibit a higher reactivity than the neopentyl alcohol of **5**, which would facilitate further nucleophilic addition to the other cyclic sulfite **4**, leading to the ring-opening polycondensation of **4** initiated by **5**. It is noted that the polymer with a narrow $M_w/M_n$ was obtained, even when the excess amount of **5** was used (entry 2, Table 4.1).

I next investigated the effects of feed ratio of initiator **(5)** on the conversions and $M_n$ (entries 3–8, Table 4.1). With the decrease of the feed ratio of **5** against **4**, the conversion of **4** decreased whereas that of **5** increased (entries 3–5, Table 4.1), which afforded the similar $M_n$ values. The decreased amount of TfOH prolonged the reaction time, probably because the reaction rate would be strongly dependent on the concentration of acid. On the other hand, when the amount of MS 3Å was decreased to 25 wt% (entry 6, Table 4.1), the conversion of **4** was dramatically improved, resulting in the formation of the polymer with higher $M_n$. In the cases of entries 7 and 8 with 5 mol% of TfOH, the reduced amount of MS 3Å (12.5 wt%) also enabled the high conversion of **4** to give the higher-molecular-weight polymer. Such results suggest that $M_n$ of **Poly-6** was moderately controllable by the change of feed ratio. The use of MS 3Å as a dehydrator might reduce the effective concentration of acid. In the case of entry 7 (Table 4.1) with 5 mol% of TfOH, the reaction hardly proceeded.

The crude material after a typical workup was precipitated into MeOH to remove the remaining **4** and **5**. The structure of the polymer as a MeOH-insoluble part was evaluated by IR, $^1$H NMR, and

MALDI–TOF mass spectra. In the IR spectrum, the absence of the characteristic signal of sulfite at around 1200 $cm^{-1}$ was observed, suggesting that the polymerization of **4** efficiently eliminates $SO_2$ to form (1→2)-linked oligosaccharide skeletons. The presence of enone absorption band at around 1660 $cm^{-1}$ was also confirmed. In the $^1H$ NMR spectrum, the signals attributed to glycyrrhetic acid and oligosaccharides appeared along with the disappearance of the protons of **4**, supporting the efficient conversion of **4**. The chemical shift of olefinic proton signal of the polymer almost agreed with that of **5**, also supporting the retention of the enone moiety after the polymerization. It has been reported that the Ag- or Hg-catalyzed glycosylation to glycyrrhetic acid skeleton gave the corresponding enol glycoside,[8b] highlighting the present reaction condition is a useful method to suppress the side reaction.

I also measured the $^{13}C$ NMR spectrum of **Poly-6** to clarify the anomeric stereochemistry (Figure S14). The β/α-stereo-ratio on the anomeric centers was roughly estimated to be 14.5:1 by the integral ratio between the carbon signals at 110–100 ppm for β carbon and those at 100–90 ppm for α carbon, considering the reported chemical shifts of natural product and synthetic derivatives.2,8 The results indicate that the polymerization would mainly undergo at SN2-like inversion manner to give the corresponding β-anomers as a kinetic product, because no specific participating group is included in the skeleton of **4**. The use of a catalytic amount of TfOH with MS 3Å might also suppress the anomerization reaction to afford the thermodynamically preferred α-anomers.

Matrix associated laser desorption/ionization time-of-flight (MALDI–TOF) mass spectrum of **Poly-6** exhibited a simple pattern with an even interval agreed with the theoretical values corresponding to the Benzyl-protected glycyrrhetic acid-terminated polymers (Figure 4.2), which finally evidenced that the polymerization of **4** accompanied with the perfect elimination of $SO_2$ to give **Poly-6** skeleton. The additional minor peaks attributed to the polymers initiated by a trace of $H_2O$ were barely detectable in the spectrum, indicating the important role of MS 3Å as a dehydrator.

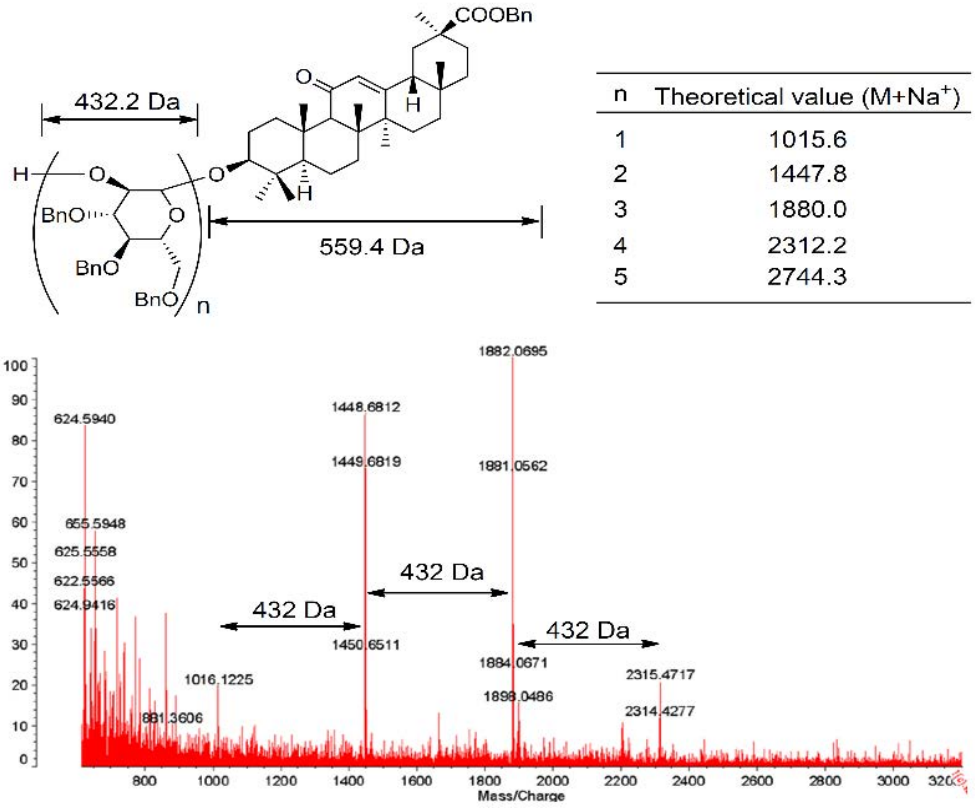


| n | Theoretical value ($M+Na^+$) |
|---|---|
| 1 | 1015.6 |
| 2 | 1447.8 |
| 3 | 1880.0 |
| 4 | 2312.2 |
| 5 | 2744.3 |

**Figure 4.2** MALDI-TOF mass apectrum of **Poly-6**

## 4.3 Conclusion

In conclusion, I demonstrated a new grafting reaction of cyclic sulfite **4** from glycyrrhetic acid **5** to give glycyrrhetic acid polyglycosides in one-pot via cationic ring-opening condensation polymerization of **4**.

The method enables the rapid preparation of glycyrrhizin derivatives consisting oligosaccharides with arbitrary polymerization degree. Because other natural glycosides bearing (1→2)-linked oligosaccharides such as cyaniding-3-*O*-sophoroside[15] and quercetin-3-*O*-sophoroside[16] have been reported, this method would be also applicable to the preparations of their derivatives. The present results may provide new insights into not only natural product syntheses but also the creation of high performance polymers based on a grafting reaction.

## 4.4 Experimental

**General methods:**

**Materials.** Molecular sieves 3Å (MS 3Å) as a dehydrator was activated by careful heating by a heat gun under vacuum. Dry dichloromethane (TCI) and trifluoromethanesulfonic acid (Kanto chemicals) were used as obtained for polymerization. The other chemicals were used without purification. Cyclic sulfite **4** was prepared according to the literature: Benksim, A.; Beaupère, D.; Wadouachi, A. *Org. Lett.* **2004**, *6*, 3913–3915.

**Measurements.** $^{1}$H NMR (400 MHz) and $^{13}$C NMR (100 MHz) spectra were recorded on JEOL JNM-

ESC400 and Bruker AVANCE II 400 spectrometers using $CDCl_3$ as the solvent, calibrated using residual undeuterated solvent and tetramethylsilane as the internal standard. FT-IR spectra were measured using a Perkin Elmer spectrum 100 spectrometer. Optical rotation was measured with an ATAGO AP-300 automatic polarimeter. SEC analyses were carried out using a chromatographic system consisting of a Shimadzu LC-20AT pump with a Shimadzu SPD-20A (UV detector) equipped with two consecutive linear polystyrene gel columns (Tosoh TSKgel $GMH_{HR}$-H and TSKgel $G3000H_{HR}$) at room temperature according to polystyrene standards using THF as an eluent (flow rate: 1.0 mL/min). MALDI–TOF MS spectra were recorded on a Shimadzu AXIMA-CFR plus mass spectrometer (matrix: CHCα).

**Typical procedure for the preparation of initiator (5)**

To a solution of glycyrrhetic acid (1.00 g, 2.12 mmol) in a mixture of acetone–DMF (10:1, 11 mL) was added $K_2CO_3$ (587 mg, 4.25 mmol) and benzyl bromide (303 μL, 2.55 mmol) at room temperature. After stirring for 40.5 h, water was added to the mixture to give white precipitates. The precipitates were collected by filtration, washed with water repeatedly, and dried in vacuo to give **5** (1.08 g, 90.8%) as a white solid: m.p. 118.0–120.0 °C; $[\alpha]_D^{25}$ +153.2 ($CHCl_3$, c. 1.00); $^1$H NMR (400 MHz, 298 K, $CDCl_3$) δ 7.40–7.33 (m, 5H), 5.55 (s, 1H), 5.19 (d, *J* = 12.4 Hz, 1H), 5.09 (d, *J* = 12.4 Hz, 1H), 3.22 (brd, 1H), 2.79 (brd, 1H), 2.31 (s, 1H), 2.04–1.91 (m, 4H), 1.80 (brd, 1H), 1.67–1.54 (m, 7H), 1.48–1.25 (m, 7H), 1.16–1.11 (m, 9H), 1.00–0.94 (m, 5H), 0.80 (s, 3H), 0.73–0.67 (s, 4H) ppm; $^{13}$C

NMR (100 MHz, 298 K, $CDCl_3$) δ 200.1, 176.2, 169.2, 136.1, 128.6, 128.5, 128.3, 128.2, 78.7, 66.2, 61.8, 54.9, 53.7, 48.2, 45.3, 44.0, 43.1, 41.0, 39.1, 37.6, 37.0, 32.7, 31.8, 31.1, 28.4, 28.3, 28.1, 27.3, 26.44, 26.37, 23.3, 18.6, 17.5, 16.4, 15.6 ppm; IR (neat) $\upsilon$ 3360, 2934, 2868, 1727, 1660, 1620, 1456, 1387, 1358, 1313, 1279, 1258, 1209, 1146, 1084, 1042, 995, 981, 955, 913, 878, 749, 645 $cm^{-1}$; MALDI–TOF MS (matrix: CHCα) calc'd for $C_{37}H_{52}NaO_4^+$ [M+$Na^+$] 583.37; found 583.85.

**Typical procedure for grafting polymerization of 4 from 5 (run 4 in Table 4.1)**

To a solution of cyclic sulfite **4** (90.3 mg, 0.18 mmol) and initiator **(5)** (20.4 mg, 0.04 mmol) in $CH_2Cl_2$ (0.30 mL) was added a freshly activated MS 3Å (ca. 45 mg) as a dehydrator at room temperature. After stirring for 1 h at room temperature, TfOH (3.2 μL, 0.04 mmol) was added to the mixture. The mixture was stirred for 94 h at the same temperature. The reaction was quenched by the addition of sat. aq. $NaHCO_3$. The products were extracted with $CHCl_3$, repeatedly. The combined organic layer was dried over $MgSO_4$, filtered, and concentrated in vacuo to give a crude material. The conversion of **4** was estimated by the $^1H$ NMR measurement of the crude material to be 76.1%. The number average molecular weight ($M_n$) was estimated by integral ratio between the olefinic proton at around 5.55 ppm and protons in a range from 4.2 ppm to 3.0 ppm to be $M_n$ 2,600 Da. The conversion of **5** was estimated by the size exclusion column chromatography (SEC, eluent: THF) of the crude solution (conc. 1.0 mg/mL) to be 98.5 % from the peak area of **5** according to the molar absorbance of **5** at 254 nm. The crude sample (60 mg) was purified for the analytical purpose through reprecipitation using

MeOH (30 mL) and $CHCl_3$ (0.1 mL) to get 7.0 mg of the polymer as a MeOH-insoluble part and 50 mg as a MeOH-soluble part. The polydispersity index ($M_w/M_n$) was also estimated by SEC analysis (eluent: THF) on the basis of polystyrene standards to be $M_w/M_n$ 1.1: $[\alpha]_D^{25}$ +63.3 ($CHCl_3$, c. 1.00); $^1$H NMR (400 MHz, 298 K, $CDCl_3$) δ 7.40–6.98 (m), 5.68 (m), 5.55 (m), 5.29–2.72 (m), 2.27–0.73 (m) ppm; IR (neat) $\upsilon$ 2919, 2851, 1727, 1659, 1497, 1454, 1361, 1311, 1260, 1211, 1050, 1026, 912, 800, 733 $cm^{-1}$.

**Figures**

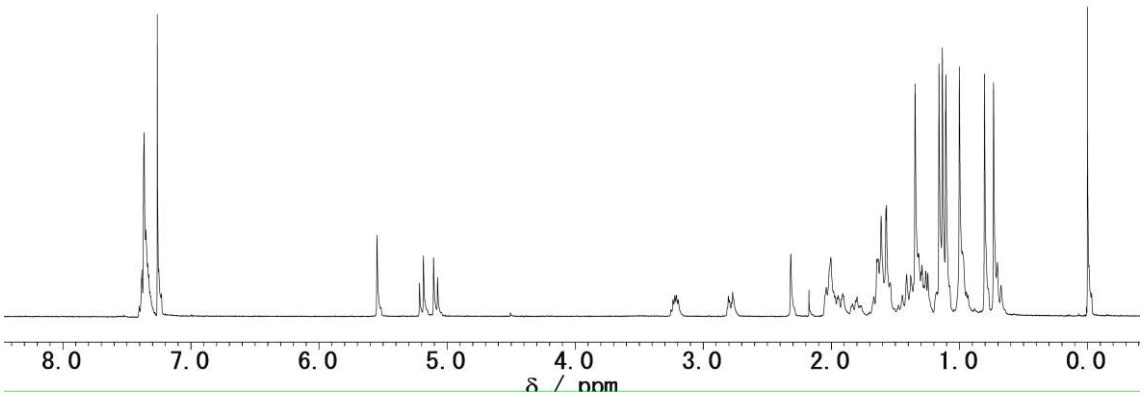


**Figure 4.3** $^1$H NMR spectrum of **5** (400 MHz, $CDCl_3$, 298 K).

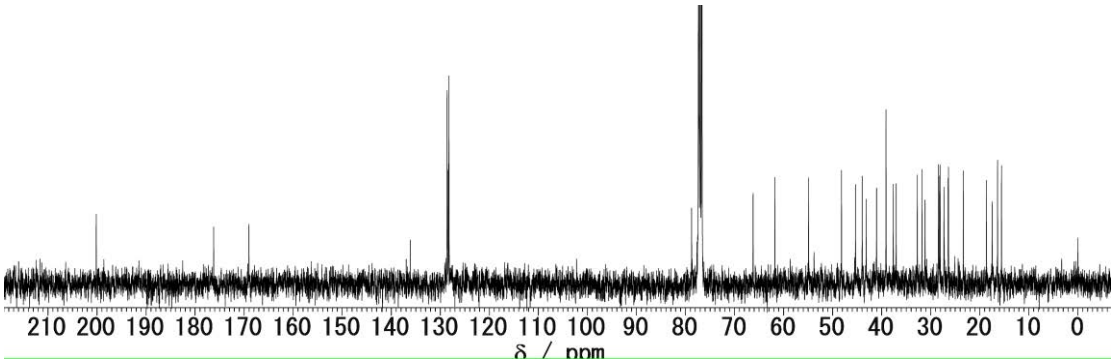


**Figure 4.4** $^{13}C$ NMR spectrum of **5** (100 MHz, $CDCl_3$, 298 K).

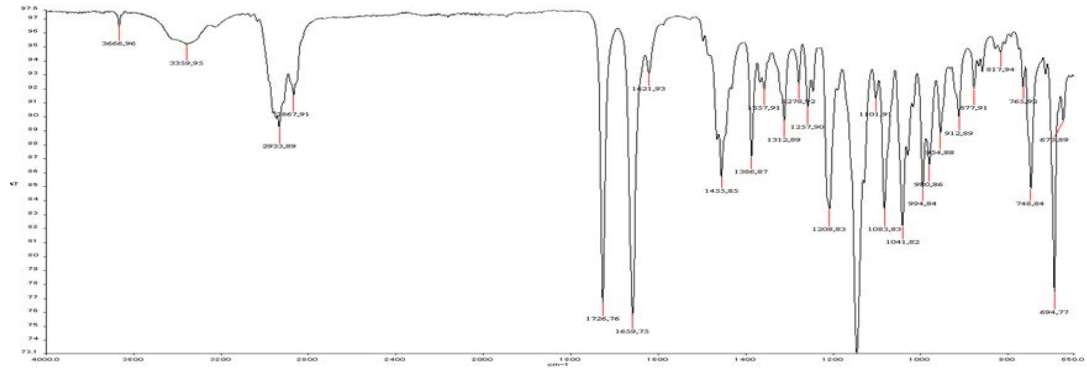

**Figure 4.5** IR spectrum of **5** (neat).

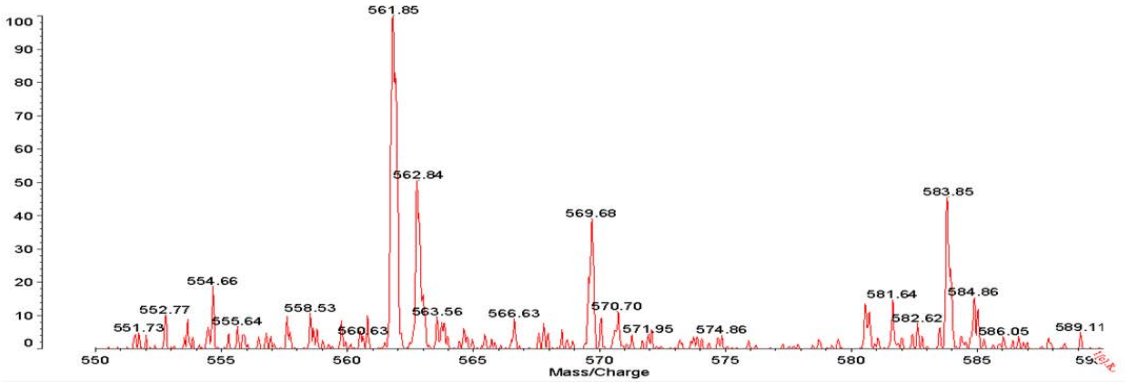


**Figure 4.6** MALDI–TOF mass spectrum of **(5)** (matrix: CHCα).

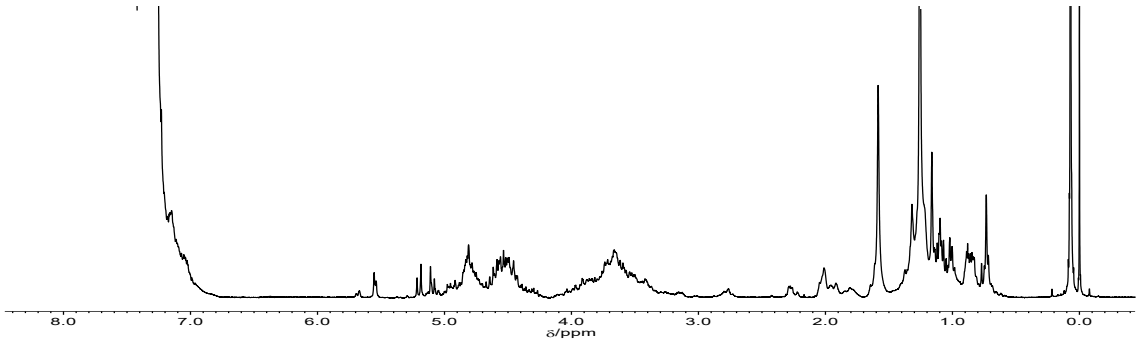


**Figure 4.7** $^{1}$H NMR spectrum of **Poly-6** (400 MHz, $CDCl_3$, 298 K).

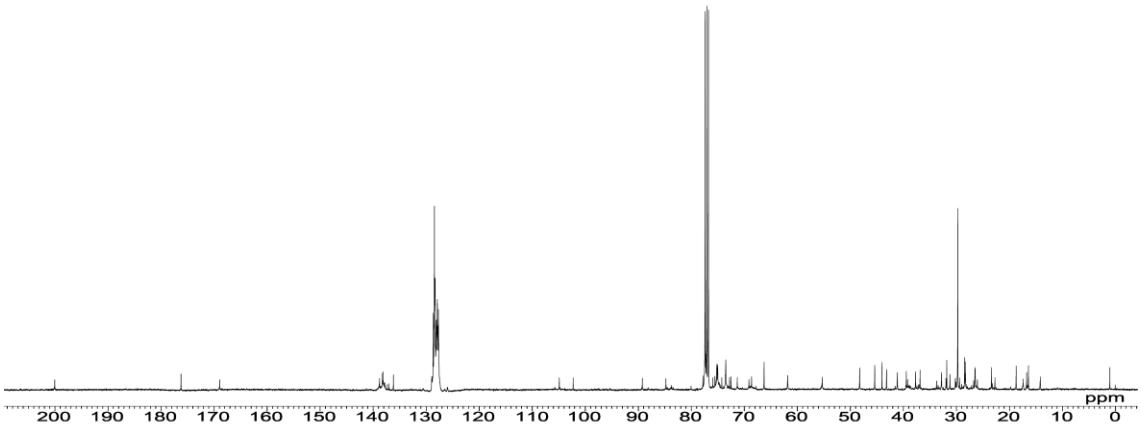


**Figure S14.** $^{13}$C NMR spectrum of **Poly-6** (100 MHz, $CDCl_3$, 298 K).

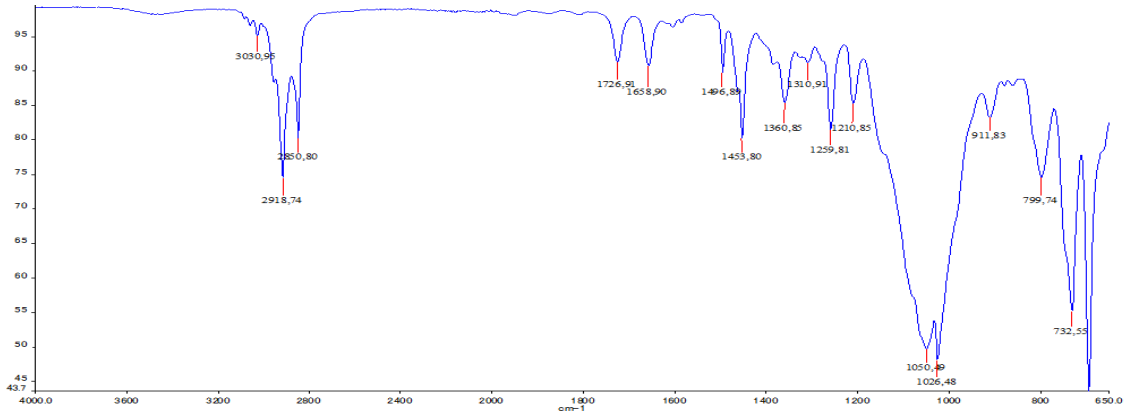


**Figure 4.8** IR spectrum of **Poly-6** (neat).

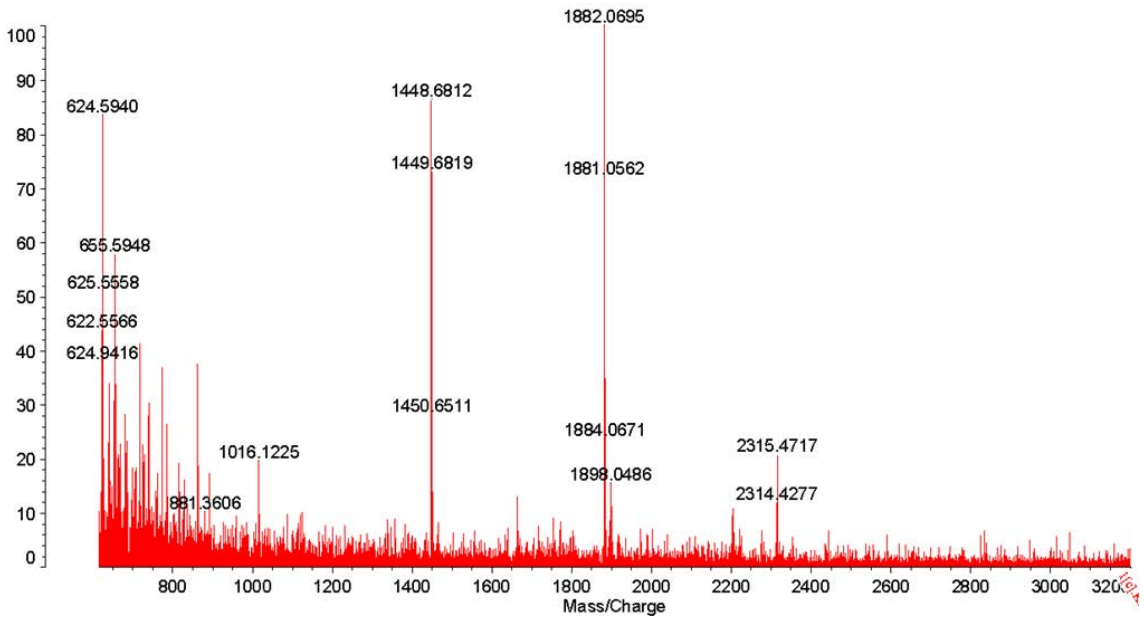


**Figure 4.9** MALDI–TOF mass spectrum of **Poly-6** (matrix: CHCα).

## References


1. For selected reviews, see; (a) Francis, G.; Kerem, Z.; Makkar, H. P. S.; Becker, K. *Br. J. Nutr*., **2002**, *88*, 587–605. (b) Park, J. D.; Rhee, D. K.; Lee, Y. H. *Phytochem. Rev.*, **2005**, *4*, 159–175. (c) Wina, E.; Muetzel, S.; Becker, K. *J. Agric. Food Chem.*, **2005**, *53*, 8093–8105. (d) Podolak, I.; Galanty, A.; Sobolewska, D. *Phytochem. Rev.*, **2010**, *9*, 425–474. (e) Synthesis and Application of a Functional Glycoside –Mainly on Glycosyltransferase–, Hamada, H. Ed., CMC publishing Co., Ltd., Tokyo, **2013**.
2. (a) Shibata, S. *Yakugaku Zasshi*, **2000**, *120*, 849–862. (b) Chaturvedula, V. S. P.; Yu, O.; Mao, G. *Eur. Chem. Bull.*, **2014**, *3*, 104–107. (c) Hayashi, H.; Sudo, H. *Plant Biotech.*, **2009**, *26*,

101−104. (d) Williams, G.; Leclercq, C.; Knaap, A. G. A. G. In Safety evaluation of certain food additives series 54, World Health Organization, Geneva, **2006**, pp. 561−613.

3. (a) Finney, R. S.; Somers, G. H. *J. Pharmacol*. **1959**, *10*, 613−620. (b) Mollica, L.; De Marchis, F.; Spitaleri, A.; Dallacosta, C.; Pennacchini, D.; Zamai, M.; Agresti, A.; Trisciuoglio, L.; Musco, G.; Bianchi, M. E. *Chem. Bio.*, **2007**, *14*, 431−441.
4. He, J.-X.; Akao, T.; Nishino, T.; Tani, T. *Bio. Pharm. Bull.*, **2001**, *24*, 1395−1399.
5. (a) Ohminami, H.; Kimura, Y.; Okuda, H.; Arich, S.; Yoshikawa, M.; Kitagawa, I. *Planta Med.* **1984**, *46*, 440−441. (b) Sen, S.; Roy, M.; Chakraborti, A. S. *J. Pharm. Pharmacol.*, **2011**, *63*, 287−296.
6. (a) Pompei, R.; Flore, O.; Marccialis, M. A.; Pani, A.; Loddo, B. *Nature*, **1979**, *281*, 689−690. (b) Ito, M.; Nakashima, H.; Baba, M.; Pauwels, R.; De Clercq, E.; Shigeta, S.; Yamamoto, N. *Antiviral Res.*, **1987**, *7*, 127−137. (c) Baba, M.; De Cleroq, S.; Nakashima, H.; Yamamoto, N. *Antiviral Res.*, **1988**, *10*, 289−299. (d) Vlietinck, A. J.; De Bruyne, T.; Apers, S.; Pieters, L. A. *Planta Med.*, **1998**, *64*, 97−109. (e) Fiore, C.; Eisenhut, M.; Krausse, R.; Ragazzi, E.; Pellati, D.; Armanini, D.; Bielenberg, J. *Phytother Res.*, **2008**, *22*, 141−148.
7. (a) Abe, N.; Ebina, T.; Ishida, N. *Microbiol. Immunol.*, **1982**, *26*, 535−539. (b) Ye, S.; Zhu, Y.; Ming, Y.; She, X.; Liu, H.; Ye, Q. *Exp. Ther. Med.*, **2014**, *7*, 1247−1252.
8. (a) Saito, S.; Kuroda, K.; Hayashi, Y.; Sasaki, Y.; Nagamura, Y.; Nishida, K.; Ishiguro, I. *Chem. Pharm. Bull.*, **1991**, *39*, 2333−2339. (b) Saito, S.; Sumita, S.; Kanda, Y.; Sasaki, Y. *Chem.*

*Pharm. Bull.*, **1994**, *42*, 1016−1027. (c) Morishima, N.; Mori, Y. *Bioorg. Med. Chem.*, **1996**, *4*, 1799−1808. (d) Hirooka, M.; Morishima, N.; Kaji, E.; Mori, Y.; Zen, S. *Yakugaku Zasshi*, **1989**, *109*, 544−559.

9. (a) Kobayashi, S.; Kashiwa, K.; Kawasaki, T.; Shoda, S. *J. Am. Chem. Soc.*, **1991**, *113*, 3079−3084. (b) Kaneko, Y.; Kadokawa, J. *Chem. Rec.*, **2005**, *5*, 36−46. (c) Yoshida, T. *Prog. Polym. Sci.*, **2001**, *26*, 379−439.
10. Halcomb, R. L.; Danishefsky, S. J. *J. Am. Chem. Soc.*, **1989**, *111*, 6661−6666.
11. Shetty, S. S.; Koyama, Y.; Nakano, T. *Chemistry lett*., **2016**, DOI:10.1246/cl.160416.
12. For related reports, see; (a) Azuma, N.; Sanda, F.; Takata, T.; Endo, T. *J. Polym. Sci.: Part A: Polym. Chem.*, **1997**, *35*, 3235−3240. (b) Kricheldorf, H. R.; Petermann, O. *Macromolecules*, **2001**, *34*, 8841−8846. (c) Nishimura, N.; Mitsunobu, O. *Tetrahedron Lett.*, **2000**, *41*, 2945−2948. (d) Lohray, B. B. *Synthesis*, **1992**, 1035−1052.
13. For related reports concerning alcohol-initiated cationic ring-opening polymerization, see: (a) Makiguchi, K.; Satoh, T.; Kakuchi, T. *Macromolecules*, **2011**, *44*, 1999–2005. (b) Shibasaki, Y.; Sanada, H.; Yokoi, M.; Sanda, F.; Endo, T. *Macromolecules*, **2000**, *33*, 4316−4320. (c) Kamber, N. E.; Jeong, W.; Waymouth, R. M. *Chem. Rev.*, **2007**, *107*, 5813−5840. (d) Iguchi, H.; Uchida, S.; Koyama, Y.; Takata, T. *ACS Macro Lett.*, **2013**, *2*, 527−530. (e) Aoki, D.; Uchida, S.; Nakazono, K.; Koyama, Y.; Takata, T. *ACS Macro Lett.*, **2013**, *2*, 461−465.

14. (a) Meslouti, A. E.; Beaupère, D.; Demailly, G.; Uzan, R. *Tetrahedron Lett.*, **1994**, *35*, 3913−3916. (b) Benksim, A.; Beaupère, D.; Wadouachi, A. *Org. Lett.*, **2004**, *6*, 3913−3915. (c) Benksim, A.; Massoui, M.; Beaupère, D.; Wadouachi, A. *Tetrahedron Lett.*, **2007**, *48*, 5087−5089.

15. Wu, X.; Gu, L.; Prior, R. L.; McKay, S. *J. Agric. Food Chem*., **2004**, *52*, 7846−7856.

16. Song, R. J.; Zhou, J. *J. Chromatogr. B*, **2015**, *995-996*, 8−14.

# Chapter 5

# General Conclusion

In this thesis, the author has described the new synthetic method of 1,2-glycosidic polymers via ring-opening condensation polymerization of a sugar- based cyclic sulfite. Cationic polymerization of the cyclic sulfite afforded (1→2)-D-glycopyranan along with the elimination of $SO_2$. The method was also applied to both grafting-onto and grafting-from polymerizations to give the corresponding glycosides. The results of this study are summarised as follows. In chapter 1, the author described the general backgrounds of polysaccharides and glycosides. Through the historical survey, the importance on the synthetic studies of 1,2-glycosidic polymers was particularly emphasized.

In chapter 2, the author discussed the chemical stability and reactivity of cyclic sulfite as a monomer, mainly by comparision with those of glycal epoxide as a conventional monomer. Kinetic studies for the degradations evaluated the higher stability of the cyclic sulfite than the epoxide. At first, the anionic ring-opening condensation polymerization of cyclic sulfite was investigated according to the model studies of nucleophilic substitution on the anomeric center. However, it was found that the anionic polymerization gave a mixture of the polymer and some other impurities containing sulfur.

In chapter 3, the author achieved the synthesis of glycosylation-active polymer bearing pentenoyl group at the polymer terminus. The anomeric stereochemistry of the polymer was moderately controllable by changing the reaction temperature. As an application, the author demonstrated the glycosylation reaction using the terminal pentenoyl group. The reaction could provide a new pathway for the creation of polysaccharide- containing graft copolymers and the cyclic polymer.

In chapter 4, I demonstrated a new grafting reaction of the cyclic sulfite from glycyrrhetic acid to

give glycyrrhetic acid polyglycosides in one-pot. The reaction enables the rapid preparation of glycyrrhizin derivatives consisting oligosaccharides with arbitrary polymerization degree.

As stated above, this thesis demonstrates the usefulness of the sugar-based cyclic sulfite as a new monomer for the first time. The author hopes that this study will be a cornerstone for the preparation of 1,2-glycosidic polymers. The present results may provide new insights into not only natural product syntheses but also the creation of high performance polymers based on a grafting reaction.